The role of CDCA in intestinal epithelial regeneration and inflammation

A dissertation for the doctoral degree of

DOCTOR RERUM NATURALIUM

Faculty of Mathematics, Informatics and Natural Sciences

Department of Biology

University of Hamburg

By

Ole Hinrichs

from Uelzen, Germany

Hamburg 2024

First reviewer: **Prof. Dr. Julia Kehr**

University of Hamburg, Faculty of Mathematics, Informatics and Natural Sciences, Department of Biology, Research Unit Molecular Plant Genetics, Hamburg, Germany

Second reviewer: **Prof. Dr. Madeleine Bunders**

Research Department Immune Ontogeny and Viral Infections, Leibniz Institute of Virology, Hamburg, Germany

Date of oral defense (disputation): April 25 2025

Contents

Table of abbreviations

AD +++	Advanced DMEM/ F-12 + + +
ANXA10	Annexin A10
AP-1	Jun proto-oncogene, AP-1 transcription factor subunit
AP1S1	Adaptor related protein complex 1 subunit sigma 1
APCDD1	APC down-regulated 1
ARPC1B	Actin related protein 2/3 complex subunit 1B
ASBT/ SLC10A2	Solute carrier family 10 member 2
ATP	Adenosine triphosphate
B2M	Beta-2-microglobulin
BMP	Bone morphogenetic protein
BSA	Bovine serum albumin
BSH	Bile salt hydrolase
CA	Cholic acid
Ca^{2+}	Calcium ion
Cas9	CRISPR associated protein 9
CCL20	C-C motif chemokine ligand 20
CCR6	C-C motif chemokine receptor 6
CD	Crohn's disease
CD16	Cluster of differentiation 16, Fc gamma receptor IIIa
CD4	Cluster of differentiation 4, CD4 molecule
CD45	Cluster of differentiation 45, protein tyrosine phosphatase receptor type C
CDC42EP5	CDC42 effector protein 5
CDCA	Chenodeoxycholic acid
cDNA	Complementary DNA
c-Myc	MYC proto-oncogene, bHLH transcription factor
CRACs	Calcium release-activated channels
CRISPR	Clustered regularly interspaced short palindromic repeats
CT	Cycle threshold
CTSZ	Cathepsin Z
CXCL8	C-X-C motif chemokine ligand 8
CXCL9	C-X-C motif chemokine ligand 9
CXCR1	C-X-C motif chemokine receptor 1
CXCR2	C-X-C motif chemokine receptor 2
CYP27A1	Cytochrome P450 family 27 subfamily A member 1

Cyp2c70	Cytochrome P450, family 2, subfamily c, polypeptide 70
CYP7A1	Cytochrome P450 family 7 subfamily A member 1
CYP8B1	Cytochrome P450 family 8 subfamily B member 1
DC	Dendritic cell
DCA	Deoxycholic acid
DMEM	Dulbecco's Modified Eagle's Medium
DMSO	Dimethylsulfoxide
dsRNA	Double-stranded RNA
DTD1	D-aminoacyl-tRNA deacylase 1
DTT	1,4-Dithiothreitol
EDTA	Ethylenediaminetetraacetic acid
EGF	Epidermal Growth Factor
egr-1	Early growth response factor 1
EM	Expansion medium
EpCAM	Epithelial cell adhesion molecule
ER	Endoplasmic reticulum
ERK	Extracellular signal-regulated kinase
EZR	Ezrin
FACS	Fluorescence-activated cell sorting
FBS	Fetal Bovine Solution
FGF19	fibroblast growth factor 19
FN1	Fibronectin 1
FOXP3	Forkhead box P3
FSC	Forward scatter
FXR/ NR1H4	Nuclear receptor subfamily 1 group H member 4
G	Glycine
GAPDH	Glyceraldehyde-3-phosphate dehydrogenase
GCA	Glycocholic acid
GCDCA	Glycochenodeoxycholic acid
GOAT	Generalized Organoid Annotation Tool
GPBAR1/ TGR5	G protein-coupled bile acid receptor 1
GPCR	G protein-coupled receptor
HEPES	4-(2-hydroxyethyl)-1-piperazineethanesulfonic acid
HLA	Human Leucocyte Antigen
IBD	Inflammatory Bowel Disease
IEL	Intestinal epithelial layer

IELs	Intraepithelial lymphocytes
IFNγ	Interferon
IL	Interleukin
IL-17	interleukin 17
IL-1β	interleukin 1 beta
IL-22	interleukin 22
IL-23	interleukin 23
IL-33	interleukin 33
IL-6	interleukin 6
IMDM	Iscove's Modified Dulbecco's Medium
IP_3	Inositol triphosphate
IRGM	Immunity-related GTPase family M protein
ISC	Intestinal stem cell
JNK	c-Jun N-terminal kinase
LCA	Lithocholic acid
LD	Live dead
LGR5	Leucine-rich repeat-containing G-protein coupled Receptor 5
LPS	Lipopolysaccharide
LYZ	Lysozyme
M cell	Microfold cell
MAPK	Mitogen-activated protein kinase
MC	*Morbus Crohn*
MCA	Muricholic acid
MFI	Median fluorescence intensity
MIF	Macrophage migration inhibitory factor
MKI76	Marker of proliferation Ki-67
mtDNA	Mitochondrial DNA
MUC1	Mucin 1
MUC2	Mucin 2
MyD88	Myeloid differentiation primary response 88
NCM	Noggin conditioned medium
NF-κB	Nuclear factor kappa-light-chain-enhancer of activated B cells
NK cell	Natural Killer cell
NKp44	Natural cytotoxicity triggering receptor 2
NLRP3	NLR family pyrin domain containing 3
NOD	Nucleotide-binding Oligomerization Domain
NR1/2	nuclear receptor subfamily 1 group I member 2

OAZ2	ornithine decarboxylase antizyme 2
OWB	Organoid washing buffer
P/S	Penicillin/ Streptomycin
p38	p38 mitogen-activated protein kinases
PAMP	Pathogen-associated molecular patterns
PBMCs	Peripheral blood mononuclear cell
PBS	Dulbecco's Phosphate Buffered Saline
PBT	PBS-Tween
PFA	Paraformaldehyde
PIP_2	Phosphatidylinositol 4,5-bisphosphate
PRR	Pattern recognition receptor
PRRC2A	proline rich coiled-coil 2A
PRSS23	Serine protease 23
RCM	R-spondin-1 conditioned medium
RORγt	Retinoic Acid Receptor-Related Orphan Receptor γt
ROS	Reactive oxygen species
RT qPCR	Reverse transcription quantitative PCR
SCFA	Short-chain fatty acid
SNHG5	small nucleolar RNA host gene 5
SOCE	Store-operated calcium entry
Sp1	Specificity protein 1
Sp3	Specificity protein 3
SRPRA	SRP receptor subunit alpha
SSC	Side scatter
ssRNA	Single-stranded RNA
T	Taurine
TCA	Taurocholic acid
TCDCA	Taurochenodeoxycholic aci
Th1 cell	T helper 1 cell
Th17 cell	T helper 17 cell
TLR	Toll-like receptor
TLR5	Toll-like receptor 5
TNF	Tumor necrosis factor
UC	Ulcerative colitis
VDR	Vitamin D receptor
WCM	WNT3a conditioned medium
WNT	Portmanteau of int and Wg for Wingless-related integration site

WNT5A	WNT family member 5A
ZNHIT3	zinc finger HIT-type containing 3
ZO-1	Tight junction protein 1

List of figures

Publication list

Parts of this thesis may be contained in future publications a peer-reviewed journals.

1. Martin E. Baumdick, Annika Niehrs**,** Frauke Degenhardt, Maria Schwerk, **Ole Hinrichs**, Ana Jordan-Paiz, Benedetta Padoan, Lucy H. M. Wegner, Sebastian Schloer, Britta F. Zecher, Jakob Malsy, Vinita R. Joshi, Christin Illig, Jennifer Schröder-Schwarz, Kimberly J. Möller, Hamburg Intestinal Tissue Study Group, Maureen P. Martin, Yuko Yuki, Mikki Ozawa, Jürgen Sauter, Alexander H. Schmidt, Daniel Perez, Anastasios D. Giannou, Mary Carrington, Randall S. Davis, Udo Schumacher, Guido Sauter, Samuel Huber, Victor G. Puelles, Nathaniel Melling, Andre Franke, on behalf of International Inflammatory Bowel Disease Genetics Consortium, Marcus Altfeld, and Madeleine J. Bunders

   HLA-DP on Epithelial Cells Enables Tissue Damage by NKp44D Natural Killer Cells in Ulcerative Colitis

   Gastroenterology 2023, 165: 946- 962

2. Jan P. Bremer, Martin E. Baumdick, Marius S. Knorr, Lucy H.M. Wegner, Jasmin Wesche, Ana Jordan-Paiz, Johannes M. Jung, Andrew J. Highton, Julia Jäger, **Ole Hinrichs**, Sebastien Brias, Jennifer Niersch, Luisa Müller, Renée R.C.E. Schreurs, Tobias Koyro, Sebastian Löbl, Leonore Mensching, Leonie Konczalla, Annika Niehrs, Florian W. R. Vondran, Christoph Schramm, Angelique Hölzemer, Karl Oldhafer, Ingo Königs, Stefan Kluge, Daniel Perez, Konrad Reinshagen, Steven T. Pals, Nicola Gagliani, Sander P. Joosten, Maya Topf, Marcus Altfeld & Madeleine J. Bunders

   GOAT: Deep learning-enhanced Generalized Organoid Annotation Tool

   bioRxiv preprint published on September 8, 2022

Abstract

Crohn's disease (CD) is a severe inflammatory disease of the intestines. At present, the exact mechanisms underlying CD are incompletely understood. However, several genetic and environmental factors leading to impaired barrier functions and hyperactive immune responses with a lack of regulatory mechanisms are considered to play important roles in CD. Recently, studies indicated that bile acid metabolism is altered in people with CD. Specifically, levels of chenodeoxycholic acid (CDCA) are increased in stool samples of individuals with CD. The hypotheses underlying this thesis project are that CDCA impairs epithelial regeneration and that CDCA enhances inflammatory processes in epithelial cells. To this end, the effects of CDCA on intestinal epithelial cells were characterized using human intestinal organoid systems. Stimulating intestinal organoids with CDCA inhibited epithelial regeneration, which implies a CDCA-mediated defect in the epithelial barrier function. Moreover, epithelial cells increased cytosolic calcium concentrations seconds after stimulation with CDCA, indicating the induction of intracellular signaling transduction pathways. A weakened intestinal epithelial barrier is an important characteristic of CD and is considered to contribute to the progression of the disease by allowing bacterial translocations from the intestinal lumen across the epithelium. To assess the effects of CDCA on the induction of proinflammatory pathways in epithelial cells in response to bacterial compounds, intestinal organoids treated with CDCA were stimulated with the TLR5 ligand flagellin. Pretreatment with CDCA enhanced TLR5 signaling, characterized by the increased production of inflammatory chemokines and cytokines, including CXCL8, CCL20, and TNF, compared to organoids that were only stimulated with flagellin. One reason for the increased production of these inflammatory mediators could be the increased epithelial TLR5 production, which was induced by CDCA. Moreover, TLR5 expression of primary intestinal stem cells derived from CD-affected individuals was higher in comparison to other epithelial cell types. Taken together, increased levels of CDCA in people with CD may enhance TLR5 signaling and intestinal inflammation. Furthermore, this organoid-based study can serve as an example for future projects to study the cellular effects of dietary factors and metabolites on the human intestinal epithelium in inflammatory diseases.

Zusammenfassung

Morbus Crohn (MC) ist eine entzündliche Darmerkrankung. Zurzeit sind die zugrundeliegenden Mechanismen nicht vollständig verstanden. Nichtsdestotrotz stehen verschiedene genetische Faktoren und Umwelteinflüsse in Verdacht, eine Schädigung der Darmbarriere und eine Überreaktion des Immunsystems auszulösen, in der immunregulatorische Kontrollmechanismen versagen. Aktuelle Studien haben gezeigt, dass der Gallensäuremetabolismus von Personen mit MC Veränderungen im Vergleich zu gesunden Menschen aufweist. Insbesondere ist die Konzentration von Chenodeoxycholsäure (CDCA) in Stuhlproben von Individuen mit MC erhöht. Die Hypothesen dieser Arbeit sind, dass CDCA die Regeneration des Darmepithels verändert und dass darüber hinaus entzündliche Prozesse in Epithelzellen verstärkt werden. Um die Effekte von CDCA auf das Darmepithel zu untersuchen, wurden Experimente mit humanen Darmorganoiden durchgeführt. Eine zweiwöchige CDCA-Stimulation hat dabei zu einer verminderten Regeneration des Darmepithels geführt, was Defekte in der Barrierefunktion des Darmepithels impliziert. Darüber hinaus induzierte CDCA wenige Sekunden nach der Stimulation einen intrazellulären Calcium-Einstrom in Epithelzellen, was auf die Initiierung von intrazellulären Signalwegen hinweist. Eine gestörte Darmbarriere ist charakteristisch für MC und trägt zur Pathogenese bei, weil es Darmbakterien erlaubt, die Epithelbarriere zu überwinden. Um den Einfluss von CDCA auf die Initiierung von entzündlichen Signalwegen in Antwort auf eine bakterielle Invasion des Darmepithels zu untersuchen, wurden zuvor mit CDCA behandelte Darmorganoide mit dem TLR5-Liganden Flagellin stimuliert. Im Vergleich zu Darmorganoiden, die nur mit Flagellin stimuliert wurden, zeigten die mit CDCA vorbehandelten Darmorganoide eine Verstärkung des TLR5-Signalwegs, was durch eine erhöhte Ausschüttung von den entzündlichen Chemokinen CXCL8 und CCL20 und dem Zytokin TNF gekennzeichnet war. Ein Grund für die vermehrte Ausschüttung dieser Entzündungsmediatoren könnte die erhöhte Expression von TLR5 sein, die durch CDCA induziert wurde. Darüber hinaus war die TLR5-Expression in primären Darmstammzellen verglichen mit anderen Epithelzelltypen in Darmproben von Individuen, die mit MC diagnostiziert wurden, erhöht. Daraus folgt, dass eine erhöhte Konzentration von CDCA im Darm von Individuen mit MC das Potential besitzt, TLR5-Signalwege und somit Entzündungen im Darm verstärken zu können. Außerdem zeigt diese Studie, wie humane Darmorganoide in Zukunft verwendet werden können, um den Einfluss von bestimmten Nahrungsmitteln und damit assoziierten Metaboliten auf das humane Darmepithel im Kontext von entzündlichen Erkrankungen zu untersuchen.

1. Introduction

1.1 The human gastrointestinal tract

1.1.1 Anatomy

The human gastrointestinal tract is a complex system composed of different organs. It is divided into the upper and lower gastrointestinal tract. The upper gastrointestinal tract comprises the oral cavity, pharynx, esophagus, stomach, and small intestine, which is further separated into the duodenum, jejunum, and ileum.[1] The lower gastrointestinal tract consists of the large intestine, which is further divided into the caecum, appendix, ascending colon, transverse colon, descending colon, sigmoid colon, rectum, and anus.[2]

Other organs that are in direct contact with the gastrointestinal tract are the liver and the pancreas, which are connected to the duodenum via the bile and pancreatic ducts (Figure 1).[3,4] Blood vessels that converge to the portal vein are in close contact with the intestinal epithelium. The portal vein reconnects the intestinal tract with the liver.[5]

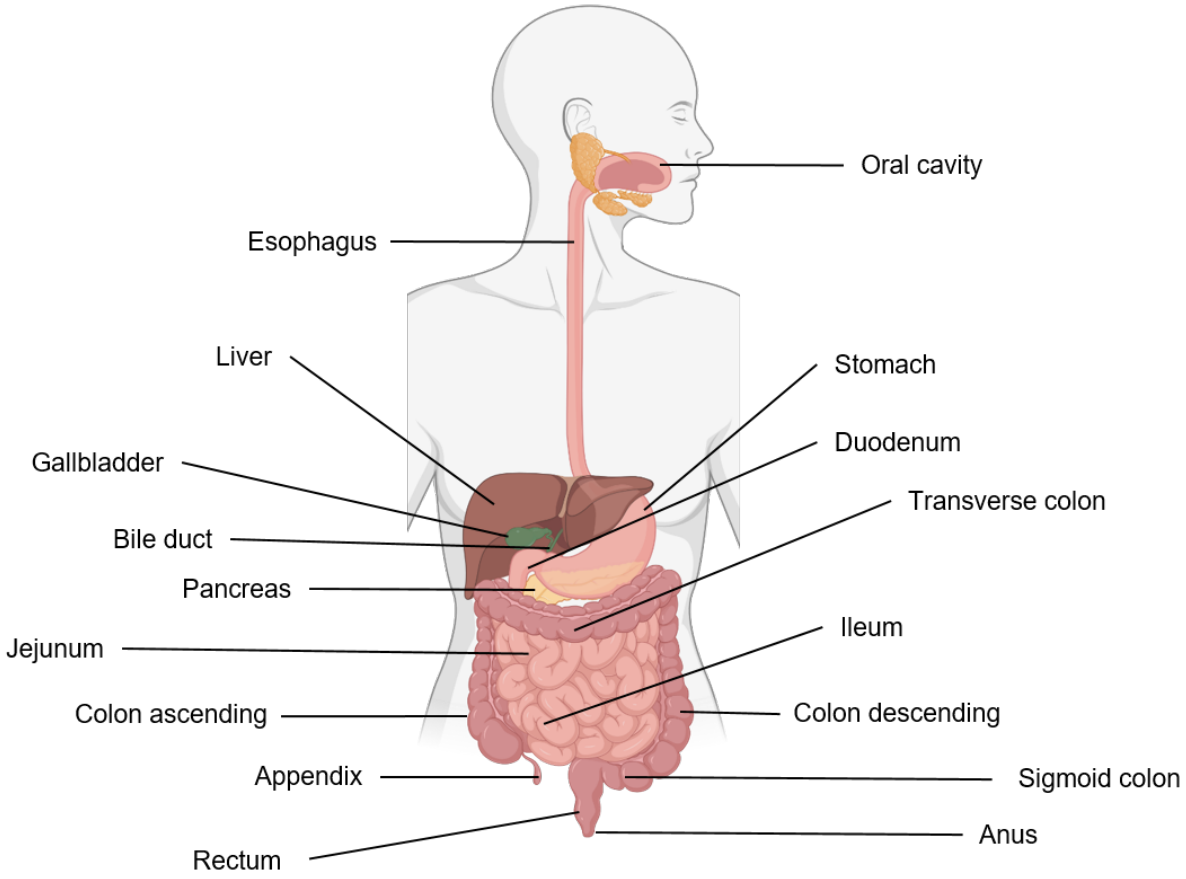

Figure 1: Anatomy of the human gastrointestinal tract. The human gastrointestinal tract consists of different organs. It starts with the oral cavity and ends with the anus.[1,2] Created with bioRender.com.

The small intestinal epithelium consists of various cell types (Figure 2) that are constantly regenerated due to the continuous proliferation of intestinal stem cells (ISCs) at the bottom of intestinal crypts.[6] Paneth cells that protect the stem cell niche by the secretion of antimicrobial factors surround ISCs.[7] ISC proliferation depends on multiple signaling pathways.[8] Direct cell-to-cell contact of ISCs and Paneth cells involves, for example, Notch signaling, which supports epithelial stem cell proliferation.[7] Below the epithelial crypt, stromal cells and myofibroblasts are located. These cells provide WNT (a portmanteau of int and Wg standing for “Wingless-related integration site”) ligands and epidermal growth factor (EGF) that are crucial for ISC maintenance and the prevention of differentiation to terminated cell types.[9,10] Further critical for the maintenance of the ISCs is the interaction of leucine-rich repeat-containing G protein-coupled receptor 5 (LGR5) with R-spondin, which additionally activates the WNT signaling pathway.[11]

WNT signaling has been identified as a pathway that enhances proliferation in epithelial cells, which is hijacked by tumor cells in colorectal cancer.[12] In the absence of WNT ligands,

β-catenin is phosphorylated and degraded.[12] Activation of Frizzled receptors such as LGR5 on the cell surface by WNT ligands leads to the dephosphorylation and translocation of β-catenin into the nucleus, which regulates transcription factors affecting the expression of genes involved in proliferation and migration.[13]

Transit amplification of ISCs describes the process of epithelial cells migrating out of the intestinal crypt and the respective stem-cell niche, leading to their differentiation.[14] Differentiation and proliferation are regulated by soluble factors in the microenvironment of villi and crypts.[15] Ligands of the WNT signaling pathway gradually decrease from the crypt to the villus.[16] In contrast, soluble bone morphogenetic proteins (BMP) promote the differentiation of stem cells.[17] Their concentrations gradually increase from the crypt to the villus.[18–20] Noggin acts as an inhibitor of BMP signaling, and its presence in intestinal crypts prevents the differentiation of intestinal stem cells.[6,21] Previous studies showed that *in vitro* and *ex vivo* stimulation of intestinal stem cells with WNT ligands and BMP signaling inhibitors maintains the stem cell phenotype, which is the basis for the generation of intestinal organoid cultures.[22,23] Differentiated epithelial cells across the villi consist of different subsets with different functional properties.[20] Enterocytes have specialized microvilli structures at the apical side and build the epithelial brush border, which enables efficient uptake of nutrients from the intestinal lumen by its increased surface.[20] Goblet cells are secretory cells that are the leading mucus producers due to the secretion of mucins.[20] Enteroendocrine cells are sensory cells that mediate signaling transduction to neurons, thereby forming an integral part of the gut-brain axis.[20]

Cells reaching the top of the villus eventually die due to apoptosis and necroptosis, resulting in their shed from the intestinal epithelium.[24] The continuous proliferation of ISCs at the bottom of crypts and the cell death of differentiated cells at the top of the villi lead to an epithelial turnover rate of four to five days.[20] The lamina propria layer is located below the epithelial layer and is populated with a high number of immune cells.[25]

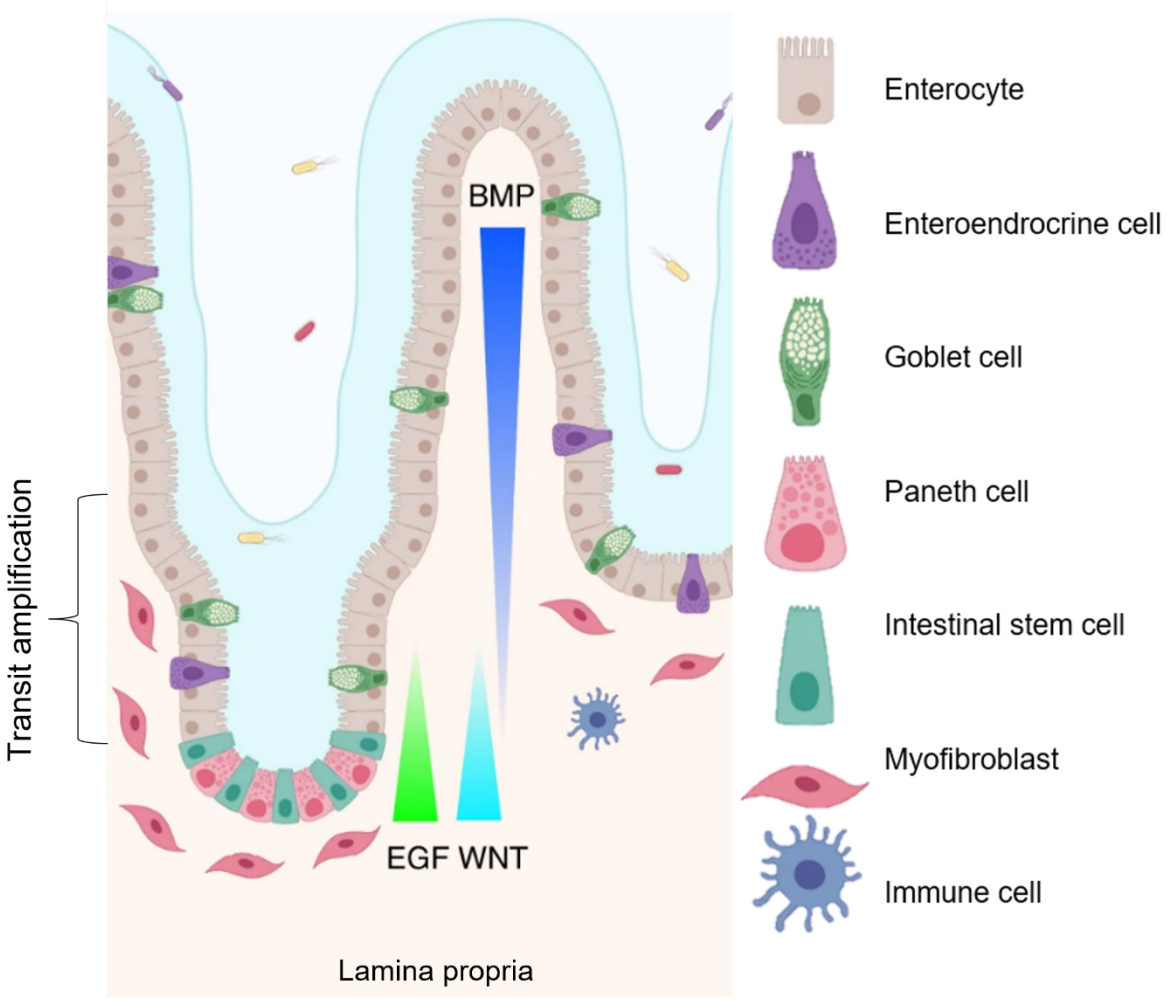

Figure 2: The small intestinal epithelium. The small intestinal epithelial cell layer contains various cell types, including enterocytes, enteroendocrine cells, Goblet cells, Paneth cells, and intestinal stem cells. In addition, myofibroblasts and immune cells can be found below the single-cell epithelial layer in the lamina propria. Gradients of epidermal growth factor (EGF), WNT, and bone morphogenic proteins (BMP) regulate the intestinal epithelial cell type composition. Adapted from Antfolk and Jensen, 2020.[26]

1.1.2 Metabolic processes

The gastrointestinal tract plays an essential role in human physiology by fulfilling different functions. One primary hallmark of the gastrointestinal tract is its ability to digest and absorb nutrients and water. Absorption is based on mechanical and biochemical disruption of food.[27] Mechanical disruption occurs in the oral cavity by transforming food to bolus, and in the stomach and small intestine by muscular contractions.[28] Biochemical digestion of food relies on enzymatic activity.[27] Specialized cell types in multiple organs secrete digestive enzymes to enable the metabolism of large molecules such as polysaccharides, lipids, proteins, and nucleic acids.[29–35] Most carbohydrates are metabolized into monosaccharides by amylases secreted in the oral cavity and the pancreas.[36] Monosaccharides, such as glucose and fructose, can enter the bloodstream via facilitative diffusion mediated by membrane transport proteins of the glucose transporter (GLUT) family.[36,37]

Large proteins are enzymatically split by proteases and peptidases in the small intestine into smaller peptides and amino acids by the hydrolysis of peptide bonds.[38] Enterocytes absorb peptides and free amino acids via solute carrier transporters.[39,40] Nucleic acids are split into nucleotides mediated by the activity of nucleases, which are secreted in the pancreas and released into the small intestine.[35]

The digestion of dietary fat is complex due to its chemical structure. The predominant forms of dietary fats are triglycerides.[41] They consist of a hydrophilic head and a hydrophobic tail, resulting in a low solubility in water.[42] Therefore, the absorption of triglycerides and other lipids is challenging and involves multiple steps of emulsification, enzymatic hydrolysis, and solubilization.[41] Lipases are secreted along the intestinal tract, starting in the oral cavity.[41] They split triglycerides into free fatty acids and monoglycerides, which form micelles in combination with bile acids.[43] Micelles shuttle the lipolytic products to the epithelial brush border, where diffusion into enterocytes can occur.[43] Bile acids are crucial in lipid digestion since their micelle complex with fatty acids, monoglycerides, cholesterol, and fat-soluble vitamins further increases the polarity and water solubility, enabling the uptake of these physiologically relevant molecules.[44]

In addition, the intestinal microbiome is involved in the digestion of certain dietary molecules.[45] For example, dietary fibers are metabolized by gut bacteria in the large intestine, resulting in the accumulation of short-chain fatty acids (SCFAs), which serve as an additional energy source for epithelial cells.[45] The microbiome biomass increases from the stomach to the large intestine and has been quantified in a previous study.[46] The colon has the largest microbial load, with 109 to 1012 microbes per milliliter, followed by the ileum, with 103 to 107 microbes per milliliter.[46] The commensal microbial community has essential functions in metabolism and also in immune regulation, and a dysregulated microbiome is

associated with several pathological conditions.[47] For example, the SCFA butyrate has been shown to have direct immunoregulatory effects on the intestinal epithelium by directly inhibiting intracellular nuclear factor 'kappa-light-chain-enhancer' of activated B-cells (NF-κB) signaling, which is a key factor for the initiation of inflammation.[48] Increased gut luminal butyrate levels have positive antiinflammatory effects in chronic intestinal diseases such as inflammatory bowel disease.[49] Next to the direct effect of microbial-derived metabolites, the presence of a diverse community of the gut microbiome is closely linked to intestinal health as it prevents the overgrowth of species with pathogenic potential by nutrient restriction.[50] The diversity of the intestinal microbiota and its microbial products is also crucial for the efficient induction, training, and function of the immune system.[51] Given the critical role of the commensal microbiota in maintaining the epithelial barrier, metabolic functions, and immune system, dysregulation of the microbiota can lead to the development of various diseases, including inflammatory and autoimmune disorders, cancers, allergies, obesity, and other metabolic conditions.[51–54] This highlights the importance of understanding the active crosstalk between nutrition and metabolic factors, microbiota, epithelial cells, immune, and other cells in the intestinal tissue.

1.2 Bile acid metabolism in humans

1.2.1 Synthesis

As mentioned above, bile acids play a crucial role in digestion by promoting the absorption of fats and fat-soluble vitamins via micelle formation in the gastrointestinal tract.[55] Bile acid metabolism is a complex interplay that involves the action of different endogenous and exogenous cell types in different organs, including the liver, the lower gastrointestinal tract, and the microbiota.[56] Bile acids are synthesized in the liver and stored in the gallbladder, which releases its content by contraction into the small intestine via the bile duct.[57] Bile acid metabolism is a complex and dynamic process that is discussed below.

The two primary bile acids, cholic acid (CA) and chenodeoxycholic acid (CDCA) are synthesized in the liver from cholesterol in two different pathways (Figure 3).[58] The classical path involves cholesterol 7 alpha-hydrolase (CYP7A1)-mediated production of 7α-hydroxycholesterol that is further processed to CA by cytochrome P450 family 8 subfamily B member 1 (CYP8B1) and CDCA by cytochrome P450 family 27 subfamily A member 1 (CYP27A1).[59] CYP27A1 mediates the alternative pathway in hepatic and non-hepatic cells.[41] The intermediate 27-hydroxycholesterol is transported through the blood to hepatocytes, where CYP7B1 catalyzes the synthesis of CDCA.[60] Some of the primary bile acids are conjugated with the amino acids glycine (G) or taurine (T) to glycocholic acid (GCA), taurocholic acid (TCA), glycochenodeoxycholic acid (GCDCA), and taurochenodeoxycholic acid (TCDCA), respectively (Figure 3).[61] Conjugation of primary bile acids increases water solubility, which is crucial for fulfilling their physiological functions in the intestine.[62] The classic pathway accounts for 90% of the total bile acid synthesis, whereas the alternative path contributes to 10% under physiological conditions.[63,64]

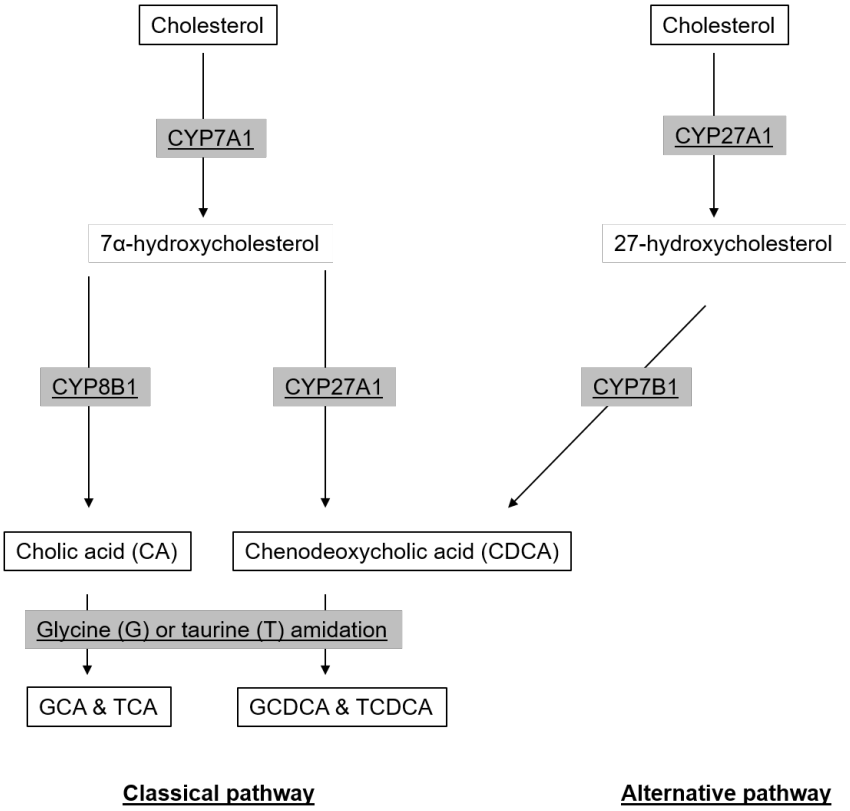

Figure 3: Primary bile acid synthesis from cholesterol in humans. In the classical pathway, cholesterol is metabolized to 7α-hydroxycholesterol, which is further processed to cholic acid by CYP8B1 or chenodeoxycholic acid by CYP27A1. In the alternative path, cholesterol is metabolized to 27-hydroxycholesterol by CYP27A1. 23-hydroxycholesterol is transported with the bloodstream to hepatocytes, where the synthesis of chenodeoxycholic acid is mediated by CYP7B1. Primary bile acids can be conjugated by amidation with glycine and taurine.[63–65]

1.2.2 Enterohepatic circulation

Enterohepatic circulation describes the recycling of bile acids released in the intestines and their transport back to the liver via the portal vein.[66] Primary conjugated bile acids are stored in the gallbladder and released into the duodenum of the small intestine upon food uptake.[57] The intestinal epithelium reabsorbs bile acids via facilitated diffusion mediated by transporters such as the solute carrier family 51 member A (SLC51A) and the solute carrier family 10 member 2 (SLC10A2).[67]

Bile acids can bind to intestinal epithelial nuclear receptors such as nuclear receptors subfamily 1 group H member 4 (NR1H4/ FXR), resulting in the secretion of fibroblast growth factor 19 (FGF19) into the portal vein.[68] FGF19, in turn, regulates bile acid synthesis in the

liver by feedback inhibition of CYP7A1.[69] Another bile acid receptor expressed in hepatocytes and intestinal epithelial cells is the vitamin D receptor (VDR), which mediates inhibition of bile acid synthesis via inhibition of CYP7A1 expression.[70] Nuclear receptor subfamily 1 group I member 2 (NR1/2) is activated by endogenous bile acids and xenobiotic substances and is involved in the detoxification pathways of its ligands.[71]

Once the bile acids are released into the intestine, they are exposed to the microbiota. The great majority of the gut microbiome are bacterial species.[72] The bacterial bile salt hydrolase (BSH) mediates the deconjugation of primary bile acids to CA and CDCA (Figure 4).[73] Unconjugated primary bile acids can be further modified by bacterial 7α-dehydroxylation and 7α epimerization to secondary bile acids such as deoxycholic acid (DCA), lithocholic acid (LCA), and other derivatives such as ursodeoxycholic acid (UDCA).[74] The main known function of primary and secondary bile acids is to emulsify dietary lipids by micelle formation.[75,76] Approximately 95% of bile acids are reabsorbed and transported back to the liver via the portal vein, where they are recycled into primary bile acids.[77] In contrast, around 5% of the bile acids released into the small intestine are not absorbed and are excreted in the stool.[77]

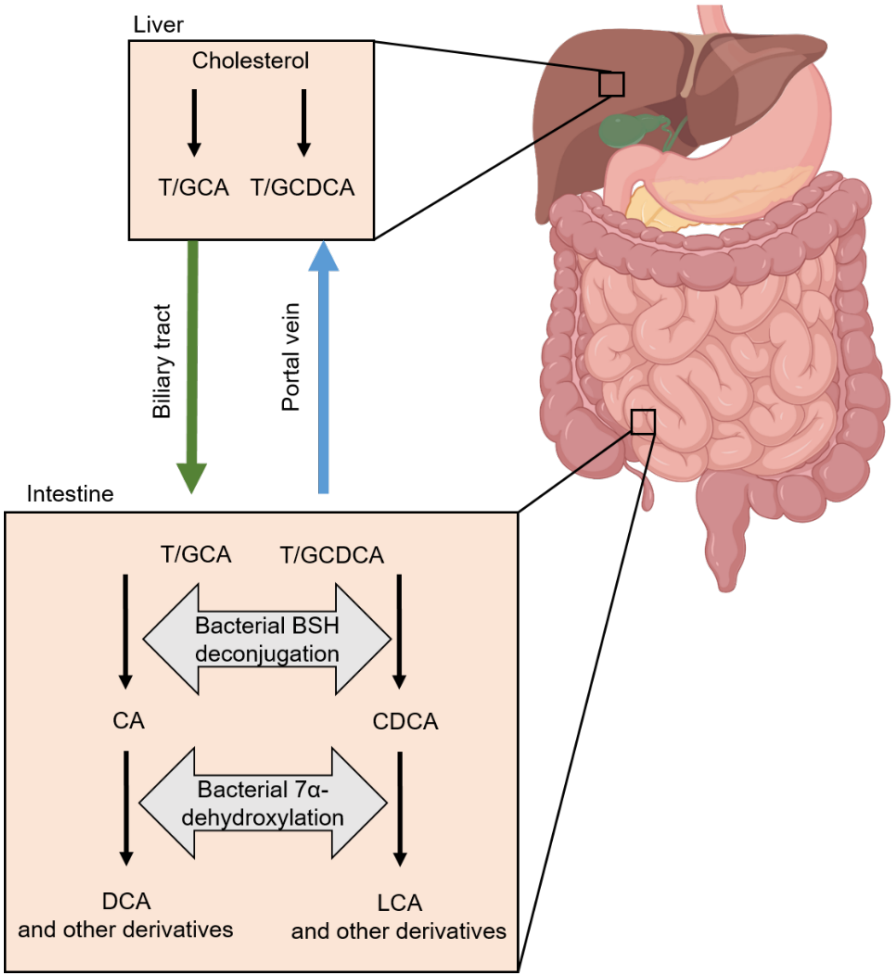

Figure 4: Enterohepatic circulation of bile acids. Bile acids are produced in the liver from cholesterol. The primary bile acids cholic acid (CA) and chenodeoxycholic acid (CDCA) are conjugated with glycine (G) or taurine (T). Conjugated bile acids are released in the small intestine with a meal uptake via the biliary tract. The bacterial bile salt hydrolases (BSH) deconjugates glycine and taurine, resulting in the presence of unconjugated primary bile acids in the intestine. The microbiome can further process unconjugated primary bile acids by 7α-dehydroxylation to deoxycholic acid (DCA), lithocholic acid (LCA), and other derivatives. Bile acids in the intestines are continuously reabsorbed and transported back to the liver via the portal vein. Adapted from Yang *et al.,* 2021.[74]

Dysregulated bile acid metabolism is reported in different diseases including diseases affecting the biliary tract, the liver, and inflammatory diseases. For example, total serum bile acids are elevated in individuals diagnosed with biliary atresia.[78] A previous large retrospective cohort study showed altered serum concentrations of bile acids in primary sclerosing cholangitis and inflammatory bowel disease, characterized by increased concentrations of the primary unconjugated CDCA.[79] It has been shown that levels of single bile acids can affect inflammatory processes by the induction of inflammatory cytokine

release.[80] For example, CDCA increased C-X-C motif chemokine ligand 8 (CXCL8) production, whereas LCA decreased its production in a human colon carcinoma cell line.[80] The same study showed a significant decrease in the transepithelial resistance, indicating increased epithelial barrier permeability.[80] However, the effects of specific bile acids are diverse and are not completely understood. Previous studies highlighted the potential of FXR activation through bile acid binding to block the NF-κB pathway and, subsequently, the downstream release of inflammatory cytokines.[81] However, activation of G protein-coupled bile acid receptor 1 (GPBAR1/ TGR5), another bile acid receptor, can entail the c-Jun N-terminal kinase (JNK) cascade, resulting in the release of proinflammatory cytokines such as IL-1β and tumor necrosis factor (TNF).[82] Furthermore, translation of findings from studies of murine bile acids is challenging due to differences in cytochrome P450 enzymes.[83] For example, in mice, the primary bile acid CDCA is hydroxylated to muricholic acid mediated by the cytochrome P450, family 2, subfamily c, polypeptide 70 (Cyp2c70), which is absent in humans.[84] Therefore, the translation of mouse data into humans requires additional models and studies with human cells. The diverse effects of bile acids on inflammatory processes highlight that more research is needed to understand the interactions of bile acids and inflammation mechanisms in the human intestines. The utilization of human intestinal organoids may have a great potential to increase this understanding.

1.3 Intestinal immune regulation

As mentioned above, the intestinal tract harbors a large microbial load including potential pathogens.[46] Therefore, the intestinal immune system is continuously challenged by microbes and needs to distinguish between beneficial commensals and harmful pathogenic microbes.[85] In addition to the cellular distinction, the intestinal immune system must be able to differentiate on a molecular level between harmless food-derived molecules and toxins produced by pathogenic microbes.[86] To ensure its effective functioning, the intestine harbors a complex system of different cell types with distinct functional traits to provide adequate host defense to pathogens and tolerance to commensals.[87] The intestinal immune system thereby plays a crucial role in maintaining intestinal functions.[87] However, when the immune responses are dysregulated, the intestinal immune system can contribute to the development of immune-mediated diseases in the intestine itself and elsewhere in the body.[88]

The intestinal immune system is present in different compartments, including the intestinal epithelium, the lamina propria, and the gut-associated lymphoid tissue (Figure 5).[89] The intestinal epithelium consists of a single-cell layer organized in crypts, harboring the intestinal stem cells, and villi, harboring differentiated epithelial cell types, as already described in chapter 1.1.[90] At the bottom of the crypts, various specialized cells create a unique microenvironment in which intestinal stem cells proliferate continuously.[91] The special niche is well protected by Paneth cells that secrete antimicrobial factors and stem cell growth factors.[92] Intraepithelial lymphocytes can reside between epithelial cells, and are involved in protective immune responses against pathogens.[93] Furthermore, a complex network of myeloid and lymphoid immune cells is involved in providing protective immunity as well as immune tolerance in the connective tissue layer called lamina propria under the epithelium.[94] Phagocytic cells, such as macrophages and dendritic cells in the epithelial area, can take up antigens and migrate to mesenteric lymph nodes, where they can prime lymphocytes to induce adaptive immune responses.[95] Subsequently, primed lymphocytes migrate to the lamina propria and execute their specific effector functions.[95] The third part of the intestinal immune system is the gut-associated lymphoid tissue that summarizes lymphatics, mesenteric lymph nodes, and Peyer's patches.[89] Peyer's patches are specialized structures involved in immune surveillance by their ability to present luminal antigens from potential microbes via microfold (M) cells to macrophages and dendritic cells.[96]

When the complex network of the intestinal immune system is malfunctioning, pathological conditions can arise.[97] In particular, in diseases such as inflammatory bowel disease, the immune system loses regulatory mechanisms and increases proinflammatory responses, leading to chronic inflammation.[98,99]

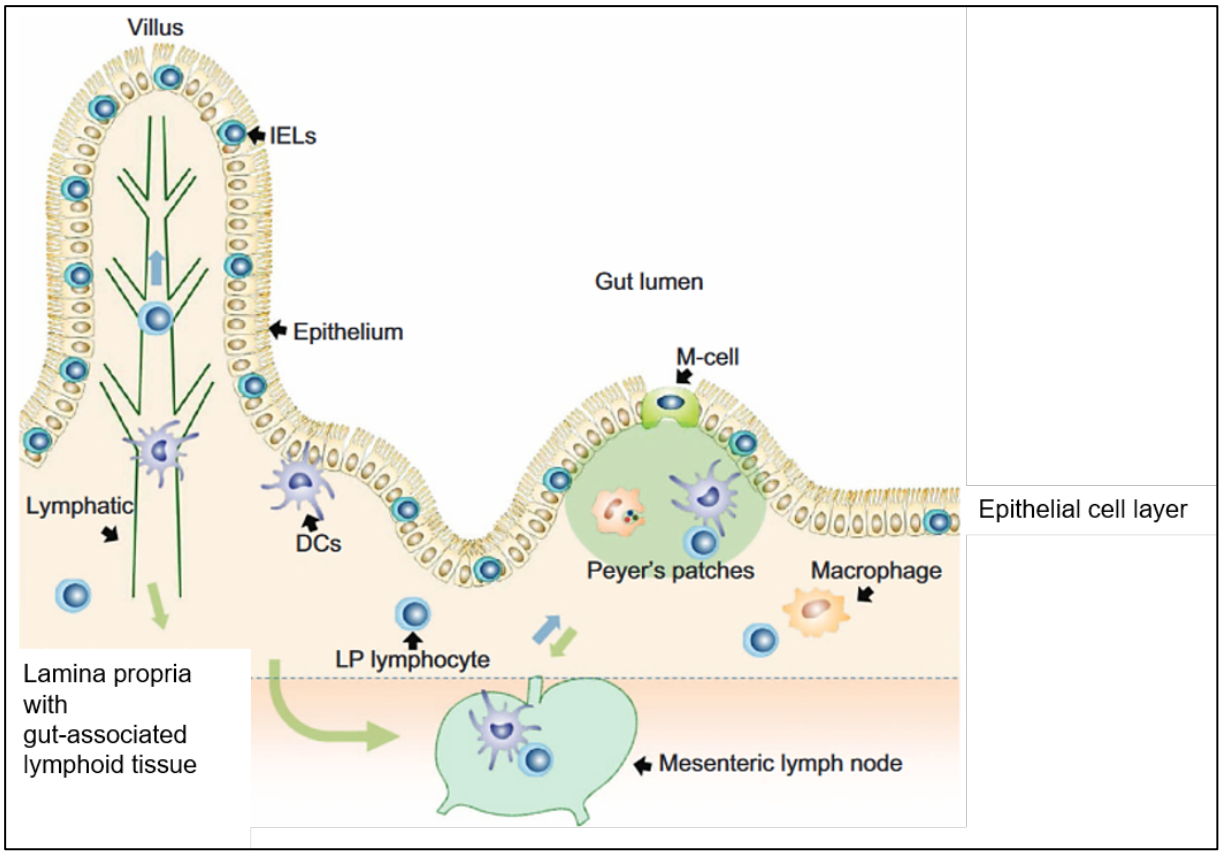

Figure 5: The intestinal immune system. The intestinal immune system comprises the epithelial cell layer and the lamina propria that contains the gut-associated lymphoid tissue**.** Professional antigen-presenting cells such as macrophages and dendritic cells (DCs) can take up antigens and migrate via the lymphatics to mesenteric lymph nodes, where lymphocyte priming can occur. Activated lymphocytes can migrate to the lamina propria and fulfill cell type-dependent effector functions. Intraepithelial lymphocytes (IELs) can reside between epithelial cells. Peyer's patches are specialized lymphoid tissues in which microfold (M-) cells can present luminal antigens directly to nearby immune cells. Adapted from Wu *et al.,* 2014.[89]

1.3.1 The role of intestinal epithelial cells in host defense and inflammation

Epithelial cells serve as the primary cellular barrier between the body and the luminal environment of the intestine, thereby playing a crucial role in the host's defense against invading microbes and pathogens.[100] The defense is mediated by several mechanisms. Goblet cells in the intestinal epithelium secrete mucins that create an intestinal mucus layer, which prevents bacteria from reaching the epithelium directly.[101] The main skeleton

component of mucus is secretory mucin 2 (MUC2).[102] Moreover, intestinal epithelial cells can secrete antimicrobial enzymes and peptides such as lysozyme and defensins that shape the commensal microbiota and maintain intestinal homeostasis.[103] Epithelial cells protect against enteric pathogens not only by such innate mechanisms but also by the activation of lamina propria immune cells.[104] Intestinal epithelial cells recognize pathogen-associated molecular patterns (PAMPs) and damage-associated molecular patterns (DAMPs), and provide corresponding signals to nearby immune cells.[100] PAMPs can activate pattern recognition receptors (PRRs), such as nucleotide oligomerization domain (NOD)-like receptors (NLRs) and toll like receptors (TLRs).[105,106] The sensing of PAMPs and signaling downstream of PRRs activates proinflammatory pathways, resulting in the secretion of cytokines, chemokines, and alarmins.[107,108] Thereby, epithelial cells change the local microenvironment, leading to the attraction and activation of various subsets of immune cells in the lamina propria.[109] Professional antigen-presenting cells such as macrophages and dendritic cells also express a wide range of TLRs, enabling them to initiate a fast immune response against invading microbes.[110] The table below shows the general cellular location of TLRs and their main respective ligands.

Table: Ligands and localization of TLRs.[111,112]

Receptor	Ligand	Location
TLR1/2	Triacylated lipoproteins	Cell surface
TLR2/6	Diacylated lipoproteins	Cell surface
TLR3	dsRNA	Endosomal
TLR4	LPS	Cell surface
TLR5	Flagellin	Cell surface
TLR7	ssRNA	Endosomal
TLR8	ssRNA	Endosomal
TLR9	CpG DNA	Endosomal
TLR10	Diacylated lipoprotein	Cell surface

TLR activation leads to the activation of adapter proteins and transcription factors such as myeloid differentiation primary response 88 (MyD88), mitogen-activated kinases (MAPK), and NF-κB, which initiates a signaling cascade that results in the expression of several chemokines and cytokines that attract and activate immune cells, thereby leading to

inflammation.[113] Chemokines can initiate different types of immune responses required for the defense against different infectious microbes by attracting different immune cells.[114] For example, CXCL8 is a main chemoattractant for neutrophils, whereas C-C motif chemokine ligand 20 (CCL20) and C-X-C motif chemokine ligand 9 (CXCL9) attract different lymphocytes.[115–118] CXCL9 promotes the recruitment of T helper 1 (Th1) cells via the respective receptor CXCR3, thereby promoting a type 1 immune response to counteract intracellular pathogens, whereas CCL20 and its respective receptor C-C motif chemokine receptor 6 (CCR6) are associated with type 3 immune responses often triggered by extracellular pathogens and fungal infections.[119]

Next to the recruitment of immune cells by chemokines, cytokines are crucial soluble factors that affect the function and survival of different cell types. For example, TNF is produced in response to TLR activation.[120] TNF binding to tumor necrosis factor receptor 1 (TNFR1) leads to apoptotic cell death in target cells.[121] In addition, proinflammatory cytokines stimulate epithelial cells to secrete antimicrobial products, and different cytokines have individual effects on mucus production.[122,123] Another cytokine that induces inflammatory responses to enhance host defense against pathogens in mucosal tissues is interleukin 17 (IL-17).[124] IL-17 is released by T cells in response to T cell receptor activation and by other cell types, such as innate lymphoid cells (ILCs), in response to inflammatory cytokines such as interleukin 6 (IL-6) and interleukin 23 (IL-23).[125,126] In target cells such as epithelial cells, IL-17 stimulates the production of antimicrobial peptides, chemokines, and cytokines, thereby promoting host defense.[127]

Damaged epithelial cells also release a class of soluble factors called alarmins that are involved in immune cell activation and tissue regeneration.[128] As an example, the alarmin interleukin 33 (IL-33) induces the secretion of interleukin 4 (IL-4) and interleukin 13 (IL-13) in target cells, thereby promoting type 2 immune responses that are proposed to be involved in the clearance of parasitic infections.[129,130]

To counteract the excessive release of pro-apoptotic and proinflammatory mediators that can lead to immune-mediated tissue damage, regulatory cell types with crucial functions are present in the intestinal mucosa. For example, CD4-positive T cell-derived interleukin 22 (IL-22) leads to epithelial regeneration by promoting the proliferation of intestinal stem cells.[131] Moreover, regulatory T cells control the proinflammatory actions of different immune cells by their secretion of antiinflammatory cytokines such as interleukin 10 (IL-10). IL-10 inhibits, for example, the expansion and the effector functions of other T cells and natural killer (NK) cells.[132]

Taken together, epithelial cells are crucial in defending against intestinal microbes via innate immune responses and the release of cytokines and chemokines, which recruit and activate

immune cells. This regulation balances protective immunity and immunological tolerance, thereby maintaining tissue homeostasis.[133]

1.4 Inflammatory bowel disease

1.4.1 Definition, symptoms, treatments

When the regulation of the intestinal immune system is disturbed, chronic inflammatory diseases such as inflammatory bowel diseases (IBD), including CD and ulcerative colitis (UC), can arise.[134] UC is characterized by continuous inflammation in the colon and rectum, whereas in CD, inflammation occurs in patches that can appear from the mouth to the rectum, including the large intestine and the small intestinal duodenum, jejunum, and ileum.[135] Persistent diarrhea, abdominal pain, rectal bleeding, weight loss, and fatigue are common symptoms shared by both conditions.[136] IBD is diagnosed by endoscopy, colonoscopy, and imaging techniques such as radiography, magnetic resonance imaging (MRI), or computed tomography scans.[136] In addition, analyses of inflammatory factors in stool and blood samples provide information about the inflammation status.[136,137]

IBD is treated based on the individual condition of the affected person and depends on the location of the inflammation in the gastrointestinal tract.[138] Glucocorticoids are frequently administered in UC and ileocecal CD.[138] However, repetitive administration of glucocorticoids is not recommended due to the systemic immunosuppressive effects and the increased risk of infections.[138] In addition, antibiotics are used to treat infectious complications and fistulas in IBD.[139] Further treatment alternatives are depicted by biologicals including for example anti-TNF monoclonal antibody therapies.[138] In addition, anti-TNF monoclonal antibody therapies can be combined with other biologicals targeting for example interleukin-12 or interleukin-23 in individuals with a high disease burden.[140] Surgical removal of affected intestinal sections is another approach that is performed in both, CD and UC.[141] Despite several treatment options, the relapse rate of IBD is very high with 50% one year after treatment stops and 90% relapse 10 years after the treatment stop, highlighting the urgency of further understanding the pathogenesis of IBD.[142]

Around 6.8 million individuals are diagnosed with IBD worldwide and the age-standardized prevalence rate increased from 79.5 in 1990 to 84.3 in 100,000 people in 2017.[143] An Italian population study showed an increase in IBD prevalence from 200 per 100,000 individuals in 2016 to 321.2 per 100,00 individuals in 2021. Similarly, the incidence increased from 6.7 to 18.0 per 100,000 individuals per year in the same period.[144] The highest age-standardized prevalence rates are in high-income North America and regions with a high socio-demographic index.[143] In Germany, the incidence of CD is 6.6 new cases per 100,000 people per year.[145] Approximately 0.7% of the population in Germany is diagnosed with CD.[146] For UC, the incidence is 4 new cases per 100,000 people per year, and the prevalence is 250 cases per 100,000 people.[145]

Dietary patterns are associated with increased incidences and progression of IBD.[147] For example, a high intake of fruits and vegetables is strongly associated with reduced incidences of UC and CD.[148] A diet consisting of high amounts of fibers is also associated with reduced progression and increased quality of life in CD.[149] In contrast, a diet containing high amounts of animal fats and dairy products with a low consumption of fruits and vegetables is associated with a high risk of developing both CD and UC.[150]

1.4.2 Pathogenesis

Despite extensive studies into IBD, the exact underlying mechanisms remain not fully understood. This is likely due to the complexity of the disease resulting from the dysregulated interplay between various cells in the intestines. Many studies investigated the influence of genetic mutations or polymorphisms in IBD development. In genome-wide association studies, it has been shown that specific genetic variants are associated with IBD.[151,152] The processes associated with genetic mutations or polymorphisms in IBD are diverse and involve a wide range of pathways and cell functions, such as the epithelial-immune cell interactions mediated by integrins, pathogen recognition as shown for nucleotide-binding oligomerization domain containing 2 (NOD2) variants, and cytokines such as *TNF* and *IL23R*.[151,152]

Additionally, previous studies showed that environmental factors such as smoking, antibiotic treatment, and psychological stress may further contribute to IBD.[153] Thus, a combination of genetic and environmental factors most likely leads to an impaired barrier function in the intestinal epithelium and subsequent inflammation (Figure 6).[154] Microbes and microbial products can then more easily translocate from the intestinal lumen to intestinal crypts and into the lamina propria, leading to innate inflammatory responses from various cell types followed by a dysregulation of adaptive responses.[155] In the chronic phase, effector cells such as macrophages and T helper 17 cell (Th17) cells continue to produce proinflammatory mediators while regulatory mechanisms mediated by regulatory T cells fail.[156,157] As a consequence, complications such as fibrosis, stenosis, abscesses, fistula, cancer, and other extra-intestinal manifestations can develop.[158] Further factors involved in IBD pathogenesis are introduced in more detail in the following subchapters.

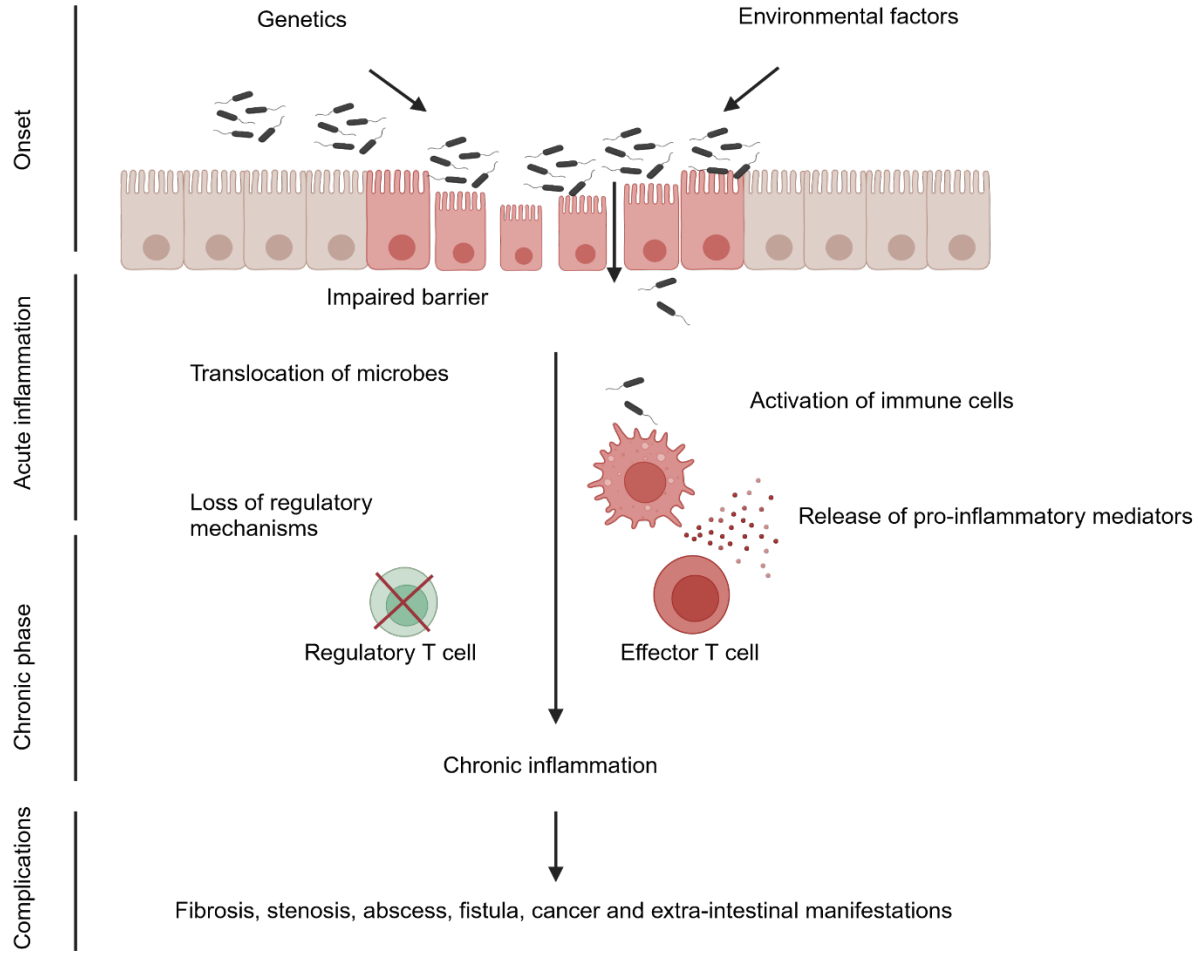

Figure 6: IBD pathogenesis. IBD results from a combination of multiple factors. In the initial pre-disease phase, genetic and environmental factors lead to impaired barrier functions of the epithelium. The translocation of microbes and their products results in an acute response with high immune cell activation that extends to a chronic phase with loss of regulatory mechanisms. Long-term chronic inflammation can result in further complications such as fibrosis, stenosis, abscess, fistula, cancer, and extra-intestinal manifestations. Adapted from Neurath, 2014.[158] Created with bioRender.com.

1.4.2.1 The intestinal epithelial barrier in IBD

The integrity of the epithelial barrier is crucial to prevent infections and chronic inflammation in the gut. Defective barrier functions are reported for both CD and UC.[159–161] The permeability of the epithelial layer is further increased by proinflammatory cytokines that are secreted by immune cells in inflamed IBD tissues, as shown for TNF and interferon-gamma (IFNγ) produced by T cells, NK cells, or ILCs.[162,163] TNF and IFNγ disrupt for example tight junctions as observed in epithelial cell lines and murine intestines.[162] Additionally, TNF and

IFNs induce apoptosis in epithelial cells.[164]

Moreover, it has been shown that mutations and polymorphisms in genes involved in epithelial barrier maintenance are associated with IBD.[165] For example, genetic variants that lead to mucin 1 (MUC1) upregulation and consequently to an altered mucus composition are associated with Crohn's disease and ulcerative colitis.[165]

Furthermore, a defective barrier is associated with epithelial stem cell dysfunctions.[166] For example, inflammation in CD correlates with decreased LGR5 expression, indicating that a loss of stem cell phenotype contributes to reduced epithelial layer regeneration and a decreased barrier function of the epithelium.[166] The disease progression is further characterized by immune-mediated epithelial damage that can, for example, result from T cells or NK cells in ulcerative colitis.[167]

1.4.2.2 Intracellular calcium signaling in IBD

Calcium signaling plays a central role in signaling transduction pathways, metabolism, gene expression, cell survival, and cell death.[168] The cytosolic calcium concentration is low at baseline but increases upon stimuli such as the binding of extracellular signaling molecules or the activation of intracellular messengers.[168] The cytosolic calcium increase depends on the influx from the extracellular milieu or the intracellular endoplasmic reticulum (ER).[168,169]

The activation of cell surface receptors, such as G protein coupled receptors (GPCRs) via the binding of their respective ligands, can activate phospholipase C, which mediates the hydrolysis of phosphatidylinositol 4,5-bisphosphate (PIP_2) to inositol trisphosphate (IP_3) that can be recognized by its respective receptor IP_3R on the ER surface, resulting in calcium ion (Ca^{2+}) release.[168] The close contact with the ER and its calcium release upon certain stimuli can lead to altered membrane potentials in mitochondria, resulting in the generation of reactive oxygen species (ROS) as a by-product of the respiratory chain.[169–171]

Previous studies showed that changes in cytosolic calcium signaling are involved in the initiation of inflammation.[172] Recently, it has been shown that an increased calcium influx in intestinal epithelial cells leads to mitochondrial dysfunction, accumulated ROS, and NLR family pyrin domain containing 3 (NLRP3) inflammasome-mediated cytokine release.[173] NLRP3 activation can be induced by mitochondrial DNA (mtDNA) that derives from damaged mitochondria after a Ca^{2+} overload.[174] In addition, it has been shown that the treatment of cells with calcium chelates inhibits the secretion of NLRP3-mediated interleukin 1 beta (IL-1β).[174–176] An intracellular calcium release can be triggered by extracellular molecules including adenosine triphosphate (ATP), which leads to the activation of purinergic receptors

and cell death in human cells.[177]

Calcium release-activated channels (CRACs) are pore-forming protein complexes that enable calcium influx.[178] Recent studies have shown that pharmacological inhibition of CRAC reduces the production of proinflammatory cytokines and activation markers in lymphocytes, including T cells and NK cells, thereby alleviating intestinal inflammation in a mouse model of colitis.[179]

Intracellular calcium can activate calcium-dependent kinases involved in MAPK pathways and calcium-dependent transcription factors such as NF-κB, resulting in the transcription of inflammatory cytokines.[180] Additionally, metabolic pathways such as glycolysis and mitochondrial respiration are regulated by store-operated calcium entry (SOCE), which is therefore involved in proliferation and effector functions in T cells.[181] Loss of function mutations in CRAC genes lead to combined immunodeficiency, highlighting its impact on immune responses and the induction of inflammation.[182]

Due to the big impact of calcium signaling on the generation of an inflammatory immune response mediated by cytokines, calcium channel blockers are proposed as potential therapeutic approaches in IBD.[183,184]

1.4.2.3 Toll-like receptor 5 (TLR5) in IBD

When the epithelial barrier in the intestine is damaged as in the case of IBD, TLRs are activated by microbes and microbial-derived intestinal contents and induce inflammatory signals to clear the invasion.[185] In the small intestinal epithelium, TLR expression depends on the cell type and the localization within the intestinal crypt-villus structure.[106] TLR5, as a receptor for bacterial flagellin, is expressed on Paneth cells and intestinal stem cells in intestinal crypts on both the basolateral and apical sides.[106,186] Previous studies showed that specific genetic variants of TLR5 are associated with IBD. For example, a non-synonymous nucleotide polymorphism of TLR5 (rs5744174) is associated with CD in children.[187] In another study, a coding variant (L616F) in the TLR5 gene was associated with CD and an increased release of CCL20.[188] Another study highlighting the importance of TLR5 in the pathophysiology of IBD showed a negative association with a dominant-negative polymorphism in the TLR5 gene.[189] Furthermore, polymorphisms in the TLR5 gene were associated with ulcerative colitis in an Indian cohort.[190] Increased expression of TLR5 correlates with inflammatory activity in UC.[191] Moreover, increased flagellin-mediated TLR5 signaling in experimental ileitis in mice leads to epithelial barrier dysfunction.[192] However, other studies have also reported increased expression of TLR5 in inflamed ileal samples of

individuals diagnosed with CD.[193] In sum, epithelial TLR5 signaling seems to play an important role in IBD.

1.4.2.4 Dysbalanced immune cell networks in IBD

As mentioned above, IBD results from a combination of environmental and genetic factors, leading to inflammatory processes in the intestines.[158] Critical mediators in the pathogenesis are immune cells that reside close to the epithelium and in the lamina propria layer and their secreted cytokines.[194]

In the lamina propria of individuals diagnosed with IBD, altered frequencies of specific immune cells have been reported.[195] Single-cell analysis of CD-affected intestinal tissues revealed that increased numbers of activated Th17 and decreased numbers of T regulatory cells are present in inflamed lesions.[195] Moreover, Th17-derived IL-17 is increased in inflamed lesions of both CD and UC-affected individuals.[196] Th1 responses have also been shown to be involved in the development of IBD.[197] CD4-positive T cells can also secrete IL-22, which induces proliferation of intestinal stem cells, thereby inducing epithelial regeneration. However, IL-22 has also been reported to be increased in IBD-inflamed mucosal tissue and may also have proinflammatory effects.[198]

Moreover, intestinal macrophages are present in the epithelial layer and the lamina propria.[199] Their physiological functions include the phagocytosis and degradation of microorganisms and dead or damaged tissue cells.[200] Additionally, they release cytokines and chemokines with multiple functions. Macrophages are potent producers of IL-10, which promotes the survival and functions of regulatory T cells.[201] Interestingly, loss of function mutations in the IL-10 gene are associated with an early disease onset in infants, indicating a protective role of IL-10 in IBD.[158] Importantly, intestinal macrophages in inflamed areas of IBD-affected intestines depict an inflammatory phenotype characterized by increased TNF expression.[202] As professional antigen-presenting cells, macrophages are also able to induce adaptive immune responses by activating T cells upon antigen presentation.[203] Dendritic cells are specialized in capturing microbes and microbial products in the lamina propria and the epithelium, and they can present microbial peptides to activate T cells.[204] In IBD-affected intestines, DCs produce more inflammatory cytokines and chemokines, including TNF and CXCL8.[205]

In a meta-analysis, Liu et al. showed associations between IBD and polymorphisms in cytokine genes *IL-1B* encoding for IL-1β, *IL-6*, and *CXCL8*.[206] Inflamed tissues in individuals with CD or UC contain a wide range of proinflammatory cytokines from various cell types.[158] Among them is CXCL8, which correlates with histological grades of active inflammation in

IBD.[207] CCL20, which recruits T and dendritic cells, is upregulated in CD and UC but not in non-IBD colitis.[208] TNF is highly elevated in the inflamed mucosa and the serum of IBD-affected individuals, and anti-TNF therapy with infliximab is frequently used to treat IBD-derived symptoms.[209] The altered abundancies of immune cells, cytokines, and chemokines in inflamed lesions of individuals diagnosed with IBD highlight the complexity of immune-mediated inflammation in IBD and the need to understand the underlying mechanisms.

1.4.2.5 Bile acid metabolism in IBD

In a metabolomics study analyzing stool samples from 56 non-IBD controls, 88 individuals with Crohn's disease (CD), and 76 with ulcerative colitis (UC), an untargeted approach revealed elevated levels of primary bile acids, particularly chenodeoxycholic acid (CDCA), in those diagnosed with IBD.[210] The study furthermore showed decreased levels of secondary bile acids in IBD-affected individuals.[210] More recently, in a longitudinal study in which 1,785 stool samples from 132 study participants with CD, UC, or without IBD were analyzed, it was shown that increased levels of the primary bile acids CA and CDCA were associated with IBD and a dysbiotic microbiome.[211] Other studies have shown altered bile acid metabolism in children with IBD.[212,213] For example, it has been demonstrated in untargeted metabolomic studies that primary conjugated bile acids are increased in stool samples of children and adults with CD or UC.[212,213]

The root cause for altered bile acid metabolism in IBD is not fully understood since the bile acid pool depends on various factors, including the enterohepatic circulation feedback loop and the microbiome-mediated alterations of bile acids. Previous studies showed that interruption of the negative feedback signaling causes an overproduction of primary bile acids in the liver.[214] For example, decreased blood levels of FGF19, the negative feedback signal for reduced bile acid production in the liver, are linked to increased production of bile acids and the development of diarrhea.[214] Interestingly, it has been shown that administration of FGF19 in a murine model of intestinal inflammation leads to changes in the bile acid pool accompanied by reduced inflammation.[215] FGF19 levels are significantly lower in individuals suffering from IBD, indicating altered signaling and potentially an increased production of primary bile acids.[216]

Furthermore, multiple studies have shown changes in the intestinal microbiota in IBD. For example, a less diverse microbiota with fewer bacterial species of the phylum Firmicutes and Bacteroidetes and more Proteobacteria is observed in stool samples of individuals with IBD.[217] The microbiota in healthy individuals contains more species of the phylum

Bacteroidetes.[217] One possibility for increased levels of primary unconjugated bile acids is an increased activity of bacterial bile salt hydrolases (BSH) that dissociates the amino acid conjugate from primary bile acids, resulting in increased levels of primary unconjugated bile acids.[73] A previous study showed BSH sequences in 591 intestinal bacterial strains within 117 genera. This study also compared different BSH phylotypes and revealed the highest activity of BSH-T3, which is only found in Lactobacillus.[218] However, Lactobacillus has been successfully used as a probiotic in IBD, indicating a protective role of BSH activity in IBD.[219]

Further modifications of primary unconjugated bile acids lead to the occurrence of secondary bile acids. 7α dihydroxylation and 7α epimerization of CA and CDCA results in DCA, LCA, and ursodeoxycholic acid (UDCA).[74] The lack of enzymes mediating these reactions is an additional potential mechanism for increased levels of CDCA. 7α dihydroxylation is a multi-step process based on bacterial bile acid-induced (*bai*) genes.[220] Interestingly, a previous study showed that the *bai* gene cluster is only present in Firmicutes species, which are less abundant in IBD-affected individuals.[217,221]

Bile acids can have direct effects on immune cells with potential consequences for IBD pathogenesis.[222] LCA decreases the LPS-induced release of proinflammatory cytokines, such as TNF, in macrophages depending on the expression of GPBAR1.[223] Bile acids can also affect CD4-positive T cells.[224] In mice, the bile acid pool composition depends on dietary and microbial factors and can induce the generation of a distinct regulatory T cell phenotype that ameliorates DSS-induced colitis.[224] In addition, it has been shown that LCA derivatives can upregulate forkhead box P3 (FOXP3) and inhibit retinoid orphan receptor gamma t (RORγt), resulting in higher frequencies of regulatory T cells and, therefore, play an essential role in immune tolerance in the gut.[225,226] LCA also decreased TNF and IFNγ release of Th1 cells through a VDR-dependent mechanism. Interestingly, LCA and bacterial genera that carry necessary enzymes for LCA synthesis are significantly reduced in the intestines of individuals diagnosed with IBD.[213] Moreover, LCA levels are inversely correlated with IL-17 expression of T cells.[213]

Bile acids can also affect epithelial cell physiology.[227] DCA and CDCA induce apoptosis in colorectal cancer cell lines.[227] Similar to the antiinflammatory effects of secondary bile acids in macrophages and T cells, DCA and LCA, but not primary bile acids, inhibit CXCL8 release of epithelial cell lines.[228] In addition, LCA and DCA promote epithelial regeneration in mouse intestinal stem cells by acting on GPBAR1/ TGR5.[229] Another study identified genetic variations in bile acid metabolism-related genes, such as *NR1H4*, which encodes the nuclear bile acid receptor FXR, in individuals with IBD.[230] Importantly, the total amount of bile acids released from the gallbladder depends on the uptake of dietary fat, which increased over the last decades in various populations.[231,232] This trend is also accompanied by increased incidences of IBD.[231] Taken together, bile acid production, modification, and signaling can

affect IBD.[233] However, the exact mechanisms of how bile acids, and especially CDCA, affect the intestinal epithelial cell layer concerning barrier functions and inflammation remain incompletely understood.

1.5 Human intestinal organoids

Until recently, studies of human tissues mostly relied on analyses of tissue-derived tumor cell lines or short-term cultivation of tissue explants. In 2009, Sato *et al.* described the generation of intestinal organoids derived from adult stem cells from intestinal tissue.[234] Organoids are three-dimensional polarized organ-like structures.[234] Up to today, they have been established for multiple organs, including the intestines and the liver.[235,236] The cellular composition of intestinal organoids resembles the *in vivo* intestinal epithelium (Figure 7), which increases the potential for clinically relevant findings compared to animal models and immortalized cell lines.[237,238] Additionally, the usage of organoids helps to reduce and replace animal studies.[239]

Two main approaches are used to generate intestinal organoids. The first one utilizes induced pluripotent stem cells and a respective differentiation protocol.[234] The second is based on the isolation and culture of adult intestinal stem cells from intestinal tissue samples.[240]

As discussed above, the development of the intestinal epithelium strongly depends on WNT signaling to maintain the stem cell phenotype, which is the basis for the continuous proliferation of intestinal stem cells in the bottom of intestinal crypts.[7] The isolation of adult stem cells from tissue and the addition of WNT provide the basis for generating intestinal organoids.[7] In addition, BMP inhibitors maintain a stem cell phenotype over several weeks *in vitro*.[241]

Tissue-specific processes such as organ development and specific diseases can be analyzed and studied with organoids by using a diverse range of established techniques, such as RNA sequencing, flow cytometry, imaging, and genome editing, making them a powerful tool for basic research.[242] The usage of adult stem cell-derived organoids from people with different diseases enables the analysis of organ-specific biological samples that may improve the translation of findings into therapies.[242]

So far, intestinal organoids have been used to study various diseases, including IBD. Organoids provide a promising tool for future IBD studies as they can be adapted to specific research questions. For example, the co-culture of organoids with lamina propria immune cells can be used to study the disturbed epithelium-immune cell communications in IBD.[243] Moreover, co-culture systems with microbes will provide more insights into the complex interactions between the intestinal microbiota and the epithelium.[244] Lastly, incorporating external dietary factors and metabolites into organoid cultures will yield further insights into how specific molecules can alter intestinal physiology at the epithelial barrier.[245]

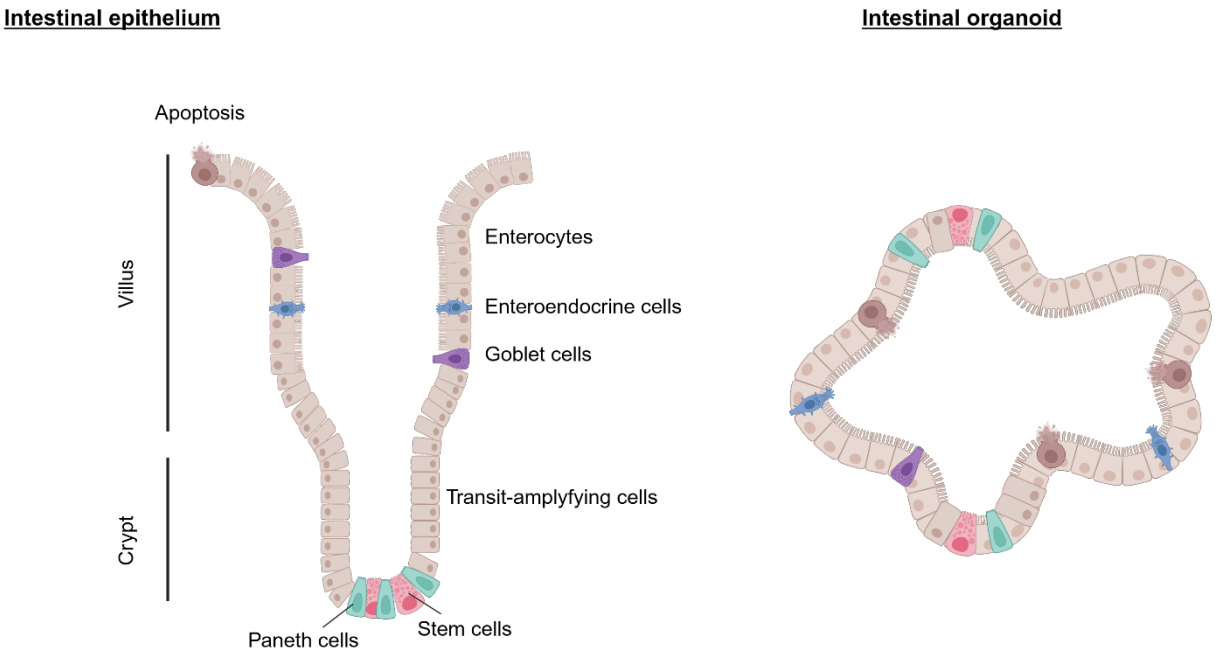

Figure 7: The intestinal epithelium and intestinal organoids. The intestinal epithelium contains crypt and villi structures. Stem cells and Paneth cells are located at the bottom of the crypts. The upper part of the crypt contains transit-amplifying cells. The villus has differentiated cell types, including Goblet, enterocytes, and enteroendocrine cells. At the top of the villus, epithelial cells undergo apoptosis and are shed into the intestinal lumen. Intestinal organoids show crypt and villus-like structures and contain the same cell types *in vivo*.[23,246] Created with bioRender.com.

1.6 Aims of the study

Several studies have linked the primary unconjugated bile acid CDCA to IBD. However, the consequences of increased CDCA concentrations in the small intestine in IBD are poorly understood, as previous studies are mainly based on mouse models and immortalized cell lines. In this study, we used human intestinal organoids derived from adult stem cells to better understand the impact of CDCA on epithelial regeneration and the induction of inflammation, in the context of IBD pathogenesis.

In this project, adult stem cell-derived organoids from multiple intestinal samples depicting multiple biological replicates were generated. These cultures were used to study the impact of CDCA on the regeneration of the intestinal epithelium in organoids. Furthermore, the ability of CDCA to induce intracellular signaling pathways in epithelial cells was assessed by visualizing intracellular calcium signals upon exposure to CDCA in organoids. Next, the influence of CDCA on flagellin-induced cytokine and chemokine expression by the intestinal epithelium was evaluated in organoids on mRNA and protein level. Moreover, differentially expressed genes in epithelial cells were determined by untargeted bulk RNA sequencing of CDCA-stimulated organoids, and the impact of CDCA on epithelial TLR5 signaling in organoids was assessed by flow cytometry and RT qPCR. Based on these experimental findings, primary epithelial cells derived from non-inflammatory and CD-affected intestinal tissues were analyzed and their TLR5 expression was compared *ex vivo*.

The obtained data are prepared for publication in a peer-reviewed journal.

2. Materials and methods

2.1 Materials

2.1.1 Plastic materials

Plastic material	Provided by
50 mL and 15 mL tubes	Greiner Bio-One
Cell strainer (70 µm)	Greiner Bio-One
CryoPure tubes, 2 mL	Sarstedt
Culture plates	Greiner Bio-One
Corning™ 96-Well Cluster Tube System	Thermo Fisher Scientific
Pipette tips	Sarstedt, Thermo Fisher Scientific
Serological pipettes	Sarstedt
Syringe	B Braun
Whatman filter (0.2 µm)	Whatman plc.
Micro tube 1.5 mL DNA LowBind	Sarstedt
LightCycler® 480 Multiwell Plate 96, clear	Roche
Sealing Tape, optically clear	Sarstedt

2.1.2 Reagents

Name	Provided by
1,4-Dithiothreitol (DTT)	Roth
2-Propanol	Sigma-Aldrich
A83-01	Bio-Techne
Advanced DMEM/F-12	Thermo Fisher Scientific
AlbuMAX™ II Lipid-Rich Bovine Serum Albumin (BSA)	Thermo Fisher Scientific
Ambion™ DNase I (RNase-free)	Thermo Fisher Scientific
Animal-Free Recombinant Human EGF	PeproTech
Aqua ad injectabilia Braun	B. Braun
autoMACS® Running Buffer	Miltenyi Biotec
B-27™ Supplement	Thermo Fisher Scientific
Cal-520(TM), AM	AAT Bioquest
Chenodeoxycholic acid	Sigma-Aldrich
Choloroform molecular biology grade	Th. Geyer
Corning™ Matrigel™	Thermo Fisher Scientific
Dimethylsulfoxide (DMSO)	Sigma-Aldrich
DNAse I	Stemcell
Dulbecco's Phosphate Buffered Saline (PBS)	Sigma-Aldrich
Ethanol	Th. Geyer
Ethanol vergällt	Th. Geyer
Ethylenediaminetetraacetic acid (EDTA)	Sigma-Aldrich
Fetal bovine serum (FBS)	Capricorn Scientific
FLA-ST (flagellin)	Invivogen
Fructose	Sigma-Aldrich

Gastrin	Sigma-Aldrich
Gibco™ HEPES (1 M)	Thermo Fisher Scientific
Gibco™ TrypLE™ Express Enzyme (1x), phenol red	Thermo Fisher Scientific
Gibco™ Zeocin™ Selection Reagent	Thermo Fisher Scientific
GlutaMAX™ Supplement	Thermo Fisher Scientific
Glycerol	Sigma-Aldrich
GlycoBlue™ Coprecipitant	Thermo Fisher Scientific
Hank's Balanced Salt Solution	Sigma-Aldrich
Gibco™ HEPES (1 M)	Thermo Fisher Scientific
Hoechst 33342, Trihydrochloride, Trihydrate	Thermo Fisher Scientific
Iscove's Modified Dulbecco's Medium (IMDM)	Thermo Fisher Scientific
Lymphocytes Separation Media	Capricorn
N2 Supplement	Capricorn
N-Acetylcysteine	Sigma-Aldrich
Nicotinamide	Sigma-Aldrich
Noggin conditioned medium (NCM)	Home-made, produced by HEK293-Noggin-Fc cells
Paraformaldehyde	Sigma-Aldrich
Penicillin/ Streptomycin (P/S)	Sigma-Aldrich
Percoll®	Sigma-Aldrich
Recovery™ Cell Culture Freezing Medium	Thermo Fisher Scientific
RNaseOUT™ Recombinant Ribonuclease Inhibitor	Thermo Fisher Scientific
RPMI-1640	Thermo Fisher Scientific
R-spondin-1 conditioned medium (RCM)	Home-made, produced by HEK293-R-spondin-1-Fc cells
SB 202190	Sigma-Aldrich

SYBR® Green	highQU GmbH
Triton™ X-100 solution	Sigma-Aldrich
TRIzol™ Reagenz	Thermo Fisher Scientific
Trypan Blue solution	Sigma-Aldrich
TrypLE™ Express	Gibco
TWEEN® 20	Th. Geyer
WNT3a conditioned medium (WCM)	Home-made, produced by WNT3a-producing L cells
Y-27632	Stemcell

2.1.3 Buffers, solutions, and medium

Name	Composition
Advanced DMEM/ F-12 + + + (AD +++)	Advanced DMEM/ F-12 98% (v/v), P/S 1% (v/v), HEPES 10 mM, GlutaMAX™ Supplement 1% (v/v)
BD intracellular staining mix	Water 90%, Permeabilization Buffer 10%
EDTA/ DTT buffer	IMDM 94% (v/v), FCD 5% (v/v), P/S 1% (v/v), EDTA 5 mM, DTT 2 mM
Freezing medium	FCS 90% (v/v), DMSO 10%
Fructose-glycerol clearing solution	Glycerol 60% (v/v), Fructose 2.5 M, Water 40% (v/v)
Intestinal organoid expansion medium (EM)	AD +++ (17.5% (v/v)), RCM (20% (v/v)), NCM (10% (v/v)), B-27 (1x), N-2 (1x), EGF (50 ng/mL), N-acetylcysteine (1.25 mM),

	Gastrin (10 nM), Nicotinamide (10 mM), A83 (500 nM), SB202190 (10 µM), WCM (50% (v/v)), Y-27632 (10 µM)
Organoid washing buffer (OWB)	Triton X-100 0.1% (v/v), BSA (2 g/l), PBS 99.9% (v/v)
Overnight medium for short-term storage of tissue samples	IMDM 79% (v/v), FBS 20% (v/v), P/S 1% (v/v)
PBS – Tween (PBT)	Tween 20 0.1% (v/v), PBS 99.9% (v/v)
PBS-BSA	BSA 10 g/l PBS
Washing medium for tissue samples	IMDM 97% (v/v), FCS 2% (v/v), P/S 1% (v/v)
Calcium measurement buffer	Ca^{2+} 1 mM 140 nM NaCl HEPES 20 mM 1 mM NaH_2PO_4 Glucose 5.5 mM pH 7.4

2.1.4 Equipment

Device	Provided by
Biosafe SC-smart	Cryotherm
Centrifuge MEGA STAR 1.6R	VWR
Cytek® Aurora System	Cytek
HB-1000 Hybridizer	UVP
HERAcell VIOS 160i Incubator	Thermo Fisher Scientific
Lightcycler 480 II	Roche
Microcentrifuge Micro Star 17	VWR
Microscope LEICA DM IL	LEICA
Neubauer chamber	Paul Marienfeld GmbH & Co. KG
Nikon TI2 (Nikon) based spinning-disk system	Nikon
Pipettes	Eppendorf AG, Integra Biosciences
Shaker GFL-3005	GFL
Spectrophotometer NanoDrop 1000	PeqLab
StrataCooler Cryo Presevation Module	Agilent
TC20™ Automated Cell Counter	BioRad
Tecan Safire	Tecan
Thermo Scientific HeraFreeze	Thermo Fisher Scientific
Thermo Scientific™ Herasafe™ KS, Class II Biological Safety Cabinet	Thermo Fisher Scientific
Thermomixer	Eppendorf AG, Integra Biosciences

2.1.5 Antibodies and primer

Extracellular staining antibodies

Target	Fluorochrome	Provided by
CD16	BV785	BioLegend
CD45	BV605	BioLegend
EpCAM	BV605	BioLegend
EpCAM	BV650	BioLegend
EpCAM	BV421	BioLegend
TLR4	BV421	BioLegend
TLR5	APC	BioLegend

Intracellular staining antibodies

Target	Fluorochome	Provided by
Ezrin	AF700	R&D Systems
LGR5	PE	R&D Systems
MUC2	FITC	Santa Cruz

Primer

Gene name	Sequence/ Provider
B2M	Fwd 5' – GCGGGCATTCCTGAAGCTGACAGCA – 3'
	Rev 5' – TACATCAAACATGGAGACAGCACTC – 3'
CCL20	Biorad
CXCL8/ IL-8	Biorad
GAPDH	Fwd 5' – CGGAGTCAACGGATTTGG – 3'
	Rev 5' – TGATGACAAGCTTCCCGTTC – 3'
IL-1β	Biorad
TLR5	Fwd 5' – TTGCTCAAACACCTGGACAC – 3'
	Rev 5' – CTGCTCACAAGACAAACGAT – 3'
TNF	Fwd 5' – CTCTTCTGCCTGCTGCACTTTG – 3'

Rev 5' – ATGGGCTACAGGCTTGTCACTC – 3'

2.1.6 Kits

Name	Provided by
Ambion DNase I (RNase-free)	Invitrogen
BD Cytofix/Cytoperm™	BD Biosciences
LIVE/DEAD Fixable Near-IR Dead Cell Stain Kit	Thermo Fisher Scientific
Human Luminex® Discovery Assay	R&D Systems
PCR Add-on Kit for Illumina	Lexogen
qScriber™ cDNA Synthesis Kit	highQU
QuantSeq 3' mRNA-Seq Library Prep Kit for Illumina (FWD)	Lexogen
RNeasy Plus Micro Kit (50)	Qiagen

2.1.7 Software & websites

Name	Provided by
bioRender	bioRender.com
FACSDiva	BD Biosciences
FlowJo 10	Tree Star Inc.
Graphpad Prism 10	Graphpad Software Inc.
Kangooroo	Lexogen
LightCycler® 480 SW 1.5	Roche
Magellan6	Tecan
Mendeley Version 1.19.8	Mendeley
Microsoft Office 2016	Microsoft
ND-1000 V3.8.1	PeqLab

NIS-Elements Imaging Software	Nikon
GOAT	In-house tool published as [247]
RStudio	R
SpectroFlo	Cytek Biosciences

2.2 Methods

2.2.1 Human intestinal sample collection

Human intestinal tissues were obtained from resected tissues at surgeries to correct reconstruction of ileostomy, tumor resection, or CD. The collection of samples in the study was approved by the ethics committee of the Freie Hansestadt Hamburg Medical Association, and all persons provided informed consent for the collection of tissues. Tissues were collected at the University Medical Center Hamburg-Eppendorf. All intestinal samples used in this study were derived from ileal sections. Samples were either processed freshly or stored at 4 °C in an overnight medium and processed the following day. Fat and muscle tissue were removed mechanically. Samples were cut into pieces of approximately 0.5 cm^2 and distributed further to generate organoids from adult stem cells and to isolate the intestinal epithelial cell layer. In total, twelve intestinal samples affected by CD or non-inflammatory diseases were analyzed in this study. When a comparison of CD and non-inflamed individuals occurred, we aimed to match the two groups for age and biological sex assigned at birth according to sample availability.

2.2.2 Generation of human intestinal organoids (HIOs) from mucosal tissue samples

Intestinal tissue pieces containing adult stem cells were obtained as described in 2.1.1. For organoid generation, three ~0.5 cm^2 tissue pieces were incubated in EDTA/ DTT buffer for 20 minutes twice and resuspended in between. After the incubation, the supernatant was filtered through a 70 µm cell strainer and centrifuged at 500 x G for five minutes at 4 °C. The supernatant was discarded, and the obtained cell pellet was resuspended in AD+++ and centrifuged again. The supernatant was discarded again, and the remaining cell pellet was resuspended in AD+++ and mixed with Matrigel in a 1:2 ratio. Adult stem cell-containing droplets of 10 µL were seeded in a pre-warmed 24-well plate. The droplets were solidified for 15 minutes and then covered with EM + 10 µM Y-27632. Cells were cultured at 37 °C and 5% CO_2. Medium change occurred every two to three days. The development of organoids was monitored by light microscopy. Cultures were passaged the first time when three-dimensional organoids became visible after 10-14 days.

2.2.3 Primary intestinal epithelial layer (IEL) cell isolation from mucosal tissue samples

During the isolation process, samples were kept on ice if not indicated differently. Fat and muscle tissues were removed mechanically. The samples were cut into ~0.5 cm^2 pieces. Three pieces were used to generate organoids (chapter 2.2.2), and the remaining tissue was used for primary cell isolation. Tissue pieces were incubated in EDTA/ DTT buffer for

20 minutes in a hybridization incubator at 37 °C. The supernatant was pipetted through a 70 µm cell strainer. The remaining tissue was incubated again with fresh EDTA/ DTT buffer. The supernatant was removed again, filtered, and pooled with the first fraction. The cell suspension was washed twice with a washing medium containing 2% FCS and counted using a Neubauer counting slide and Trypan Blue solution. When sufficient material was present, the sample was further enriched for epithelial and immune cells by performing a density gradient centrifugation using Lymphocyte Separation Media. Cells were resuspended in 10 mL Hank's Balanced Salt Solution and layered on 4 mL Lymphocyte Separation Media. Tubes were centrifuged for 22 minutes at 1000 x G with minimum acceleration and deceleration. The middle cell layer was carefully harvested, washed with a washing medium, and counted using a Neubauer counting slide and Trypan Blue.

2.2.4 Passaging organoids

Organoid growth was examined regularly by light microscopy. Based on the density and the morphology of the organoids, the splitting ratio was determined before starting with the passaging procedure. First, the culture medium was removed from the well and discarded. Organoid-containing Matrigel droplets were dissolved in ice-cold AD+++ and transferred to a 15 mL conical tube. Organoids were centrifuged at 300 x G and 4 °C for five minutes. The supernatant containing Matrigel was removed and discarded. Organoids were resuspended in 1 mL AD+++. Organoids were disrupted mechanically by pipetting them 40 times thoroughly with a 200 µL tip plugged below a 1000 µL tip. The tube was filled with 4 mL AD+++ and centrifuged again with 400 x G and 4 °C for five minutes. The supernatant was removed, and cells were resuspended in AD+++ and Matrigel (1:2) and seeded in pre-warmed 24-well plates. Three 10 µL droplets were seeded per well. Droplets solidified for 15 minutes before they were covered with 500 µL pre-warmed EM. The medium was changed every two to three days until the following passage by removing and discarding the old medium without touching the Matrigel droplets. Fresh pre-warmed EM was then carefully placed in the wells covering the droplets. Organoids were cultured at 37 °C and 5% CO_2.

2.2.4 Dissociating HIOs to single epithelial cells

Organoid dissociation to single cells was achieved by an enzymatic digest. Firstly, the culture medium was removed and discarded. Matrigel droplets containing organoids were harvested by resuspension in ice-cold AD+++. Then, cells were centrifuged at 4 °C 500 x G for five minutes, and the supernatant was removed and discarded. The pellet was resuspended in TrypLE™ Express Enzyme (1X), phenol red, incubated at 37 °C for five minutes, and pipetted up and down 20 times. The suspension was assessed under the microscope to verify the disruption of organoids to single cells. If not fully dissociated, organoids were

incubated at 37 °C for another two minutes. The single-cell suspension was diluted 1:20 with PBS to prepare for flow cytometry analysis. Then, cells were centrifuged at 500 x G for five minutes and resuspended in PBS. If the single cells were used to reseed organoids, the suspension was diluted 1:20 with AD+++ and centrifuged at 500 x G 4 °C for five minutes. The supernatant was discarded, and the cells were resuspended again in AD+++. Organoid-derived single cells were counted using a TC20™ Automated Cell Counter and Trypan Blue solution. Ten thousand single cells were seeded per well in a 24-well plate. Cells were embedded in a mixture of Matrigel and AD+++ in a ratio of 1:2. The droplets containing single cells were allowed to solidify for 15 minutes before being covered with 500 µL of EM supplemented with 10 µM Y-27632. Medium was replaced every two to three days. Y-27632 was added during the first week of culture.

2.2.5 Cell freezing and thawing

Cells analyzed and cultured for this project derived from peripheral blood (2.2.6), intestinal epithelial layer cell isolation, or cultured organoids. Peripheral blood mononuclear cells (PBMCs) and intestinal epithelial cells were frozen in FBS + 10% DMSO. In brief, the cell pellet was first resuspended in FBS. Following the resuspension, the same volume of FBS + 20% DMSO was added in tiny drops. Cells were then transferred into cryopreservation tubes and to a 4 °C cold StrataCooler Cryo Preservation Module, allowing a temperature decrease of 0.1 °C/minute to increase cell viability. The StrataCooler Cryo Preservation Module was then transferred to a -80 °C freezer and transferred to liquid nitrogen, holding a temperature below -160 °C on the next day. In order to freeze organoids, the culture medium was aspirated and discarded. Then, Matrigel droplets containing organoids were resuspended in ice-cold Recovery™ Cell Culture Freezing Medium and transferred to cryopreservation tubes. Samples were placed into a 4 °C cold StrataCooler Cryo Preservation Module, moved to a -80 °C freezer, and transferred into liquid nitrogen with -160 °C the next day.

For cell thawing, cryopreservation tubes were placed into a 37 °C warm water bath until the samples were thawed almost completely. Then, cells were transferred quickly into a 15 mL conical and diluted with 10 mL corresponding medium or buffer. PBMCs analyzed with flow cytometry were filled up with 10 mL PBS. Intestinal epithelial layer cells used for flow cytometry analysis were filled with 10 mL washing buffer. Cells were centrifuged at 500 x G for five minutes, and the supernatant was discarded. Organoids cultured after thawing were filled with 10 mL of AD+++ and centrifuged at 500 x G at 4 °C for 5 minutes. This washing step was repeated a second time, and then, the organoid pellet was resuspended in AD+++, mechanically disrupted, and reseeded as described in chapter 2.2.4.

2.2.6 PBMC isolation from human blood

PBMCs were isolated from peripheral blood from voluntary donations of a healthy cohort upon informed consent from all individuals with approval by the ethics committee of the Freie Hansestadt Hamburg Medical Association. PBMCs were isolated by density gradient centrifugation. 30 mL of blood were carefully layered on 15 mL Lymphocyte Separation media. Samples were centrifuged with acceleration and deceleration set to the minimum at 500 x G for 30 minutes at room temperature. The PBMC layer was aspirated and transferred to a new tube. Tubes were filled with Hanks′ Balanced Salt solution and centrifuged at 500 x G for five minutes with maximum acceleration and deceleration. The supernatant was discarded, and cells were rewashed with Hanks′ Balanced Salt solution. PBMCs were counted using a TC20™ Automated Cell Counter and Trypan Blue solution.

2.2.7 Flow cytometry

The cells for flow cytometry analysis were derived from PBMCs or organoids that were dissociated to the single cells, according to Chapter 2.2.4. Cells were resuspended in PBS and centrifuged at 500 x G for 5 minutes. The supernatant was discarded, and the washing step was repeated. The cell pellet was resuspended in a prepared mixture of surface antibodies in PBS and incubated for 20 minutes at room temperature, protected from light. After the incubation, additional PBS was added to the samples before washing. The labeled cell pellet was fixed by adding 4% polymeric formaldehyde (PFA) to the cells. Cells were fixed for 20 minutes at room temperature and protected from light. Following the fixation, labeled and fixed cells were rewashed with PBS and finally measured at the CytekTM 5-Laser Aurora flow cytometer.

Intestinal epithelial layer-derived cells were thawed, as described in Chapter 2.2.5. The cells were washed and extracellularly stained as described for PBMCs and organoids. After the extracellular staining, the primary epithelial cells were washed with 200 µL MACS buffer. Then, cells were fixed and permeabilized by incubating them in BD Cytofix/Cytoperm™ for 20 minutes at room temperature. 10x BD Perm/Wash was added to the cells, which were then centrifuged at 500 x G for five minutes. The supernatant was discarded, and cells were stained with antibodies with intracellular targets in 10x BD Perm/wash. Cells were incubated for 20 minutes in the dark at room temperature. Then, 200 µL PBS was added, cells were centrifuged, resuspended in PBS, and finally measured at the CytekTM 5-Laser Aurora flow cytometer.

Table 7: Human intestinal organoid panel 1

Target	Fluorochrome	Dilution
CD16	BV785	1:100
EpCAM	BV605	1:100
LIVE/DEAD™ Fixable Near-IR	NIR	1:1000
TLR4	BV421	1:100
TLR5	APC	1:100

Table 8: Human intestinal organoid panel 2

Target	Fluorochrome	Dilution
CD16	BV785	1:100
EpCAM	BV650	1:100
LIVE/DEAD™ Fixable Near-IR	NIR	1:1000
TLR4	BV421	1:100
TLR5	APC	1:100

Table 9: Intestinal epithelial layer cell panel

Target	Fluorochome	Dilution
Ezrin (intracellular)	AF700	1:100
LGR5 (intracellular)	PE	1:25
MUC2 (intracellular)	FITC	1:100
CD45	BV605	1:100
EpCAM	BV421	1:100
LIVE/DEAD™ Fixable Near-IR	NIR	1:1000
TLR5	APC	1:100

2.2.8 Immunofluorescence analyses of intestinal organoids

Immunofluorescence staining of intestinal organoids was performed as previously described by Dekkers *et al*., 2019. In brief, organoids grown from single cells were washed with ice-cold PBS without disrupting the Matrigel. Ice-cold cell recovery solution was added to each well and incubated on ice for 60 min on a horizontal shaker (60 r.p.m) to dissolve the Matrigel. Pipette tips were pre-coated with PBS-BSA and then used to transfer organoids into pre-coated PBS-BSA 15 mL tubes. Tubes were filled with 10 mL cold PBS and then centrifuged at 70 x g for 3 minutes at 4 °C. The supernatant was discarded, and organoids were carefully

resuspended in 1 mL PFA for fixation using a pre-coated tip. Organoids were incubated at 4 °C for 45 minutes. After the fixation, the tube was filled up to 10 mL with 4 °C cold PBT gently mixed, incubated for 10 minutes at 4 °C, and centrifuged at 70 x g for 5 minutes at 4 °C. The supernatant was discarded, and the organoids were resuspended in 400 µL OWB and transferred to low-adherent fluorescence-activated cell sorting (FACS) tubes. Organoids were allowed to settle to the bottom of the tube. Then, 200 µL of the supernatant were carefully discarded, and 200 µL of OWB containing primary antibodies for TLR5 and Tight junction protein 1 (ZO-1) (2x concentration) were added to the tube. The samples were incubated overnight at 4 °C shaking. Then, 1 mL of OWB was added for washing. After organoids settled to the bottom of the tube, 1 mL OWB was aspirated and discarded. Then, 1 mL of OWB was added, and samples were incubated for 2 hours. 1 mL of supernatant was removed, and the washing was repeated thrice. Then, 200 µL of secondary antibodies in OWB (2x concentration) were added to 200 µL organoid suspension, incubated overnight with phalloidin and Hoechst at 4 °C, and protected from light. Stained organoids were washed three times. Then, organoids were transferred to a 1.5 mL tube and left untouched for a while, allowing them to settle to the bottom of the tube. In order to prepare the samples for imaging, they were cleared by removing as much OWB as possible and by resuspension in fructose-glycerol clearing solution with a 200 µL tip with a cut-off end. The organoids were then incubated for 20 minutes at room temperature. Then, the organoids were transferred to the slide and covered with a coverslip. Spinning-disk microscopy was performed on a Nikon TI2 (Nikon) based spinning-disk system and the NIS-Element at the Leibniz Institute of Virology Microscopy facility. Images were analyzed using the NIS-Elements Imaging Software from Nikon.

Immunofluorescence staining reagents

Target	Reagent	Dilution
Nuclei	HOECHST 33342	1:2000
Actin	AF647 Phalloidin	1:400
ZO-1	Goat ZO-1 Polyclonal Antibody	1:50
TLR5	Rabbit TLR5 Polyclonal Antibody	1:500
Secondary	Donkey anti-Goat antibody, AF488	1:100
Secondary	donkey anti-rabbit AF546	1:100

2.2.9 RNA isolation of organoids for reverse transcription quantitative PCR (RT qPCR)

For mRNA expression analysis by RT qPCR, cells harvested from three droplets of Matrigel-containing organoids were harvested in 500 µL TRIzol™ Reagent and stored at -80 °C until

RNA isolation was performed according to the manufacturer's instructions. In brief, samples were thawed on ice and incubated for five minutes at room temperature. RNA, DNA, and protein contents were separated by adding 100 µL chloroform, mixing, and shaking. Samples were incubated at room temperature for three minutes and then centrifuged at 12,000 x g at 4 °C for 15 minutes. The upper aqueous phase containing total RNA was carefully collected and transferred to a new RNase-free tube. RNA precipitation occurred by adding 250 µL 2-propanol and 2 µL GlycoBlue™ Coprecipitant. Samples were incubated for 15 minutes at 4 °C and then centrifuged for 15 minutes with 12,000 x g at 4 °C. The supernatant was discarded, and the pellet was resuspended in 300 µL 75% ethanol. Then, samples were centrifuged for 5 min at 7,500 x g at 4 °C, and the supernatant was discarded. The RNA pellet was air-dried for 10 to 15 minutes and then resuspended in 21 µL water. Finally, the samples were incubated for 10 minutes at 55 °C to dissolve the RNA completely. One microliter of RNA solution was used to measure the concentration with a NanoDrop spectrophotometer.

2.2.10 RNA purification for RT qPCR

RNA was then treated with a mixture of RNaseOUT™ Recombinant Ribonuclease Inhibitor and Ambion™ DNase I (RNase-free) to purify and protect the RNA according to the manufacturer's instructions from degradation. In brief, RNaseOUT™ (4 mM), 10x Ambion buffer, and DNase I (80 U/mL) were mixed and added to 20 µL RNA. After a shaking incubation at 37 °C, the reaction was stopped by incubation with EDTA solution (2.5 mM) for 10 minutes at 65 °C.

2.2.11 Reverse transcription (RT) for RT qPCR

To generate complementary DNA (cDNA), the qScriber™ cDNA Synthesis Kit was used according to the manufacturer's instructions. In brief, one µg of RNA solution was mixed with water, 5X qScriber™ Reaction Mix, and 20X qScriber™ Enzyme Blend to a 20 µL reaction mix and placed in a thermocycler. Cycler settings are summarized in the table below. Synthesized cDNA was stored at -20 °C until quantitative PCR with SYBR Green was performed.

Table 11: cDNA thermocycler settings

Time	Temperature
5 min	25 °C
30 min	42 °C
5 min	85 °C
	Hold at 4 °C

2.2.12 Quantitative PCR (qPCR)

Generated cDNA was used for a quantitative PCR using SYBR Green according to the manufacturer's instructions to quantify gene expression. In brief, reaction mixtures of 10 µL were prepared, and qPCR was performed in a LightCycler 96 System. Water, primers (10 µM), and SYBR Green reagent were mixed in a pre-PCR room. 0.5 µg of cDNA was added in a room separated from the previous working steps to avoid cDNA contaminations. Primers targeting *CXCL8*, *TNF*, *CCL20*, and *IL-1β* were obtained from Biorad. Primer sequences for glyceraldehyde-3-phosphate dehydrogenase (*GAPDH*), beta-2-microglobulin (*B2M*), and toll like receptor 5 (*TLR5*) are shown in Chapter 2.1.5. The cycler settings are summarized in the table below.

Table 12: Lightcycler settings

PCR step	Temperature	Time	Cycles
Initial denaturation	95 °C	5 min	1
Denaturation	95 °C	5 seconds	40
Annealing/ extension	60 °C	30 seconds	40
Melting curve	95 °C	15 seconds	1
	60 °C	15 seconds	1
	95 °C	Continuous	
Cooling	4 °C	Continuous	

2.2.13 Bulk RNA sequencing of HIOs

According to the manufacturer's instructions, organoids were harvested, and RNA was isolated with an RNeasy Plus Micro Kit (50) from Qiagen. Isolated RNA was eluted in 14 µL RNase-free water, and 3.5 µL was used for Qubit analysis to determine the quality and the concentration of the isolated RNA performed by the Next Generation Sequencing facility at

the Leibniz Institute of Virology. 390 ng RNA were used for the library preparation with the Lexogen 3' mRNA-Seq Library Prep Kit for Illumina (FWD) and the PCR Add-on Kit according to the manufacturer's instructions. Briefly, RNA was used as a template to generate a first-strand cDNA. After RNA removal, the second strand was synthesized and purified to create the DNA library. The library was amplified using a PCR Add-on Kit. The cycle number for the endpoint PCR was calculated according to the manufacturer's instructions as 13. Amplified libraries were sent to Novogene for NovaSeq PE150 partial lane sequencing with 6.6 million reads per sample. Counts were aligned to the *Homo sapiens* reference genome and quantified using the Kangooroo web tool to generate the count matrix. The count matrix and metadata were loaded in R (Version 2023.06.1) and analyzed using the DESeq2 package.

2.2.14 Human Luminex® Discovery Assay

To quantify the production and release of cytokines and chemokines from human intestinal organoids into the culture supernatant, we performed a Human Luminex® Discovery Assay with a Human Premixed Multi-Analyte Kit. All steps have been performed according to the manufacturer’s instructions. Briefly, 50 µL of standard or supernatant was added to each well. Then, the Microparticle Cocktail was added and incubated for 2 hours at room temperature on a shaker at 800 rpm. Following the incubation, the liquid was removed, and particles were washed by adding and removing the provided wash buffer. This step was repeated three times. Then, 50 µL of diluted Biotin-antibody cocktail was added to each well, protected from light, and incubated for one hour at room temperature on a shaker at 800 rpm. After three additional washing steps, 50 µL of diluted Streptavidin-PE was added and incubated for 30 minutes. After incubation, samples were washed again, resuspended in 100 µL wash buffer, and measured using a Bio-Plex 200 System (BioRad).

2.2.15 Cytosolic calcium measurement

The culture medium of intestinal organoid cultures was aspirated and discarded to determine cytosolic calcium signals in response to CDCA in live organoids. Organoids in Matrigel were dissolved with ice-cold AD+++ and transferred to a conical tube. Organoids were centrifuged at 200 x g and 4 °C for 5 minutes. The supernatant was discarded, and organoids were carefully resuspended in 1 mL AD+++. Then, organoids were centrifuged again, resuspended in a staining buffer containing 5 µM Cal520, and incubated for 20 min at 37 °C in the dark. Then, fresh AD+++ was added and again incubated for 20 minutes. Loaded organoids were washed twice with calcium measurement buffer.

Imaging slides were coated in two steps with 5 µL BSA (5 mg/mL) for 5 minutes and 5 µL of PLL. After air-drying the slides, rubber O-rings were fixed on the slide with silicon grease to

create a reaction chamber. Organoids in calcium measurement buffer were added to the chambers and placed below a spinning disk microscope with a 40-fold oil magnification objective. Samples were stimulated with respective reagents for 240 seconds. Images were acquired with a complementary camera. Cal520 fluorescence was induced with a 488 nm laser and detected with a 525/50 emission filter. Data processing and analysis occurred in Fiji, Excel, and Prism. Organoid staining, live-cell imaging, and analysis were performed by Miriam Kopdag and Björn-Philipp Diercks from the University Hospital Hamburg-Eppendorf - Department of Biochemistry and Molecular Cell Biology.

3. Results

3.1 Generation of organoids from human intestinal tissue samples

Human adult intestinal stem cell-derived organoids were generated to study the influence of CDCA on epithelial regeneration and inflammation. Therefore, intestinal sections were obtained after surgery from different individuals diagnosed with non-inflammatory diseases. To generate organoids from these tissue samples that contain intestinal crypts and epithelial adult stem cells, established protocols published in 2009 and 2011 by the research group of Hans Clevers were used.[235,248]

Human intestinal organoids can be cultured in media of different compositions that affect the proliferation of intestinal stem cells and their differentiation to other epithelial cell types.[249] To establish organoid cultures from fresh intestinal tissue samples, EM containing stem cell growth factors such as WNT, noggin, and R-spondin is used.[92] This medium ensures the maintenance of the stem cell phenotypes in the three-dimensional organoid culture.[23] Upon changing the culture condition to differentiation medium (DM), intestinal stem cells differentiate into other epithelial cell types, leading to a transition from a cystic three-dimensional structure to a crypt-villus structure with apical-basolateral polarization.[250]

Since previous studies have highlighted the importance of intestinal stem cells in tissue regeneration and inflammation, organoids grown in EM were used to study the effects of CDCA on the intestinal epithelium in this thesis.[251] The three-dimensional structure of intestinal organoids in EM organoids was assessed by immunofluorescence (Figure 8).

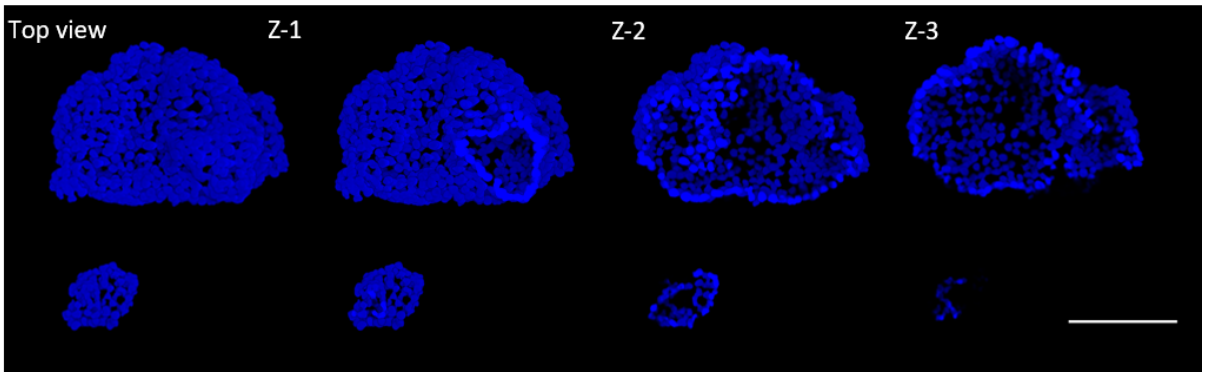

Figure 8: Three-dimensional structure of a human intestinal organoid. Organoids were grown from organoid-derived single cells for 14 days and then nuclei stained as described in Dekkers et al., 2019 [252] using HOECHST. Images show one organoid from the top and in different Z-stacks (Z-1 to Z-3). Scale bar = 100 µm.

3.2 Effects of CDCA on intestinal epithelial regeneration

As mentioned above, the intestinal epithelium is a dynamic single-cell layer that is continuously regenerated based on the proliferation capacity of crypt-based intestinal stem cells.[253] Disturbance of the proliferation lead to defective epithelial barrier functions that can result in the invasion of microbes from the intestinal lumen into the lamina propria with strong inflammatory responses, as seen in CD.[166] To investigate if varying CDCA concentrations can affect epithelial regeneration, we monitored the growth of organoids over 14 days by microscopy and subsequently quantified the development by using the Deep learning-enhanced Generalized Organoid Annotation Tool (GOAT) (Figure 9).[254] GOAT detects individual organoids by instant segmentation in brightfield microscopy images and allows the quantification of the size and the number of organoids per image (Figure 10).[247]

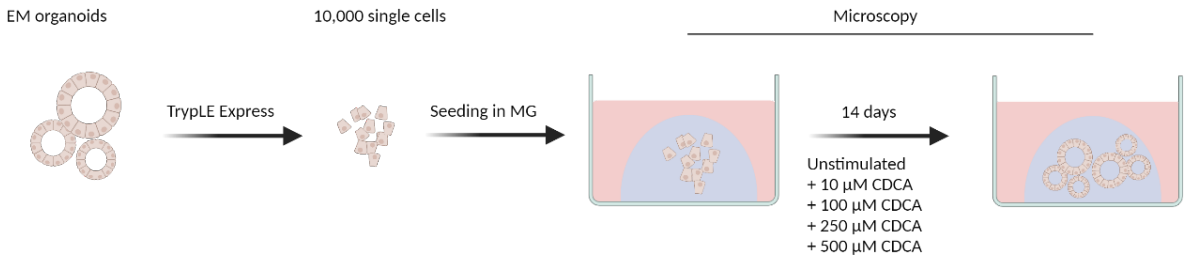

Figure 9: Workflow to study the effects of CDCA on intestinal epithelial regeneration. Organoids were treated with TrypLE Express to obtain single cells. 10,000 single cells per well were seeded in Matrigel (MG) for each condition. The growth was monitored by light microscopy for 14 days. Created with Biorender.

Figure 10 a shows the identification and quantification of organoids in microscopy images. CDCA in varying concentrations had differential effects on the epithelial cells, shown by different organoid numbers and sizes. The average organoid size decreased with increased CDCA concentrations. Furthermore, the number of organoids in the 250 and 500 µM conditions was extremely low after 14 days.

Figure 10 b shows the organoid development over a period of 14 days in cultures derived from three different samples. The average organoid size in the unstimulated and the 10 µM condition showed no significant difference. Intestinal organoids stimulated with 100 µM CDCA showed decreased organoid sizes compared to unstimulated organoids, visible on day 11 and day 14. 250 µM and 500 µM CDCA almost completely inhibited long-term

organoid development, with 250 µM CDCA only allowing small organoid formation, whereas 500 µM CDCA blocked organoid formation in all three cultures. All tested organoid cultures responded similarly to varying CDCA concentrations. After 14 days, intestinal organoids were significantly smaller in cultures treated with 100 µM CDCA compared to unstimulated organoids (Figure 10 c).

In conclusion, human intestinal organoid development is inhibited by concentrations from 100 µM or higher, indicating that an altered bile acid metabolism with increased levels of CDCA impaired epithelial regeneration. Since extracellular signaling transduction depends on cytosolic calcium signaling, we next assessed if CDCA induced the release of calcium ions into the cytosol.[255]

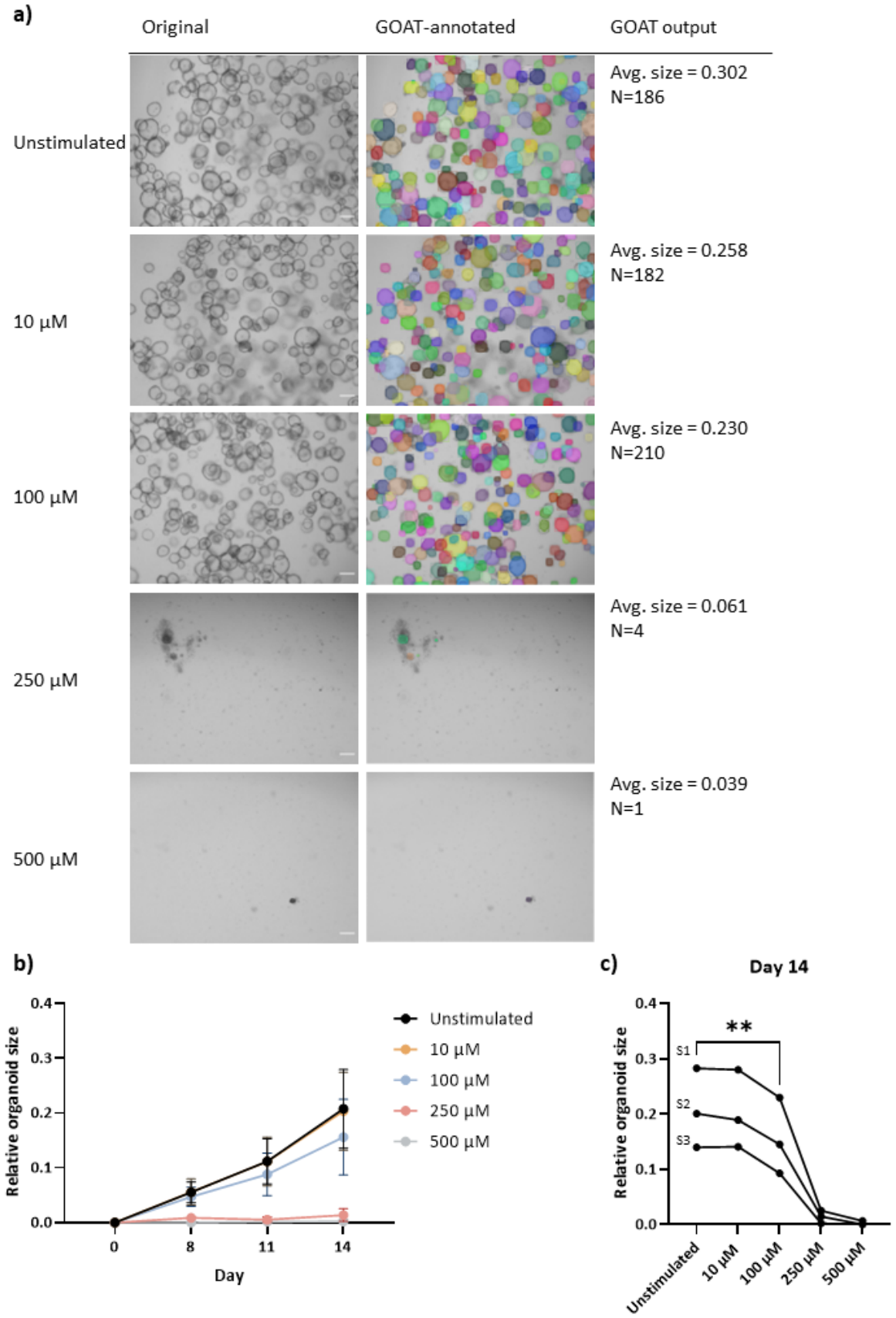
a)
Original
GOAT-annotated
GOAT output
Unstimulated
Avg. size = 0.302
N=186
10 µM
Avg. size = 0.258
N=182
100 µM
Avg. size = 0.230
N=210
250 µM
Avg. size = 0.061
N=4
500 µM
Avg. size = 0.039
N=1
b)
Relative organoid size
0.4
0.3
0.2
0.1
0.0
0
8
11
14
Day
Unstimulated
10 µM
100 µM
250 µM
500 µM
c)
Day 14
**
S1
S2
S3
Relative organoid size
Unstimulated
10 µM
100 µM
250 µM
500 µM

Figure 10: Influence of CDCA on intestinal epithelial regeneration. Organoids from N = 3 non-inflamed tissue samples were cultured in EM supplemented with indicated concentrations of CDCA or left unstimulated. All images were analyzed using the organoid quantification algorithm GOAT. a) Representative images showing organoids cultured for 14 days with increasing CDCA concentrations. The right column shows respective images annotated by GOAT. b) Organoid growth kinetics showing relative organoid sizes over time. Each data point is the mean organoid size of organoids from three different samples with six images per condtion. Error bars indicate the standard deviation. c) Growth comparisons after 14 days. Scale bar = 200 µm. The horizontal bars indicate the significance of the paired t test statistic. **p ≤0.01.

3.3 Influence of CDCA on epithelial cytosolic calcium signals

Calcium ions play a substantial role in signaling transduction and previous studies have shown the importance of cytosolic calcium influx in epithelial integrity and inflammation.[256,255] As organoid development was inhibited by CDCA, indicating an impaired epithelial barrier, we further mimicked bacterial exposure on the epithelium by stimulating organoids from multiple samples with bacterial flagellin. To assess if CDCA and flagellin can induce a cytosolic calcium influx in the intestinal epithelial cell model of human organoids, we used a microscopic approach where organoids were labeled with the cytosolic calcium labeling dye Cal520. These experiments were performed in collaboration with Miriam Kopdag and Björn-Philipp Diercks from the University Hospital Hamburg-Eppendorf - Department of Biochemistry and Molecular Cell Biology. We investigated whether CDCA and bacterial flagellin have the potential to activate intracellular processes by the induction of calcium release and if this response is affected by a 14-day long-term exposure to CDCA (Figure 11). EM was supplemented with 100 μM CDCA, which has a visible effect on organoid growth but still allowed sufficient growth and biomass accumulation for the analysis. DMSO was used as a solvent for CDCA. Therefore, we used the same DMSO concentration (v/v = 0.01%) as a negative control. Previous publications showed cytosolic calcium influx in organoids in response to ATP.[257] We could confirm these findings in all tested organoids from the individual samples and used ATP as a positive control in our experiments (Figure 11).

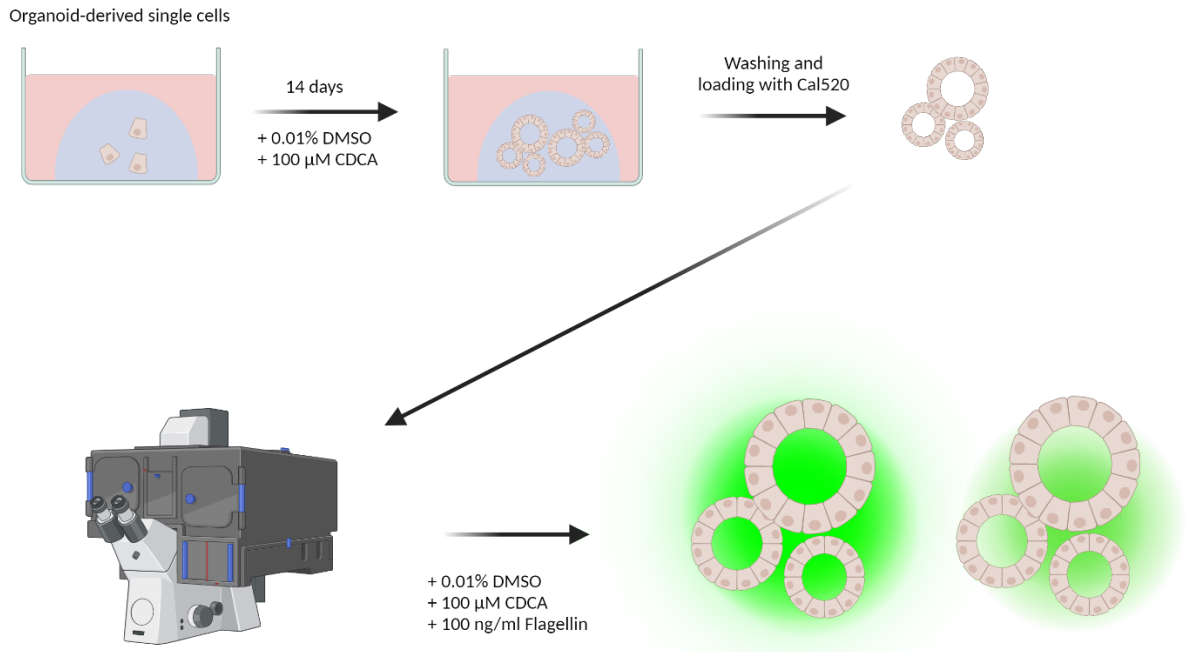

Figure 11: Workflow to study the effects of CDCA on cytosolic calcium signaling in the intestinal epithelium. Organoid-derived single cells were seeded and cultured in DMSO (control) or CDCA for 14 days. The medium was changed every two to three days. On day 14, organoids were carefully harvested, washed, and loaded with Cal520. Organoids were placed under a confocal microscope, and cytosolic calcium influx was monitored during the stimulation with DMSO, CDCA, flagellin, and ATP.

Snapshots of Cal520-labelled organoids were taken over time before, early after, and late after the indicated stimulations. Before each stimulation, the fluorescence intensities of individual cells within one organoid differed, most likely due to individual cellular processes of the living cells in different stages. DMSO did not induce a calcium response. CDCA induced a calcium influx in an acute stimulation with and without prior long-term exposure to CDCA. At early time points after stimulation with CDCA or ATP, an increased cytosolic calcium signal was observed, which was decreased late after the stimulation. The fluorescence intensities of CDCA and ATP-stimulated cultures differed between individual cells within the same organoid. Flagellin did not induce a calcium response independent of prior long-term CDCA stimulation (Figure 12 a).

Organoids from five individual samples, including three non-inflammatory samples and two CD-affected samples, were tested. DMSO did not induce a calcium influx in any of the organoid cultures. CDCA led to a calcium influx with varying intensities in all organoids from

the individual samples. The calcium signal was also induced when organoids were cultured for 14 days in CDCA before an acute CDCA stimulation (Figure 12 b and c).

The CDCA-induced calcium signal exhibited different temporal dynamics than the ATP-induced signaling, as the calcium signal after CDCA stimulation appeared later and was maintained until the endpoint of the measurements at 250 seconds in organoids generated from each sample. In organoids generated from two out of three non-inflammatory samples, acute CDCA stimulation induced a higher calcium influx in untreated organoids compared to those pre-cultured with CDCA for 14 days (Figure 12 b). Organoids from the two CD-affected samples differed in calcium signal intensities (Figure 12 c). Organoids generated from CD-affected sample 4 showed the strongest calcium response to ATP compared to organoids generated from other samples. The initial strong signal was lost after 120 seconds and followed by a second increase that was not as intense but remained stable until the end of the measurement. Intestinal organoids generated from sample 5 showed the highest calcium signal intensity early after ATP stimulation and no secondary signal. CDCA led to weak calcium signals at later time points in organoids generated from this sample.

In conclusion, CDCA-induced cytosolic calcium release was detected with varying intensities in intestinal organoids generated from CD-affected and non-inflamed intestinal tissue samples. Calcium signaling could also be induced in intestinal organoids pretreated for 14 days in CDCA before an acute CDCA stimulation. Within our measurement period, flagellin stimulation did not induce an increase in cytosolic calcium concentrations in epithelial cells in intestinal organoids. These findings indicate that CDCA activates signaling pathways in epithelial cells that could induce various cellular responses. As previous studies showed that cumulated cytosolic calcium signals can promote cytokine production, we further investigated if CDCA also affects the cytokine production of epithelial cells.[258]

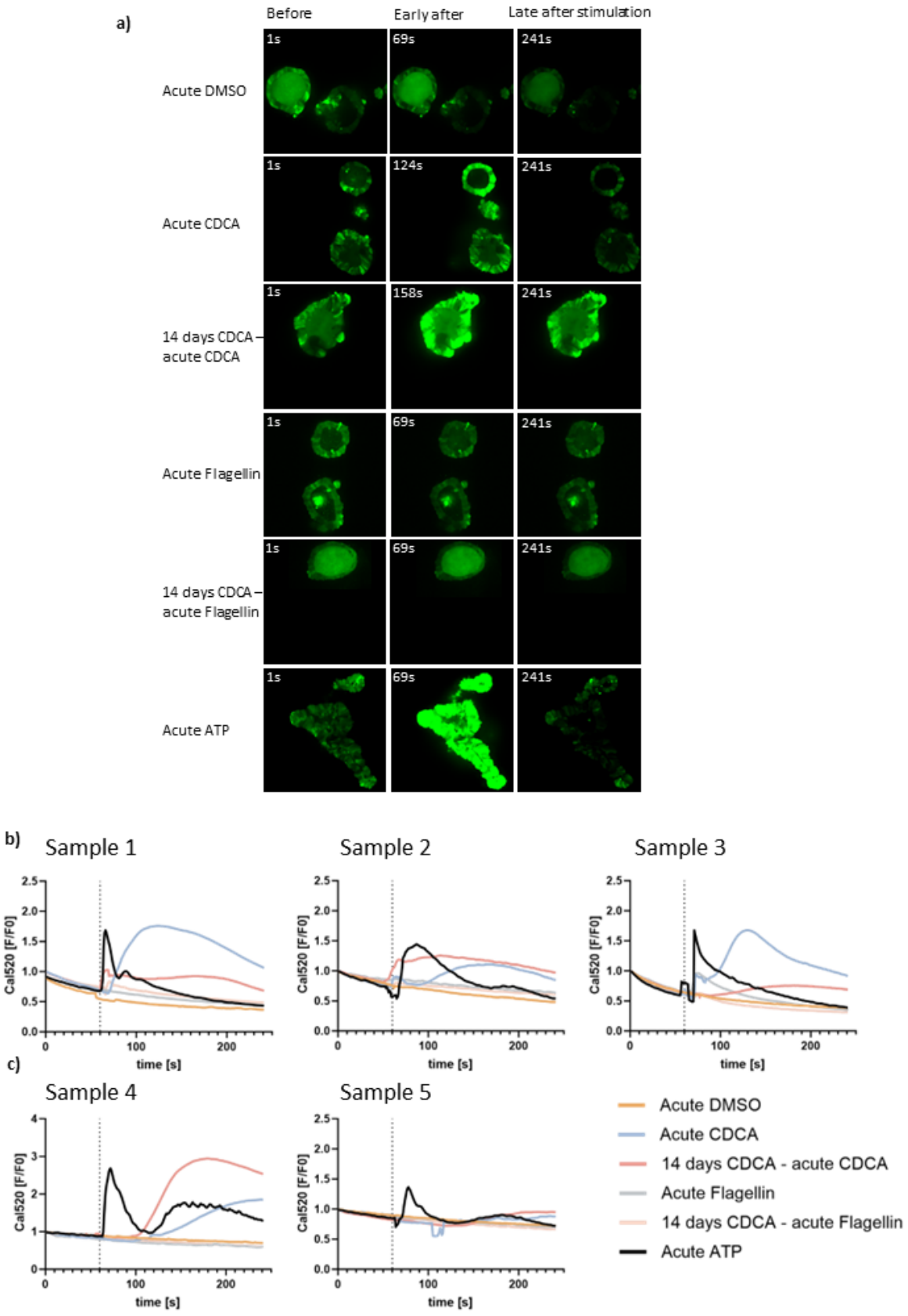
a)
Before
Early after
Late after stimulation
Acute DMSO
1s
69s
241s
Acute CDCA
1s
124s
241s
14 days CDCA – acute CDCA
1s
158s
241s
Acute Flagellin
1s
69s
241s
14 days CDCA – acute Flagellin
1s
69s
241s
Acute ATP
1s
69s
241s
b)
Sample 1
Sample 2
Sample 3
c)
Sample 4
Sample 5
Cal520 [F/F0]
time [s]
Acute DMSO
Acute CDCA
14 days CDCA - acute CDCA
Acute Flagellin
14 days CDCA - acute Flagellin
Acute ATP

Figure 12: Effects of CDCA on cytosolic calcium signaling in the intestinal epithelium. Organoids from N = 3 non-inflamed and N = 2 inflamed CD tissues were grown for 14 days from single cells in EM supplemented with 100 μM CDCA, 0.01% DMSO (negative control), 100 μM CDCA, 100 ng/mL flagellin, or 10 μM ATP (positive control). The dotted line indicates the time point of stimulation at 60 seconds. Results are shown as fluorescence intensity relative to baseline fluorescence. a) Representative images showing cytosolic calcium signals before, early, and late after the indicated stimulation. b) Summarized data showing calcium signaling dynamics of organoids generated from non-inflamed intestinal samples. c) Summarized calcium signaling data of organoids generated from CD-affected intestinal samples.

3.4 Influence of CDCA and flagellin on intestinal epithelial cytokine production

Previous studies showed that cumulated intracellular calcium signaling promotes the production of cytokines.[258] As we observed increased calcium signaling in organoids exposed to CDCA, we further assessed if CDCA also induces increased cytokine release of epithelial cells in organoids. Furthermore, we showed impaired organoid development upon long-term CDCA exposure, indicating reduced barrier functions of the affected epithelium. This can physiologically enable microbes to cross the epithelial barrier. Consequently, pattern recognition receptors located on intestinal stem cells in intestinal crypts could be activated. Epithelial cell exposure to microbes and microbial products was mimicked again by the addition of bacterial flagellin, the ligand of TLR5. TLR5 signaling is crucial for protective immunity against pathogens but may also contribute to the development of chronic pathological inflammatory conditions such as IBD.[192,259]

It was hypothesized that CDCA modifies TLR5 signaling and, consequently, its mediated cytokine release. To test this hypothesis, CDCA-pretreated organoids were stimulated with the TLR5 ligand flagellin for 24 hours. The mRNA and protein levels of cytokines and chemokines, which are frequently expressed in response to TLR5 activation, were quantified by RT qPCR and a Human Luminex® Discovery Assay in organoid cultures generated from up to seven non-inflamed tissue samples (Figure 13).

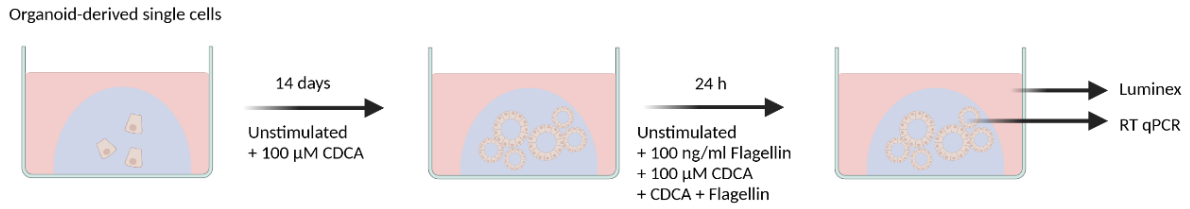

Figure 13: Workflow to study the effects of CDCA and flagellin on epithelial chemokine and cytokine production. Organoid-derived single cells were cultured for 14 days in the presence or absence of CDCA and then stimulated with flagellin and CDCA for 24 h. The cells were harvested in Trizol for RT qPCR, and the supernatant was collected for Luminex Discovery Assay.

3.4.1 Epithelial mRNA levels of cytokines and chemokines upon CDCA and flagellin stimulation

Previous studies showed that downstream signaling of TLR5 results in increased transcription of multiple genes encoding for cytokines and chemokines, including *TNF*,

CCL20, *IL-1β*, and *CXCL8*. By using RT qPCR, we assessed the transcription of these targets and whether the respective mRNA levels were altered in CDCA-pretreated epithelial cells.

Stimulation with flagellin resulted in a significant increase of *IL-1β* and *CCL20* transcription by epithelial cells in organoids (Figure 14). The same trend was observed for *TNF* and *CXCL8* mRNA levels in CDCA-stimulated organoids compared to unstimulated organoids although not reaching significance.

Stimulation of intestinal organoids with CDCA alone increased the expression of *TNF* and *CCL20* only marginally compared to unstimulated organoids.

To evaluate the effect of CDCA on TLR5 signaling in intestinal epithelial cells, CDCA-pretreated organoids were stimulated with CDCA and flagellin, and compared to flagellin-only stimulated organoids that were not pre-treated with CDCA. Flagellin-induced expression of *TNF* and *CXCL8* in epithelial cells was not affected by CDCA. However, organoids pretreated with CDCA showed increased flagellin-induced expression of *CCL20* and *IL-1β* compared to organoids only stimulated with flagellin (Figure 14).

In conclusion, flagellin-induced *CCL20* and *IL-1β* expression by epithelial cells was further increased by CDCA, indicating that CDCA affects TLR5 signaling in epithelial cells. As post-transcriptional regulation can further impact cytokine and chemokine production, we quantified cytokine and chemokine levels in the culture supernatant by using a Human Luminex® Discovery Assay.

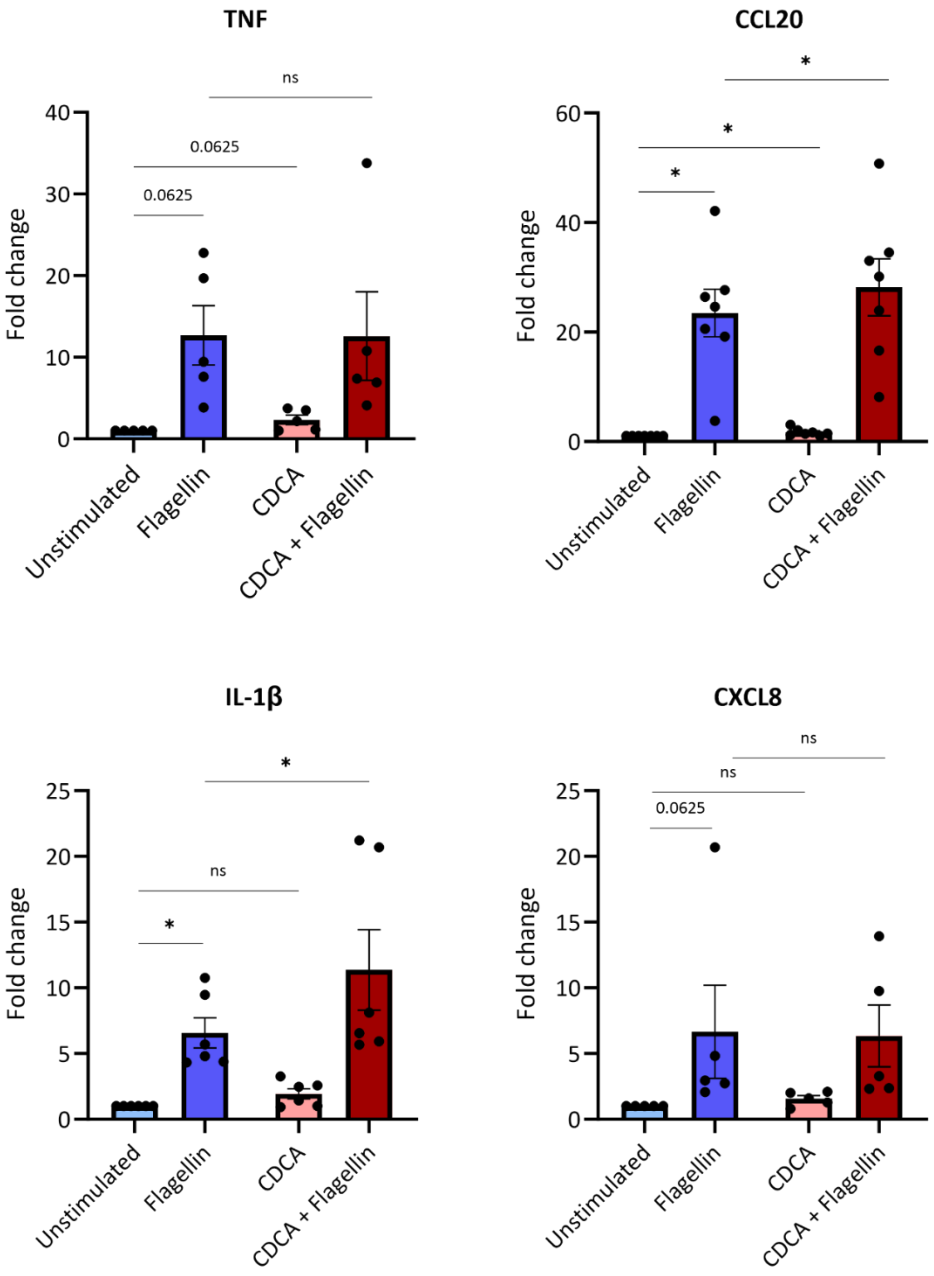

Figure 14: Effects of CDCA and flagellin on epithelial chemokine and cytokine expression. Organoids from N = 5 (*TNF* and *CXCL8*), N = 7 (*CCL20*), and N = 6 (*IL-1β*) non-inflamed tissues were cultured in EM supplemented with 100 µM CDCA or left unstimulated. After 14 days, organoids were further stimulated with 100 ng/mL flagellin for 24 hours and harvested in Trizol. RT qPCR data show the 2^{-ddCT} values normalized to a housekeeping gene and the unstimulated condition. The mean of biological replicates and the respective standard errors are shown. Horizontal bars indicate the significance of the Wilcoxon matched pairs signed rank test. *p ≤ 0.05.

3.4.2 Epithelial cytokine production upon CDCA and flagellin stimulation

The results above showed increased mRNA levels of *CCL20* and *IL-1β* after flagellin stimulation in organoids pretreated with CDCA. To assess if flagellin-induced cytokine levels in the culture supernatant were also affected by the pretreatment with CDCA, we used a Human Luminex® Discovery Assay approach that enabled the simultaneous quantification of multiple cytokines in the supernatant of organoid cultures. The concentrations of multiple cytokines and chemokines, including CXCL8, TNF, CCL20, CXCL9, and IL-1β and the alarmin IL-33, were measured in this regard (Figure 15). The experiments were performed with organoids derived from seven non-inflamed tissue samples.

In the unstimulated conditions, TNF was not detected, whereas CXCL8, CCL20, IL-33, CXCL9, and IL-1β were detected in unstimulated organoid cultures with varying concentrations. CXCL8 and CCL20 showed the highest concentrations in the supernatant of organoid cultures at baseline. IL-33 and IL-1β showed a low baseline production. All cytokine and chemokine concentrations in the supernatants increased significantly when organoids were stimulated with flagellin compared to unstimulated organoids. CDCA-only stimulation of organoids did not alter the levels of any cytokines, chemokines, or alarmins in the supernatant of the cultures. Remarkably, pretreatment with CDCA increased the flagellin-induced release of CXCL8 significantly compared to flagellin-only stimulated cultures. The same trend was observed for CCL20 and TNF, whereas flagellin-induced production of IL-33, CXCL9, and IL-1β was not affected by the CDCA pretreatment.

The flagellin-induced increased release of TNF, CCL20, IL-1β, and CXCL8 corresponded to the increased expression of the corresponding genes determined by RT qPCR. The trend of increased flagellin-induced CCL20 levels in the supernatant of organoid cultures upon pretreatment with CDCA was in line with the increased expression of this gene determined by RT qPCR.

These findings indicate altered TLR5 signaling mediated by CDCA in epithelial cells during flagellin exposure. CDCA synergistically increased the flagellin-mediated production of CXCL8 significantly. In addition, CCL20 and TNF showed a trend towards a higher production in organoids pretreated with CDCA followed by a flagellin stimulation in comparison to organoids that were treated with flagellin only, which highlights the potential of CDCA to contribute to inflammatory processes in the intestinal epithelium. To assess whether the expression of other genes relevant to TLR5 signaling is affected by CDCA, untargeted bulk RNA sequencing on organoids treated with CDCA was performed next.

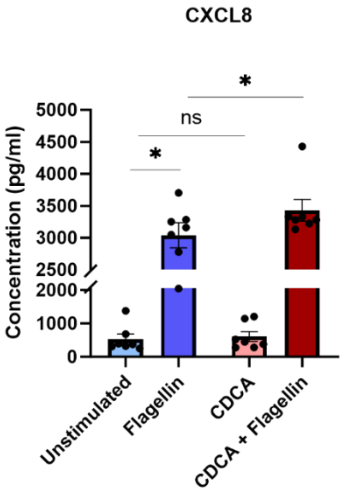
CXCL8
Concentration (pg/ml)
5000
4500
4000
3500
3000
2500
2000
1000
0
*
ns
*
Unstimulated
Flagellin
CDCA
CDCA + Flagellin

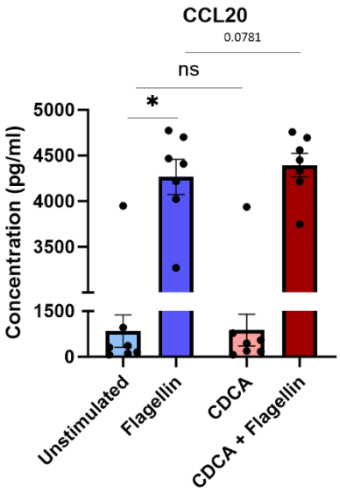
CCL20
0.0781
ns
*
Concentration (pg/ml)
5000
4500
4000
3500
1500
0
Unstimulated
Flagellin
CDCA
CDCA + Flagellin

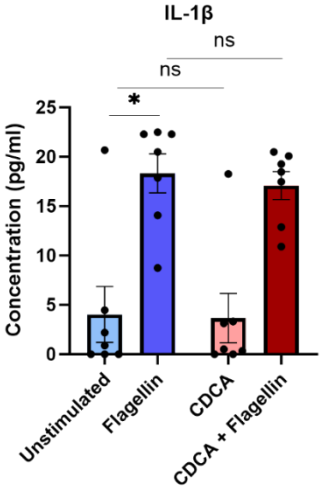
IL-1β
ns
ns
*
Concentration (pg/ml)
25
20
15
10
5
0
Unstimulated
Flagellin
CDCA
CDCA + Flagellin

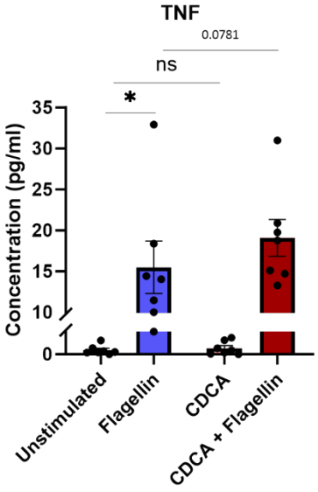
TNF
0.0781
ns
ns
*
Concentration (pg/ml)
35
30
25
20
15
10
0
Unstimulated
Flagellin
CDCA
CDCA + Flagellin

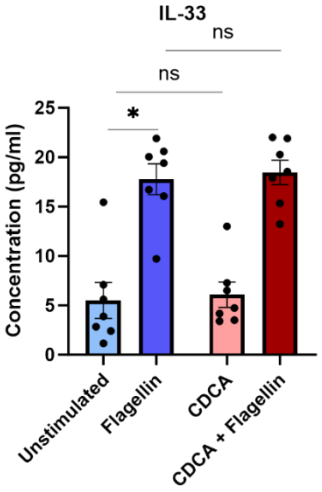
IL-33
ns
ns
*
Concentration (pg/ml)
25
20
15
10
5
0
Unstimulated
Flagellin
CDCA
CDCA + Flagellin

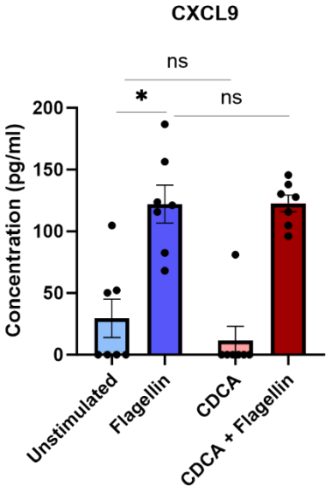
CXCL9
ns
*
ns
Concentration (pg/ml)
200
150
100
50
0
Unstimulated
Flagellin
CDCA
CDCA + Flagellin

Figure 15: Effects of CDCA and flagellin on epithelial chemokine and cytokine production. Organoids from N = 7 non-inflamed tissue samples were cultured in EM supplemented with 100 µM CDCA or left unstimulated. After 14 days, organoids were stimulated with 100 ng/mL flagellin for 24 h. The supernatant was collected and stored at -80 °C until indicated cytokine, chemokine, and alarmin levels were quantified by a Human Luminex® Discovery Assay. The mean of biological replicates and its respective standard error are shown. Horizontal bars indicate the significance of the Wilcoxon matched-pairs signed rank test. *$p \leq 0.05$.

3.5 Differential gene expression of intestinal organoids exposed to CDCA

To get further insights about potential mechanisms that mediate altered TLR5 signaling in CDCA-stimulated organoids, we performed untargeted bulk RNA sequencing with organoids generated from four non-inflamed intestinal samples. EM medium containing 0.01% DMSO (control) or 100 µM CDCA was renewed every two to three days. The organoids were harvested four hours after the last stimulation. RNA was isolated and quality-checked in-house. The purified RNA was used for library preparation, and the samples were sequenced by Novogene. Data were analyzed using R. The experimental workflow is shown in Figure 16.

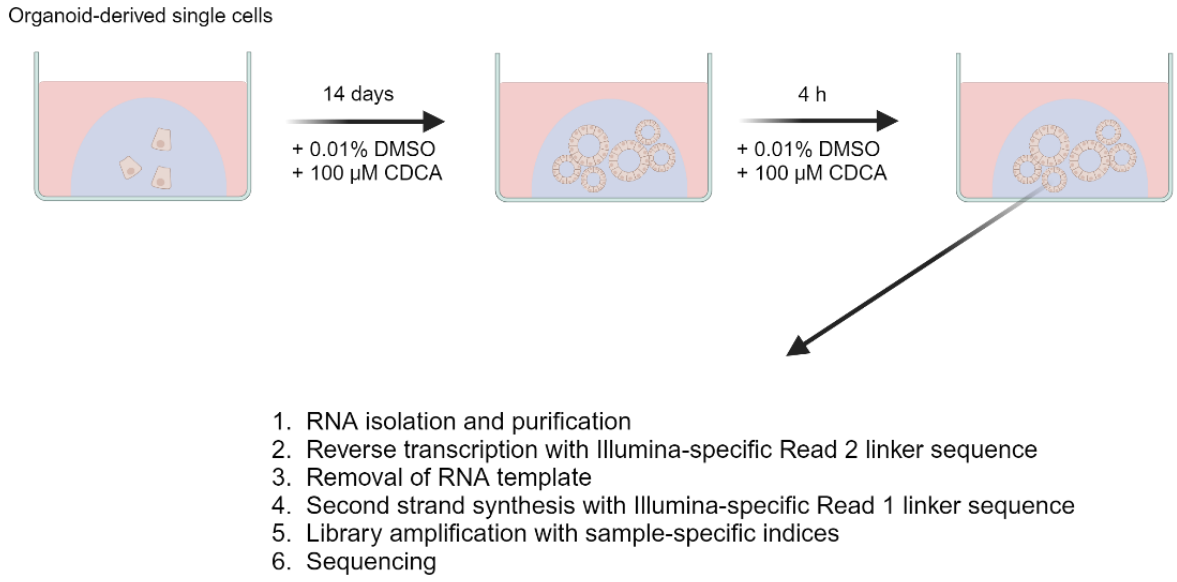

Figure 16: RNA sequencing workflow to study effects of CDCA on epithelial gene expression. Organoids were treated with TrypLE Express to obtain single cells. 10,000 single cells per well were seeded for both conditions. EM medium containing 0.01% DMSO (control) and 100 µM CDCA was renewed every two to three days. Organoids were harvested 4h after the last stimulation on day 14 and processed as indicated.

Principal component analysis showed altered overall gene expression upon stimulation with CDCA. The separation of data points is based on their treatment with DMSO or CDCA (PC1: 37% variance) (Figure 17 a). Further analysis revealed differential expression of 17 out of

14510 expressed genes in CDCA-treated organoids after correction for multiple testing. Five genes were significantly downregulated, whereas twelve genes were significantly upregulated (Figure 17 b and c).

These genes are involved in various cellular processes. Interestingly, among the differentially expressed genes, candidates were included that are involved in cellular growth and inflammation, highlighting their potential to be involved in the pathogenesis of CD.

D-aminoacyl-tRNA deacylase 1 (*DTD1*) was significantly downregulated in CDCA-treated organoids. *DTD1* is involved in the initiation of DNA replication by binding DNA unwinding elements.[260] Its downregulation could indicate a defective proliferation capacity of intestinal stem cells and, therefore, a defective intestinal epithelial regeneration and reduced integrity of the epithelial cell layer.

MUC1 was significantly upregulated in organoids treated with CDCA. The *MUC1* gene encodes a trans-membrane mucin that functions as a physical barrier in healthy tissues, thereby providing protection against microbes.[261] However, it has been shown that MUC1 regulates the release of chemokines in a NF-κB dependent mechanism, highlighting its potential to affect infectious and inflammatory diseases.[262] A previous study also identified the enrichment of MUC1 in intestinal enterocytes of individuals with CD by a meta-analytical approach.[263]

Fibronectin 1 (FN1) was significantly overexpressed in CDCA-treated organoids. FN1 is part of the extracellular matrix and is increased in fibrotic tissues of individuals with CD.[264] Annexin A10 (ANXA10) is highly increased in inflamed ileal tissues of individuals with CD.[193] However, the cellular functions of ANXA10 in CD are not well understood. It is a calcium-dependent phospholipid-binding protein of the annexin family that is involved in various processes including apoptosis, vesicle trafficking, calcium signaling, growth control, and cell division.[265,266] *ANXA10* expression was increased in response to CDCA stimulation of intestinal organoids.

In conclusion, CDCA exposure induces an altered gene expression in epithelial cells that has potential consequences for a wide range of biological processes including cell growth and inflammation. However, this untargeted approach with a limited sample size does not explain the altered cytokine and chemokine productions in response to bacterial flagellin. To gain further insights into the mechanisms driving the increased release of epithelial cytokines in response to CDCA, targeted RT qPCR and flow cytometry were performed on organoids generated from additional tissue samples. This allowed for the assessment of the flagellin receptor TLR5 on epithelial cells and an investigation into whether its expression is affected by long-term CDCA stimulation.

a) Principal component analysis

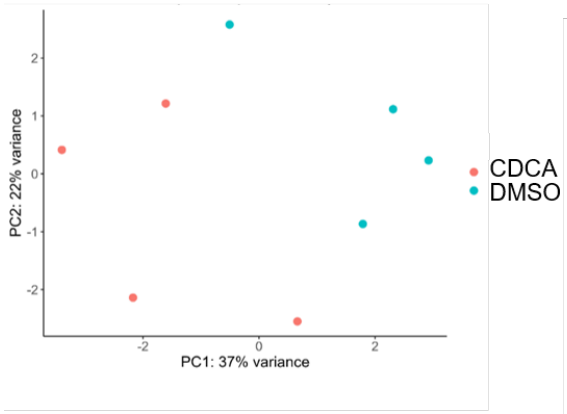

b) Volcano plot of differentially expressed genes

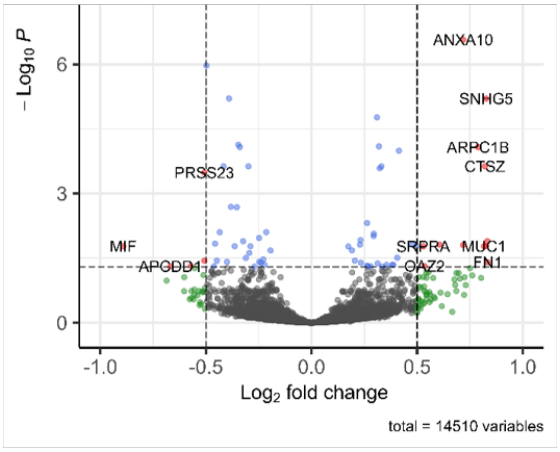

c) Heatmap of differentially expressed genes

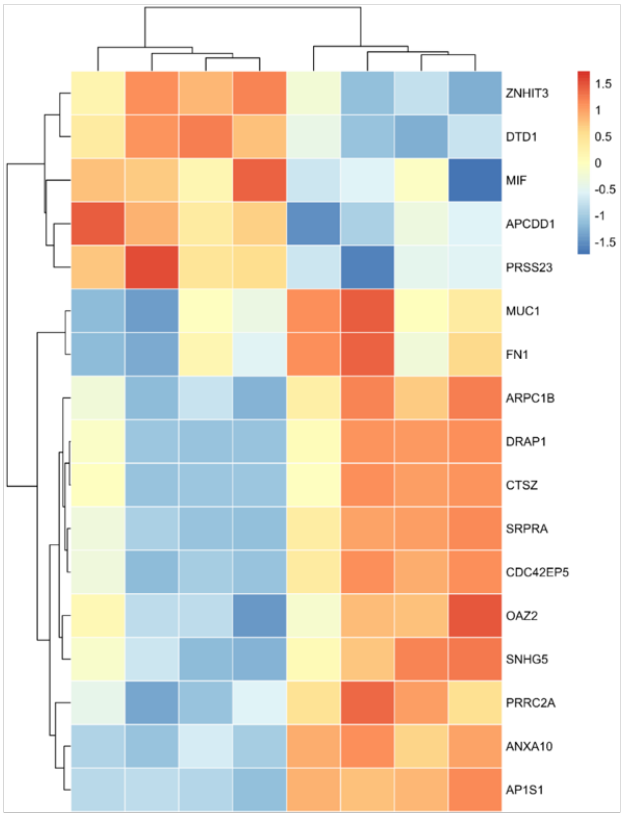

Figure 17: Effects of CDCA on epithelial gene expression. Organoids generated from N = 4 non-inflamed tissues samples were cultured from organoid-derived single cells and cultured in EM supplemented with DMSO (0.01%) or CDCA (100 μM) for 14 days. Total RNA was isolated and quality checked. The library was prepared and sequenced. Data were analyzed using R. a) Principal component analysis of DMSO and CDCA-treated organoids. b) Volcano plot showing differential gene expression in CDCA-treated organoids. Genes are considered as significantly changed if log2fold change ≥ 0.5 and adjusted p-value ≤ 0.05 indicated by bracket lines in the plot. c) Heatmap of differentially expressed genes.

3.6 Influence of CDCA on epithelial TLR5 in intestinal organoids

The experiments above demonstrated that CDCA pretreatment enhanced TLR5 signaling in epithelial cells within organoids, as evidenced by increased epithelial production of CXCL8 and, to a lesser extent, TNF and CCL20, in flagellin-stimulated intestinal organoids. To investigate the underlying mechanisms contributing to these findings, the expression of TLR5 in epithelial cells in organoids was quantified. As in the previous experiments, organoid-derived single cells were seeded and cultured in the presence or absence of 100 µM CDCA for 14 days. On day 14, intestinal organoids were stimulated with CDCA and flagellin, and TLR5 expression was quantified 24 hours after the last stimulation by flow cytometry and RT qPCR (Figure 18).

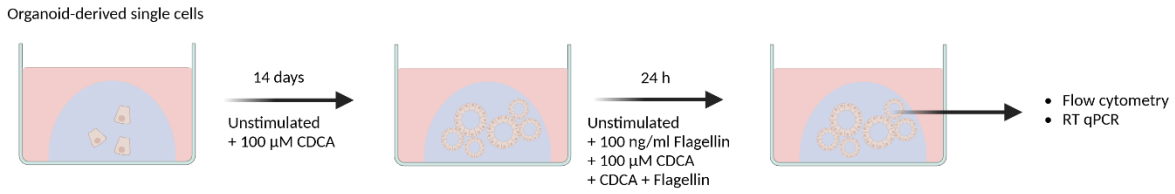

Figure 18: Workflow to study the effect of CDCA on epithelial TLR5 expression. Organoid-derived single cells were cultured for 14 days in the presence or absence of 100 µM CDCA and then stimulated with flagellin and CDCA for 24 h. The cells were harvested in Trizol for RT qPCR or directly processed for flow cytometry.

To quantify the cell surface expression of TLR5 by flow cytometry, the measured events were gated for single cells based on their SSC-A, FSC-A, and SSC-H patterns. Single cells were subsequently gated on live cells using a dye that enters dying and dead cells (Figure 19 a).

The median fluorescence intensity (MFI) of TLR5 on single viable epithelial cells was determined and visualized in histograms (Figure 19 b). For gating purposes, unstained epithelial cells from organoids were used as a negative control, and PBMC-derived CD14-positive monocytes were used as a positive control.

Figure 19 c shows the mean MFI of six organoid cultures derived from individual samples. In comparison to baseline expression, the MFI of TLR5 on flagellin-stimulated epithelial cells decreased, although not statistically significant, indicating effective stimulation. The same effect was observed in epithelial cells derived from CDCA-pretreated organoids that were stimulated with flagellin. Notably, TLR5 MFI was significantly increased on CDCA-pretreated

organoids compared to the unstimulated condition.

Similarly, mRNA levels of TLR5 in epithelial cells were increased upon CDCA stimulation. (Figure 19 d). Data are shown as fold change expression normalized to a housekeeping gene and the unstimulated condition. Flagellin stimulation did not result in a significant decrease of *TLR5* mRNA levels in organoids compared to the unstimulated condition. Flagellin stimulation in CDCA-pretreated organoids tended to lower levels of mRNA *TLR5* compared to CDCA-pretreated organoids without flagellin stimulation.

In conclusion, these two methods showed increased CDCA-mediated expression of TLR5 on the protein and the mRNA level, indicating that CDCA affects TLR5 signaling by influencing TLR5 expression on a transcriptional level. To further assess whether this was mimicked by intestinal epithelial cells from individuals with CD, we determined TLR5 expression on epithelial cells from non-inflamed and CD-affected intestinal tissues *ex vivo*.

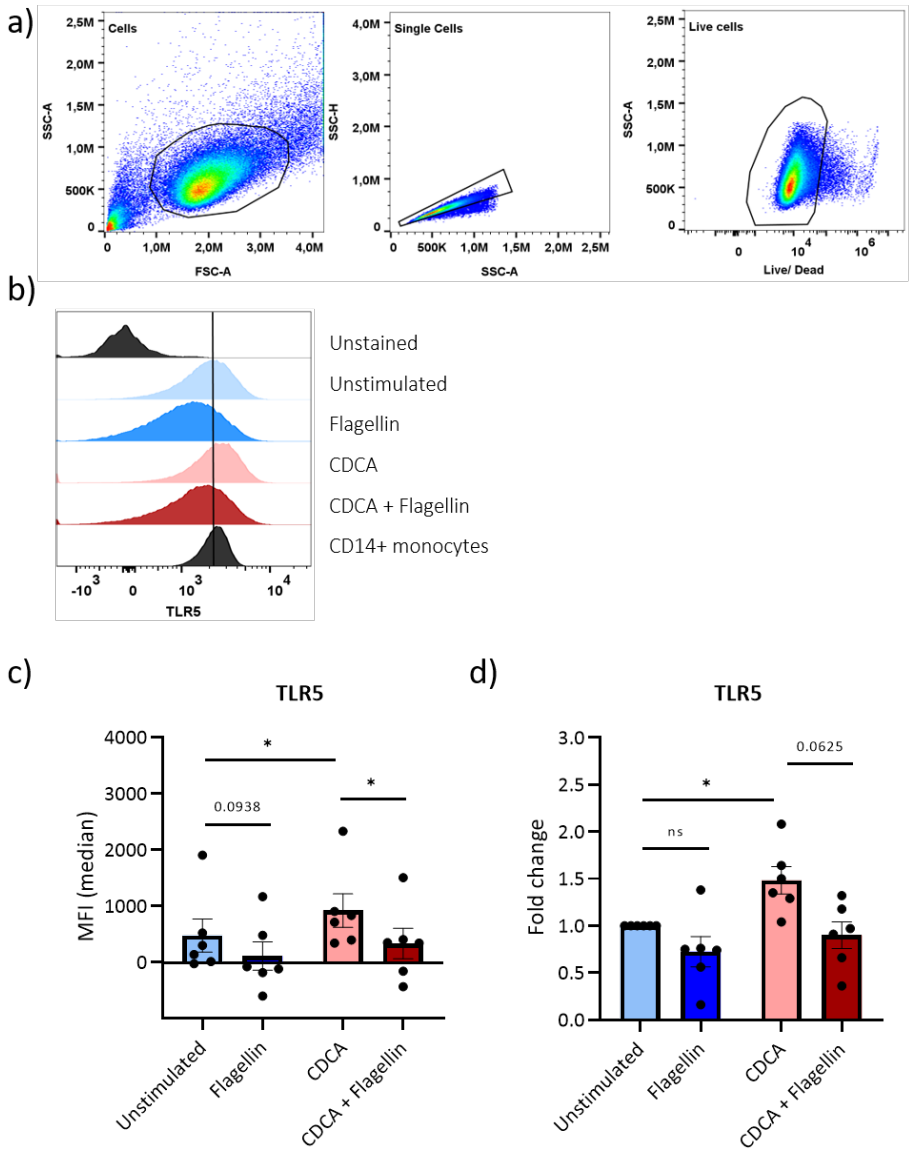

Figure 19: Effect of CDCA on epithelial TLR5 expression. Organoids from N = 6 non-inflamed tissue samples were cultured for 14 days in EM in the presence or absence of 100 µM CDCA. On day 14, organoids were stimulated with 100 ng/mL flagellin for 24 h. Cells were stained directly for flow cytometry analysis or harvested in Trizol for RT qPCR analysis. a) Gating strategy to identify single live epithelial cells. b) Histograms comparing the levels of TLR5 in single live cells under different conditions. c) Summarized flow cytometry data showing the Median Fluorescence Intensity (MFI) of TLR5 in single viable cells in indicated conditions. d) Summarized RT qPCR data showing the 2^{-ddCT} values normalized to a housekeeping gene and the unstimulated condition as fold change to the unstimulated condition. Horizontal bars indicate the significance of the Wilcoxon matched-pairs signed rank test. *p ≤ 0.05.

3.7 *Ex vivo* intestinal epithelial TLR5 expression

Previous studies have shown that CDCA concentrations are increased in stool samples of individuals with CD.[185] The findings above demonstrate that CDCA stimulation leads to increased TLR5 expression by epithelial cells *in vitro* in EM intestinal organoids derived from non-inflamed ileum samples. Based on these data, we hypothesized that epithelial cells from intestinal tissue affected by active CD express higher amounts of TLR5. To test this hypothesis, primary epithelial cells from CD-affected intestinal tissue and non-inflamed tissue were analyzed, and the frequencies of TLR5-positive cells were quantified by flow cytometry. Single intestinal epithelial cells were obtained by the incubation of small intestinal tissue pieces with EDTA/ DTT buffer, filtering, and washing (Figure 20). Cells were frozen and cryopreserved in liquid nitrogen until antibody staining and flow cytometry analysis (Figure 21).

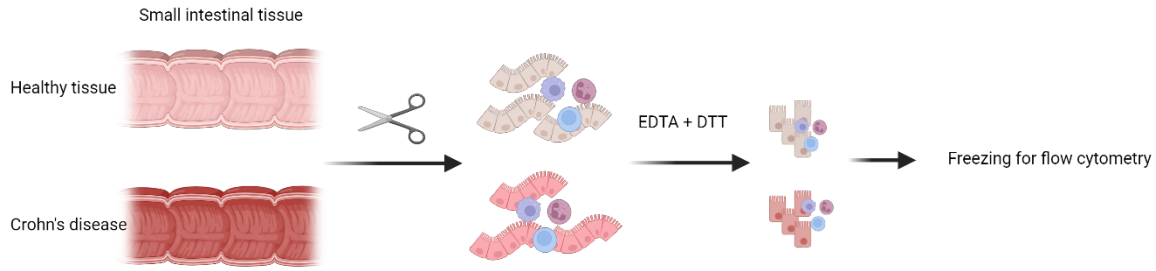

Figure 20: Workflow to study epithelial *ex vivo* TLR5 expression. Samples were obtained from people with non-inflammatory diseases and Crohn's disease after surgery. Fat and muscle layers were mechanically removed, and cells were isolated by EDTA/ DTT treatment. Single-cell solutions were cryopreserved and stored until flow cytometry staining.

The intestinal epithelial cells were incubated with an antibody mix to determine target protein expression. Cells were gated on single live cells based on SSC-A, FSC-A, and SSC-H, as described above. Next, the viable cells were identified by the absence of the live/dead dye that stains explicitly dying and dead cells. To establish an internal positive control for TLR5, monocytes were identified within the CD45-positive population based on their SSC-A and FSC-A characteristics (Figure 21 b). CD45-negative and epithelial cell adhesion molecule (EpCAM)-positive epithelial cells were separated into LGR5 high positive (stem cells) and LGR5 low cells (non-stem cells) (Figure 21 a).

As shown in Figure 21 c, the frequencies of TLR5-positive epithelial cells in LGR5 high and LGR5 low populations in non-inflamed (N = 6) and Crohn's disease samples (N = 6) were compared.

In LGR5 low cells of non-inflamed intestinal tissues, the median frequency of TLR5-positive cells was low and did not differ significantly from LGR5 high cells (Figure 21 d). In contrast, in LGR5 high cells of CD-affected individuals, the median frequency of TLR5-positive cells was significantly higher compared to LGR5 low cells (Figure 21 e). However, the frequencies of TLR5-positive cells in LGR5 high subsets did not differ between non-inflamed and Crohn's disease samples (Figure 21 f).

In conclusion, our data show that LGR5 high-positive stem cells in CD show higher frequencies of TLR5-positive cells relative to LGR5 low-positive cells. This difference cannot be observed in non-inflamed tissue samples, indicating that in CD, stem cells differ from non-stem cells in their expression of TLR5. However, frequencies of TLR5-positive stem cells in CD and non-inflamed samples did not significantly differ. Considering the dynamics of bile acid metabolism and the complex and intensive processing protocol of tissue samples, further studies are needed to evaluate TLR5 expression by epithelial cells in CD-affected intestines.

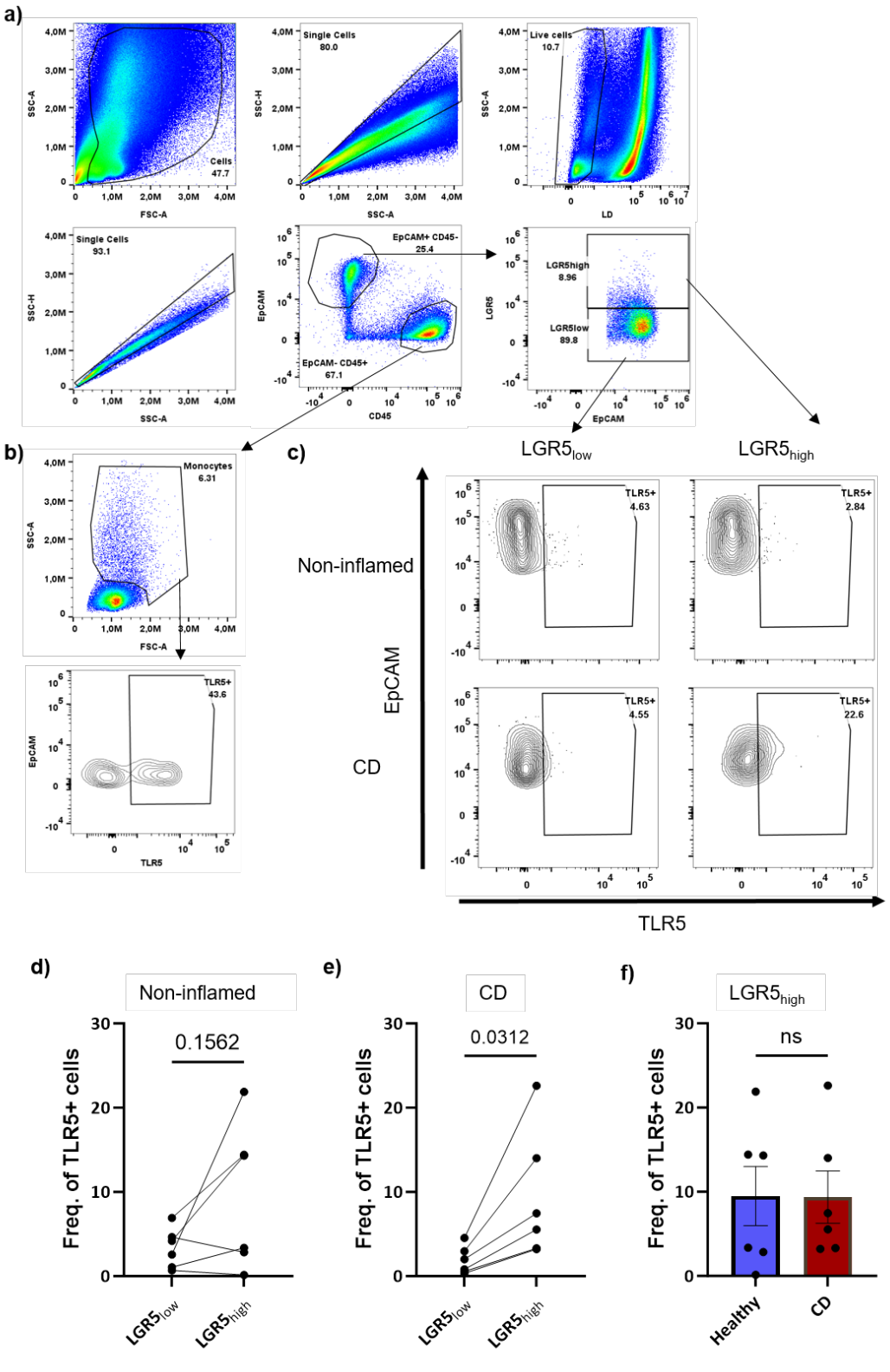
a)
Cells
47.7
Single Cells
80.0
Live cells
10.7
Single Cells
93.1
EpCAM+ CD45-
25.4
EpCAM- CD45+
67.1
LGR5high
8.96
LGR5low
89.8
b)
Monocytes
6.31
TLR5+
43.6
c)
LGR5low
LGR5high
Non-inflamed
CD
EpCAM
TLR5
TLR5+
4.63
TLR5+
2.84
TLR5+
4.55
TLR5+
22.6
d)
Non-inflamed
0.1562
Freq. of TLR5+ cells
LGR5low
LGR5high
e)
CD
0.0312
Freq. of TLR5+ cells
LGR5low
LGR5high
f)
LGR5high
ns
Freq. of TLR5+ cells
Healthy
CD

Figure 21: *Ex vivo* epithelial TLR5 expression by CD-affected and non-inflamed intestinal tissue samples. N = 6 non-inflamed tissue samples and N = 6 inflamed CD tissue samples were obtained freshly after surgery from University Hospital Hamburg Eppendorf and processed within one day. The intestinal epithelial layer was isolated and stored at -180 °C until the antibody staining and measurement. a) Gating strategy: Cells were gated on single live and further on EpCAM-positive and CD45-negative cells and separated into LGR5 low and LGR5 high-positive cells. b) CD45-positive cells were gated on monocytes based on FSC and SSC. Monocytes separated into TLR5-positive and negative cells, which determined the gate setting. c) Representative flow plots showing increased TLR5 frequencies in LGR5 high positive stem cells in CD-affected intestines. d) Summarized data showing frequencies of TLR5-positive epithelial cells in LGR5 low and high-positive cells from non-inflamed intestines. e) Summarized data showing frequencies of TLR5-positive cells in LGR5 low and high-positive cells from CD-affected intestines. f) Comparison of TLR5 frequencies in LGR5 high-positive cells from non-inflamed and CD-affected tissues.

4. Discussion

Previous studies highlighted the increased abundance of CDCA in the intestines of individuals with CD.[267,268] In this project, the influence of CDCA on intestinal epithelial cells was investigated using a human intestinal organoid model. CDCA stimulation negatively affected epithelial cell regeneration in a concentration-dependent manner, as shown by decreased intestinal organoid sizes. In addition, CDCA stimulation resulted in cytosolic calcium influx by epithelial cells independent of prior long-term CDCA exposure, highlighting its potential to activate various signaling pathways. Given the reduced epithelial growth due to CDCA exposure, we mimicked defective epithelial barrier functions by stimulating organoids with bacterial flagellin, which is the ligand for TLR5. TLR5 signaling induced by flagellin stimulation resulted in a significantly increased expression of *CCL20* and *IL-1β* by epithelial cells in intestinal organoids. The same trend was observed for *TNF* and *CXCL8* gene expression after flagellin stimulation in epithelial cells. CDCA synergistically increased the flagellin-induced expression of *CCL20* and *IL-1β* in epithelial cells derived from organoid cultures. In addition, flagellin-induced TLR5 signaling resulted in the increased production of CXCL8, CCL20, IL-1β, TNF, IL-33, and CXCL9, detected in organoid culture supernatants. CDCA synergistically increased the flagellin-induced production of CXCL8, indicating that CDCA increases TLR5 signaling in epithelial cells. The same trend was seen for CCL20 and TNF production by epithelial cells upon CDCA pretreatment before flagellin stimulation of epithelial cells in organoids. In an untargeted bulk RNA sequencing approach, differentially expressed genes in response to CDCA were identified. These genes have potential functions in epithelial regeneration and inflammation while being not directly linked to TLR5 signaling. To directly quantify the expression of TLR5 at the protein and mRNA levels, a targeted approach using flow cytometry and RT qPCR was employed with an increased sample size. CDCA treatment resulted in elevated mRNA and protein levels of TLR5 in epithelial cells within organoids, likely explaining the heightened secretion of cytokines and chemokines induced by TLR5 signaling after CDCA pretreatment. Lastly, intestinal stem cells of individuals with CD also showed higher TLR5 expression levels compared to other epithelial cells in CD-affected intestines *ex vivo*. However, TLR5 expression did not differ significantly between epithelial cells from non-inflamed and CD-affected tissues. Figure 22 summarizes the results of the current study in a model. This project highlights the potential of intestinal organoids to study the impact of metabolic factors, such as bile acids, on intestinal health. By combining experimental analyses with clinical data, future studies may help to identify pathophysiological mechanisms in the intestinal epithelium contributing to IBD, which may identify targets to improve treatment options for IBD.

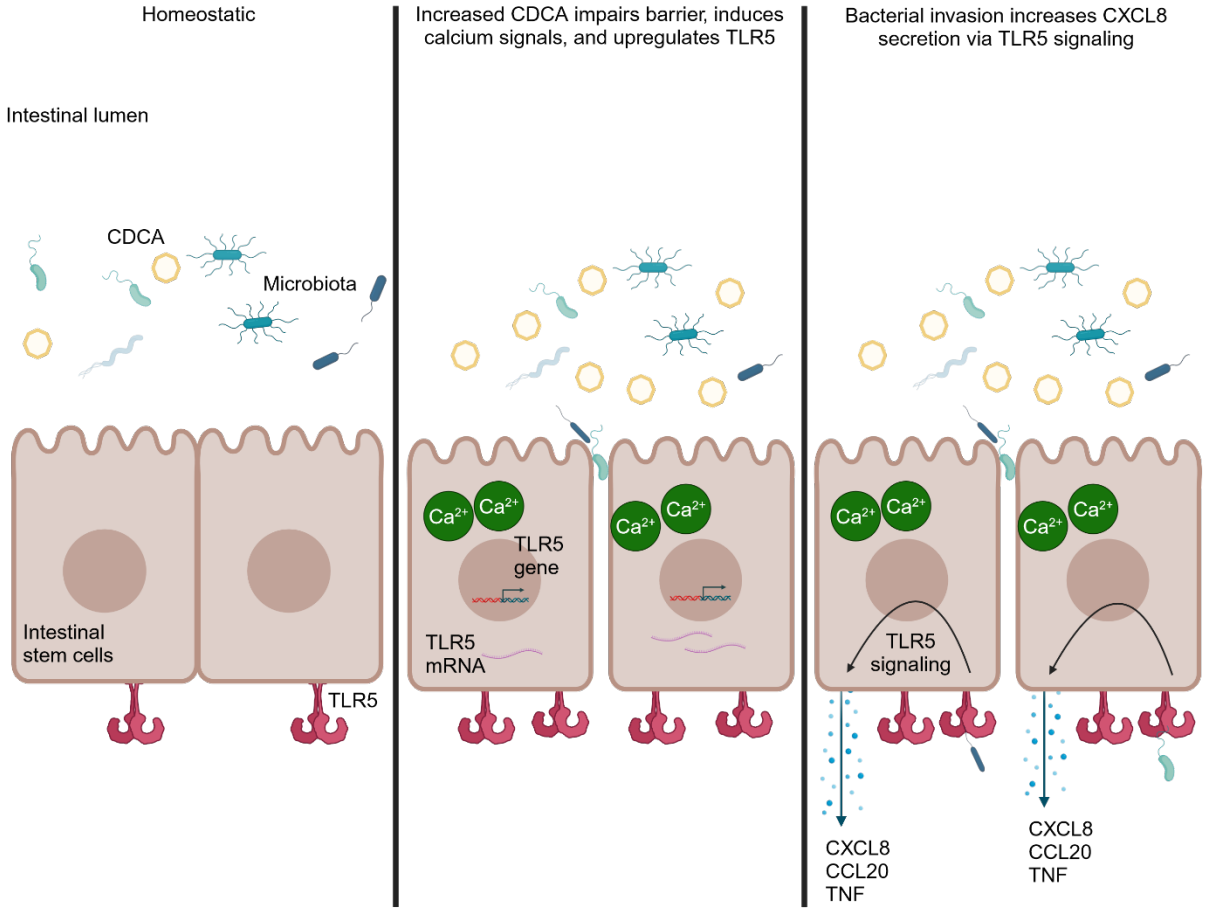

Figure 22: Model of CDCA-induced impaired intestinal epithelial barrier function and inflammation. Increased CDCA levels can impair barrier function and upregulated TLR5 on epithelial cells. Further, CDCA induces calcium signaling, and TLR5 activation leads to increased release of proinflammatory chemokines and cytokines such as CXCL8, CCL20, and TNF. Created with bioRender.com

4.1 Effects of CDCA on epithelial regeneration

We used human intestinal organoids to study the effect of different CDCA concentrations on epithelial regeneration. In these experiments 1 and 10 µM CDCA did not affect organoid sizes. Fourteen days of culture in 100 µM CDCA significantly reduced organoid sizes, indicating defects in epithelial regeneration. 250 and 500 µM CDCA did not allow organoid generation. The physiological concentration of bile acids in the small intestine depends on the reabsorption rate and their modification by intestinal microbes.[213] The postprandial bile acid concentration ranges from 2 to 10 mM in the human small intestinal lumen.[269] Another study showed that the postmortem bile acid pool in the cecum is composed of 7-8% CDCA, indicating that the concentrations used in the experiments in the current study are within the physiological range.[270]

The exact mechanisms by which increased CDCA levels impair organoid generation remain to be elucidated. Nevertheless, our results align with previous studies. For example, a previous publication showed DCA and CDCA-mediated apoptosis via oxidative stress mechanisms in human colon adenocarcinoma cell lines 30 minutes to 2 hours after stimulation. According to the authors, bile acid-induced apoptosis is a result of oxidative stress with increased production of reactive oxygen species (ROS) due to the activity of the plasma membrane oxidases nicotinamide adenine dinucleotide phosphate oxidase (NAD(P)H) and phospholipase A2 (PLA_2).[271] Interestingly, ROS production was shown to be induced by highly hydrophobic bile acids CDCA and DCA but not by less hydrophobic bile acids CA and UDCA.[272] Another study showed that CDCA increases ROS production and impairs mitochondrial membrane potentials induced by caspase-9 and caspase-3 pathways.[273]

Increased ROS production can lead to cell death via different mechanisms, including apoptosis, ferroptosis, autophagy-mediated cell death, and necroptosis.[274] Whether ROS-mediated cell death is also responsible for reduced organoid formation and reduced epithelial regeneration, as shown in our project, remains to be answered. Future studies could utilize ROS-specific fluorescent markers that could be detected by flow cytometry. This would also highlight the potential use of antioxidants to prevent the cytotoxic effects of CDCA-induced oxidative stress and barrier dysfunction. The abundance of oxidative stress in the inflamed mucosa of individuals diagnosed with IBD has already been reported by the quantification of 8-oxo-2'-deoxyguanosine as a biomarker of oxidized DNA in biopsies.[275] In line with that, some studies have shown the beneficial effect of dietary antioxidants in individuals with IBD.[276] However, not all the studies could show such beneficial effects.[277] Another approach to reduce ROS production in IBD is, for example, the inhibition of ROS-producing enzymes. A recent study showed promising results in reducing ROS production in cancer cells by

inhibiting NAD(P)H oxidase *in vitro*.[278]

We performed bulk RNA sequencing on CDCA-stimulated organoids and found differential gene expression in stimulated organoids. We saw increased expression of ANXA10. Although its functions are largely unknown, previous studies showed a potential role of this protein in regulating growth, making this protein a potentially important target for future research on epithelial regeneration.[279] ANXA10 is significantly downregulated in liver hepatocellular carcinoma and its overexpression inhibits the growth of immortalized hepatocellular cell lines *in vitro*.[279] However, the effect of increased ANXA10 expression in intestinal epithelial cells in the context of IBD is unknown. Still, it might be involved in IBD pathogenesis since it is also highly overexpressed in the CD-affected ileum.[193] If ANXA10 could be involved in reduced epithelial regeneration, thereby leading to defects in the epithelial barrier, needs further investigations. Intestinal organoids from individuals with UC also show increased expression of ANXA10.[280] A multi-omics study showed increased expression of ANXA10 in microbiota dysbiotic individuals with IBD.[267]

Additionally, we saw reduced expression of DTD1. Previous studies showed an essential role of the DTD1 protein in initiating DNA replication by interactions with unwinding elements.[281] Whether the differential expression of these two candidates is responsible for the reduced growth of human organoids and how CDCA regulates their expression requires further research.

Impaired barrier function in IBD is a major driver of pathogenesis.[282] Investigating the molecular mechanisms behind the CDCA-induced epithelial growth defects has the potential to identify targets that may improve treatment options for CD-affected individuals that also show a dysregulated bile acid metabolism.

4.2 Effects of CDCA on flagellin-induced cytokine expression by epithelial cells

The results above showed reduced organoid growth, indicating dysregulated barrier functions due to CDCA exposure. To mimic epithelial invasion by motile bacteria, we stimulated CDCA-treated organoids with bacterial flagellin. Flagellin induced the expression of chemokines and cytokines by epithelial cells. Notably, we observed increased flagellin-induced mRNA levels of *CCL20* and *IL-1β* when organoids were pretreated with CDCA. This synergistic effect of CDCA was not observed for *CXCL8* and *TNF.* However, the short lifespan of mRNA necessitates appropriate timing of cell harvest after stimulation. In the experiments, mRNA expression was determined after 24 hours of flagellin stimulation, which might be too late to detect differences in some cases. To complement these results, we utilized a Luminex Discovery Assay, enabling the quantification of secreted proteins in the cell culture supernatant. In these analyses specifically, significantly increased levels of CXCL8 and trends of increased TNF and CCL20 levels in culture supernatants were observed when organoids were pretreated with CDCA before the flagellin stimulation. These findings highlight the importance of considering the potential temporal dynamics of different gene expressions and posttranscriptional regulation.

To investigate the underlying mechanism for increased TLR5 signaling, an untargeted and a targeted approach were taken. Although some genes were differentially transcribed upon CDCA stimulation of organoids, obvious candidates for increased TLR5 signaling were not observed, likely due to the limited numbers of samples included in the bulk RNA sequencing. However, when quantifying TLR5 protein and mRNA directly by flow cytometry and RT qPCR, increased TLR5 expression in organoids stimulated with CDCA was observed. Increased levels of TLR5 upon CDCA stimulation could explain the increased production of CXCL8 and the trend of increased release of CCL20 and TNF due to increased signaling downstream of TLR5 activation. However, CDCA may also affect specific cytokines as only a few and not all of the genes downstream of TLR5 signaling were higher expressed when organoids were treated with CDCA prior to flagellin stimulation. This highlights the importance of future studies to investigate the effect of CDCA on posttranscriptional regulation mechanisms that influence genes downstream of TLR5 signaling as, for instance, IL-1β, IL-33, and CXCL9. One possible explanation is that in epithelial cells, regulatory mechanisms downstream of TLR5 signaling balance the secretion of cytokines and that CXCL8, CCL20, and TNF are not or less affected by such regulations. A potential mechanism that could inhibit the secretion of mature IL-1β is the cleavage of pro-IL-1β to its mature form by caspase-1.[283] However, previous studies have shown that CDCA increases

caspase-1 activation in mouse liver macrophages, which would increase production and secretion of IL-1β.[284] Until now it is unclear how CDCA may affect caspase-1 activity and, therefore, mature IL-1β secretion in humans.

Previous studies of intestinal samples affected by IBD have shown an increased abundance of CXCL8, CCL20, and TNF in inflamed regions.[208,285,286] CXCL8 functions as a chemoattractant for cells expressing its respective receptors, C-X-C motif chemokine receptor 1 (CXCR1) and C-X-C motif chemokine receptor 2 (CXCR2), that are mainly present on neutrophils, thereby mediating a fast innate immune response.[287] Interestingly, neutrophils are also found in inflamed intestinal tissues of individuals diagnosed with IBD.[288] CXCR1 and CXCR2 have also been shown to be expressed on other cell types, such as epithelial and endothelial cells, fibroblasts, and neurons, indicating additional functions beyond immune cell recruitment, such as tissue homeostasis and regeneration.[289] In addition, a trend towards increased CCL20 and TNF production upon flagellin stimulation by CDCA-pretreated epithelial cells was observed compared to flagellin-only treated organoid cultures. CCL20 is a chemoattractant for cells expressing the respective receptor CCR6.[290] CCR6 is expressed by various T cell types, including Th17 cells, which are detected in higher frequencies in IBD intestinal tissue samples than in non-inflamed tissues.[291] An increased release of CCL20 promotes the induction of adaptive immune responses initiated by T cells.[292] TNF binding to its respective TNF receptors leads to the induction of proinflammatory processes, including apoptotic cell death and lymphocyte maturation, thereby playing a fundamental role in infectious and inflammatory diseases.[293] IL-33, an alarmin that is involved in the initiation of type 2 immune responses, was released by epithelial cells in organoids in response to flagellin.[128] However, its levels in organoid cultures were unchanged by pretreatment with CDCA, indicating that CDCA does not increase type 2 immunological responses mediated by IL-33 in the intestinal epithelium.

To study the direct impact of an altered cytokine and chemokine microenvironment induced by CDCA and flagellin on intestinal immune cells, future studies could utilize co-culture models of epithelial organoids with immune cells. Previously we have shown that a TNF-containing inflammatory cytokine environment can contribute to immune-mediated tissue damage by NK cells in the context of UC, highlighting the importance of studying the cytokine and chemokine profiles that are generated by the intestinal epithelium.[167]

TNF is involved in the polarization of macrophages to proinflammatory M1-like macrophages.[294] The CDCA-mediated increased release of TNF in flagellin-stimulated epithelial cells may thereby contribute to increased accumulation of this macrophage subtype.

In IBD, increased activation and accumulation of proinflammatory M1-like macrophages in inflamed intestinal lesions have been reported.[295] In addition to the secretion of proinflammatory cytokines, M1 macrophages have also been shown to contribute to barrier defects by inducing epithelial cell apoptosis and altered expression of tight junctional proteins.[296] Interestingly, anti-TNF therapy leads to the induction of regulatory macrophage phenotypes involved in healing processes during IBD.[296]

Here, we could show that increased levels of epithelial cytokines and chemokines released in response to a combination of CDCA and flagellin correspond to cytokines and chemokines that have been found in inflamed IBD-affected intestines, indicating a potential pathophysiological role of CDCA by the increase of flagellin-induced chemokine and cytokine responses in the intestinal epithelium.

4.3 Effects of CDCA on TLR5 expression

We could observe increased expression of TLR5 in organoids stimulated with CDCA on mRNA and protein levels, indicating that CDCA alters the transcriptional regulation of TLR5 rather than affecting protein stability or posttranscriptional regulation.

The TLR5 gene contains regulatory elements, including transcription factor binding sites for jun proto-oncogene, AP-1 transcription factor subunit (AP-1), Sp-family of transcription factors, NF-κB, early growth response factor 1 (egr-1), and MYC proto-oncogene, bHLH transcription factor (c-Myc) upstream of the transcription start site.[297] In a colon carcinoma cell line, the Sp-family of transcription factors is the primary regulator of TLR5 transcription.[297] TLR5 transcription is regulated by the dephosphorylation or acetylation of Sp1 by serine or threonine phosphatases and simultaneous phosphorylation of Sp3 by extracellular signal-regulated kinase - mitogen-activated protein kinase (ERK-MAPK) signaling.[297] This results in the movement of Sp1 from the promoter region and the binding of Sp3, co-activator p300 recruitment, histone acetylation, and transcription.[297] Interestingly, butyrate, a microbiota-derived metabolite in the intestinal lumen, can alter this transcriptional regulation.[297] Additionally, pharmacological inhibition of the Sp-family of transcription factors with mithramycin ameliorates rodent colitis.[298] Our bulk RNA sequencing data did not show CDCA-induced differential expression of respective transcription factors. However, regulation of transcription factors mostly depends on (de-)phosphorylation or translocation into the nucleus and should, therefore, be investigated in the future with other approaches, such as western blotting and imaging techniques.[299]

MAPK signaling pathways play essential roles in cellular signaling transduction and affect various cellular processes. So far, different MAPK pathways involving different key mediators have been identified, including ERK1/2, JNK, and p38 mitogen-activated protein kinases (p38). Interestingly, ERK1/2 and JNK pathways can result in the phosphorylation of Sp1 showing the potential to also activate TLR5 gene expression.[300,301] Multiple bile acids, including CDCA, can activate ERK-MAPK signaling cascades.[302] Interestingly, previous studies showed the ERK-MAPK activation via unconjugated bile acids depends on reactive oxygen species.[302] Moreover, MAPK signaling involves a cytosolic calcium influx.[303,304] Importantly, CDCA induced a cytosolic calcium influx in intestinal organoids, highlighting the potential to induce such pathways.

Further experiments are needed to understand the molecular mechanisms of how CDCA increases TLR5 expression in the intestinal epithelium. Activation of the ERK-MAPK pathway and Sp-1/3-mediated promoter activation of TLR5 may play a substantial role in this context.

TLR5 expression by epithelial cells depends on the localization within the intestinal epithelial layer.[305] Previous studies suggest that TLR expression is absent in the distal colon

but present on both the apical and the basolateral site of the proximal colon.[106] In the ileum, TLR5 expression is limited to the crypts.[106] Previous studies showed increased TLR5 expression in CD-affected intestines on RNA but not on a protein level.[193] However, it is unclear what triggers this increased expression. In our experiments, we detected TLR5 expression in LGR5-positive stem cells and, to a limited extent, in other epithelial cell types with low expression of LGR5. Interestingly, the difference in TLR5 expression in stem cells and other epithelial cells was present in CD individuals but not in healthy individuals, indicating that TLR5 expression can increase upon barrier dysfunctions. However, the sample size is limited to six CD and six non-inflamed tissue samples. Samples were collected upon surgical removal and processed as soon as possible. Moreover, due to freezing and thawing procedures, the TLR5 expression on the surface of cells may have changed until the analysis was performed. Therefore, future studies should investigate TLR5 expression directly after procurement of the samples without prior cryopreservation or directly with immunohistochemistry stainings of fixed tissue samples. Furthermore, future studies should directly investigate the relationship of CDCA levels and TLR5 expression in the intestinal epithelium. For the intestinal samples we obtained, no data about the bile acid content in affected intestines were available. Such studies could directly link the relationship of the bile acid pool in inflamed lesions of CD affected intestines and investigate whether TLR5 expression and CDCA concentrations in inflamed lesions correlate.

TLR5 is expressed by various cell types, not only epithelial cells but also for example lamina propria dendritic cells, which play a major role in the induction of Th17 cells that are associated with the pathogenesis of IBD.[306] TLR5 activation must be carefully regulated since its binding to flagellin initiates strong inflammatory immune responses to counteract the potential bacterial infection.[307] However, bacteria in the gut microbiome must not be harmful as some commensal species are important in the generation of immunological tolerance and by fulfilling beneficial metabolic functions.[308] Therefore, the localization and regulation of TLR5 expression in the intestinal mucosa is critical. It will be interesting to further investigate whether CDCA that enters the lamina propria due to increased abundance and barrier defects can also increase TLR5 expression by dendritic and other immune cells.

4.4 Organoids in immunometabolism research

In this project, the effect of CDCA on epithelial regeneration and inflammation was investigated by using organoids from human intestines. We used EM organoid cultures that have been shown to contain mainly intestinal stem cells but also other epithelial cell types, including Paneth cells, which have been shown to express TLR5.[106,248] Importantly, research

questions requiring other epithelial cell types can be addressed with this model since the differentiation of intestinal stem cells to different epithelial cell types can be induced by adapting culture conditions.[309]

We provide an example of how the inflammatory capacities of the human intestinal epithelium in response to dietary factors and metabolites can be studied. Many candidates have been shown to affect the mucosal immune system in the gut, including different fatty acids and short-chain fatty acids.[310,311] However, most of these studies were performed with immortalized cell lines or mouse models, which differ significantly from the human *in vivo* situation. Also, the bile acid pool differs between humans and mice.[312] In mice, CDCA is further hydroxylated to muricholic acids (MCAs) with distinct signaling capacities.[84] The reaction is mediated by Cyp2c70 that is absent in humans.[313] As no enzyme with related catalytic properties exists in humans, MCAs are absent in humans.[313]

For dietary lipids, it has been shown that diets with high amounts of saturated fatty acids increase inflammation and the risk of chronic diseases.[314] Palmitic acid can directly affect the release of proinflammatory cytokines such as IL-6 and CXCL8 by macrophages and T cells.[315,316] The underlying mechanisms of the inflammatory response are not well understood. Previous studies indicated that palmitic acid can directly act as an agonist of TLR4, whereas other studies proposed that an altered lipidome changes the macrophage phenotype towards a proinflammatory M1 phenotype.[317,318] Moreover, palmitic acid has a direct effect on the gut epithelial barrier and inflammatory cytokine production by epithelial cells in a mouse model.[319] As the great majority of these studies have been performed in immortalized cell lines or animal models, it is unclear how translatable these findings are to the human *in vivo* situation. Organoids and organoids co-cultured with immune cells depict an alternative model for studying the direct effects of palmitic acid and other fatty acids on the human intestinal epithelium as they can be added directly to the cultures.

In addition to organoid co-cultures with immune cells, organoid co-cultures with bacteria have been established.[244] Further improvements of such systems can be used in the future to increase the understanding of the complex interplay between the dietary factors inducing bile acids, microbiota, intestinal epithelium, and immune cells in humans. Similar to cell lines and *in vivo* models, organoids can be genetically modified by clustered regularly interspaced short palindromic repeats and CRISPR associated protein 9 (CRISPR-Cas9), which can be utilized to study the effect of specific genes on human intestinal physiology.[320] Moreover, several companies provide organs-on-chip models with microfluidic systems that enable research on organ crosstalk.[321] This is particularly useful for the intestines since they collaborate closely with other organs, such as the liver and the central nervous system. Especially the dynamics of bile acid metabolism and enterohepatic circulation in different parts of the intestines and between different organs such as the liver and the bile duct can,

therefore, be studied in a setting that mimics the human situation more closely than other models.

4.5 Conclusion

In this thesis, the effects of CDCA on epithelial regeneration and inflammation were investigated. Using intestinal organoids generated from human intestinal samples, this study showed that CDCA impairs epithelial regeneration, indicated by reduced organoid sizes. CDCA also initiates intracellular calcium signals and increases epithelial flagellin-induced production of proinflammatory chemokines and cytokines in organoids. This increase may be explained by increased TLR5 expression of epithelial cells that were pretreated with CDCA. Considering the increased abundance of CDCA in IBD-affected intestines, these observations may contribute to decreased intestinal barrier functions and increased proinflammatory responses in CD-affected intestines. Future studies are needed to understand the intracellular effects of bile acids in the intestinal epithelium, which lead to the observed outcomes.

5. References

1. Treuting, P. M., Valasek, M. A. & Dintzis, S. M. Upper Gastrointestinal Tract. *Comparative Anatomy and Histology* 155–175 (2012) doi:10.1016/B978-0-12-381361-9.00011-1.

2. Treuting, P. M., Arends, M. J. & Dintzis, S. M. Lower Gastrointestinal Tract. in *Comparative Anatomy and Histology* 213–228 (Elsevier, 2018). doi:10.1016/b978-0-12-802900-8.00012-9.

3. Cigliola, V. *et al.* Role of connexins and pannexins in the pancreas. *Pancreas* **44**, 1234–1244 (2015).

4. Sibulesky, L. Normal liver anatomy. *Clin Liver Dis (Hoboken)* **2**, (2013).

5. Guan, H., Zhang, X., Kuang, M. & Yu, J. The gut–liver axis in immune remodeling of hepatic cirrhosis. *Front Immunol* **13**, 946628 (2022).

6. Andersson-Rolf, A., Zilbauer, M., Koo, B. K. & Clevers, H. Stem cells in repair of gastrointestinal epithelia. *Physiology* **32**, 278–289 (2017).

7. Farin, H. F., Van Es, J. H. & Clevers, H. Redundant sources of Wnt regulate intestinal stem cells and promote formation of Paneth cells. *Gastroenterology* **143**, (2012).

8. Takahashi, T. & Shiraishi, A. Stem Cell Signaling Pathways in the Small Intestine. *Int J Mol Sci* **21**, (2020).

9. Fevr, T., Robine, S., Louvard, D. & Huelsken, J. Wnt/β-Catenin Is Essential for Intestinal Homeostasis and Maintenance of Intestinal Stem Cells. *Mol Cell Biol* **27**, 7551–7559 (2007).

10. Abud, H. E., Chan, W. H. & Jardé, T. Source and Impact of the EGF Family of Ligands on Intestinal Stem Cells. *Front Cell Dev Biol* **9**, (2021).

11. de Lau, W., Peng, W. C., Gros, P. & Clevers, H. The R-spondin/Lgr5/Rnf43 module: regulator of Wnt signal strength. *Genes Dev* **28**, 305 (2014).

12. Verheyen, E. M. & Gottardi, C. J. Regulation of Wnt/β-catenin signaling by protein kinases. *Developmental Dynamics* **239**, 34–44 (2010).

13. Fevr, T., Robine, S., Louvard, D. & Huelsken, J. Wnt/β-Catenin Is Essential for Intestinal Homeostasis and Maintenance of Intestinal Stem Cells. *Mol Cell Biol* **27**, 7551–7559 (2007).

14. Hsu, Y. C., Li, L. & Fuchs, E. Transit-Amplifying Cells Orchestrate Stem Cell Activity and Tissue Regeneration. *Cell* **157**, 935–949 (2014).

15. Hageman, J. H. *et al.* Intestinal Regeneration: Regulation by the Microenvironment. *Dev Cell* **54**, 435–446 (2020).

16. Farin, H. F. *et al.* Visualization of a short-range Wnt gradient in the intestinal stem-cell niche. *Nature 2016 530:7590* **530**, 340–343 (2016).

17. Beumer, J. *et al.* BMP gradient along the intestinal villus axis controls zonated enterocyte and goblet cell states. *Cell Rep* **38**, 110438 (2022).

18. Sanman, L. E. *et al.* Transit-Amplifying Cells Coordinate Changes in Intestinal Epithelial Cell-Type Composition. *Dev Cell* **56**, 356-365.e9 (2021).

19. Gregorieff, A. *et al.* Expression Pattern of Wnt Signaling Components in the Adult Intestine. *Gastroenterology* **129**, 626–638 (2005).

20. Van Der Flier, L. G. & Clevers, H. Stem cells, self-renewal, and differentiation in the intestinal epithelium. *Annu Rev Physiol* **71**, 241–260 (2009).

21. Clevers, H. The Intestinal Crypt, A Prototype Stem Cell Compartment. *Cell* **154**, 274–284 (2013).

22. Haramis, A. P. G. *et al.* De Novo Crypt Formation and Juvenile Polyposis on BMP Inhibition in Mouse Intestine. *Science (1979)* **303**, 1684–1686 (2004).

23. Sato, T. *et al.* Long-term expansion of epithelial organoids from human colon, adenoma, adenocarcinoma, and Barrett's epithelium. *Gastroenterology* **141**, 1762–1772 (2011).

24. Günther, C., Neumann, H., Neurath, M. F. & Becker, C. Apoptosis, necrosis and necroptosis: cell death regulation in the intestinal epithelium. *Gut* **62**, 1062–1071 (2013).

25. Pimentel-Muiños, F. X. Autophagy in the gastrointestinal system and cross talk with microbiota. *Autophagy in Health and Disease* 321–333 (2022) doi:10.1016/B978-0-12-822003-0.00016-4.

26. Antfolk, M. & Jensen, K. B. A bioengineering perspective on modelling the intestinal epithelial physiology in vitro. *Nat Commun* **11**, (2020).

27. Sensoy, I. A review on the food digestion in the digestive tract and the used in vitro models. *Curr Res Food Sci* **4**, 308–319 (2021).

28. Patricia, J. J. & Dhamoon, A. S. Physiology, Digestion. *StatPearls* (2022).

29. Wright, E. M., Martín, M. G. & Turk, E. Intestinal absorption in health and disease—sugars. *Best Pract Res Clin Gastroenterol* **17**, 943–956 (2003).

30. Thorens, B. & Mueckler, M. Glucose transporters in the 21st Century. *Am J Physiol Endocrinol Metab* **298**, E141 (2010).

31. Heda, R., Toro, F. & Tombazzi, C. R. Physiology, Pepsin. *StatPearls* (2023).

32. Lin, L., Yee, S. W., Kim, R. B. & Giacomini, K. M. SLC Transporters as Therapeutic Targets: Emerging Opportunities. *Nat Rev Drug Discov* **14**, 543 (2015).

33. Sheng, L., Luo, Q. & Chen, L. Amino Acid Solute Carrier Transporters in Inflammation and Autoimmunity. *Drug Metab Dispos* **50**, 1228–1237 (2022).

34. Iqbal, J. & Hussain, M. M. Intestinal lipid absorption. *Am J Physiol Endocrinol Metab* **296**, (2009).

35. Beck, I. T. The role of pancreatic enzymes in digestion. *Am J Clin Nutr* **26**, 311–325 (1973).

36. Wright, E. M., Martín, M. G. & Turk, E. Intestinal absorption in health and disease—sugars. *Best Pract Res Clin Gastroenterol* **17**, 943–956 (2003).

37. Thorens, B. & Mueckler, M. Glucose transporters in the 21st Century. *Am J Physiol Endocrinol Metab* **298**, E141 (2010).

38. Heda, R., Toro, F. & Tombazzi, C. R. Physiology, Pepsin. *StatPearls* (2023).

39. Lin, L., Yee, S. W., Kim, R. B. & Giacomini, K. M. SLC Transporters as Therapeutic Targets: Emerging Opportunities. *Nat Rev Drug Discov* **14**, 543 (2015).

40. Sheng, L., Luo, Q. & Chen, L. Amino Acid Solute Carrier Transporters in Inflammation and Autoimmunity. *Drug Metab Dispos* **50**, 1228–1237 (2022).

41. Iqbal, J. & Hussain, M. M. Intestinal lipid absorption. *Am J Physiol Endocrinol Metab* **296**, (2009).

42. Ahmed, S., Shah, P. & Ahmed, O. Biochemistry, Lipids. *StatPearls* (2023).

43. Cheng, H. M., Mah, K. K. & Seluakumaran, K. Fat Digestion: Bile Salt, Emulsification, Micelles, Lipases, Chylomicrons. *Defining Physiology: Principles, Themes, Concepts. Volume 2* 63–65 (2020) doi:10.1007/978-3-030-62285-5_18.

44. Ros, E. Intestinal absorption of triglyceride and cholesterol. Dietary and pharmacological inhibition to reduce cardiovascular risk. (2000).

45. Den Besten, G. *et al.* The role of short-chain fatty acids in the interplay between diet, gut microbiota, and host energy metabolism. *J Lipid Res* **54**, 2325 (2013).

46. Donaldson, G. P., Lee, S. M. & Mazmanian, S. K. Gut biogeography of the bacterial microbiota. *Nature Reviews Microbiology 2015 14:1* **14**, 20–32 (2015).

47. Vijay, A. & Valdes, A. M. Role of the gut microbiome in chronic diseases: a narrative review. *European Journal of Clinical Nutrition 2021 76:4* **76**, 489–501 (2021).

48. Canani, R. B. *et al.* Potential beneficial effects of butyrate in intestinal and extraintestinal diseases. *World Journal of Gastroenterology : WJG* **17**, 1519 (2011).

49. Chen, J. & Vitetta, L. Butyrate in Inflammatory Bowel Disease Therapy. *Gastroenterology* **158**, 1511 (2020).

50. Spragge, F. *et al.* Microbiome diversity protects against pathogens by nutrient blocking. *Science (1979)* **382**, (2023).

51. Belkaid, Y. & Hand, T. W. Role of the Microbiota in Immunity and Inflammation. *Cell* **157**, 121–141 (2014).

52. Liu, B. N., Liu, X. T., Liang, Z. H. & Wang, J. H. Gut microbiota in obesity. *World J Gastroenterol* **27**, 3837 (2021).

53. Round, J. L. & Mazmanian, S. K. The gut microbiota shapes intestinal immune responses during health and disease. *Nature Reviews Immunology 2009 9:5* **9**, 313–323 (2009).

54. Zheng, D., Liwinski, T. & Elinav, E. Interaction between microbiota and immunity in health and disease. *Cell Research 2020 30:6* **30**, 492–506 (2020).

55. Staels, B. & Fonseca, V. A. Bile Acids and Metabolic Regulation: Mechanisms and clinical responses to bile acid sequestration. *Diabetes Care* **32**, S237 (2009).

56. Roberts, M. S., Magnusson, B. M., Burczynski, F. J. & Weiss, M. Enterohepatic Circulation. *Clinical Pharmacokinetics 2002 41:10* **41**, 751–790 (2012).

57. Ziessman, H. A., O'Malley, J. P. & Thrall, J. H. Hepatobiliary System. *Nuclear Medicine* 159–214 (2006) doi:10.1016/B978-0-323-02946-9.50012-X.

58. Pandak, W. M. & Kakiyama, G. The acidic pathway of bile acid synthesis: Not just an alternative pathway. *Liver Res* **3**, 88–98 (2019).

59. Chiang, J. Y. L. Bile Acid Metabolism and Signaling. *Compr Physiol* **3**, 1191 (2013).

60. Ren, S. *et al.* Regulation of oxysterol 7α-hydroxylase (CYP7B1) in the rat. *Metabolism* **52**, 636–642 (2003).

61. Nagana Gowda, G. A., Shanaiah, N., Cooper, A., Maluccio, M. & Raftery, D. Bile Acids Conjugation in Human Bile Is Not Random: New Insights from 1H-NMR Spectroscopy at 800 MHz. *Lipids* **44**, 527 (2009).

62. Carey, M. C. Bile acids and bile salts: ionization and solubility properties. *Hepatology* **4**, 66S-71S (1984).

63. Grant, S. M. & Demorrow, S. Bile Acid Signaling in Neurodegenerative and Neurological Disorders. *International Journal of Molecular Sciences 2020, Vol. 21, Page 5982* **21**, 5982 (2020).

64. Fiorucci, S. & Distrutti, E. Linking liver metabolic and vascular disease via bile acid signaling Molecular Medicine. *Trends Mol Med* **28**, 51–66 (2022).

65. Fuchs, C. D. & Trauner, M. Role of bile acids and their receptors in gastrointestinal and hepatic pathophysiology. *Nature Reviews Gastroenterology & Hepatology 2022 19:7* **19**, 432–450 (2022).

66. Cai, J. S. & Chen, J. H. The Mechanism of Enterohepatic Circulation in the Formation of Gallstone Disease. *J Membr Biol* **247**, 1067 (2014).

67. Ballatori, N., Christian, W. V., Wheeler, S. G. & Hammond, C. L. The heteromeric organic solute transporter, OSTα–OSTβ/SLC51: A transporter for steroid-derived molecules. *Mol Aspects Med* **34**, 683–692 (2013).

68. Kliewer, S. A. & Mangelsdorf, D. J. Bile Acids as Hormones: The FXR-FGF15/19 Pathway. *Dig Dis* **33**, 327 (2015).

69. Somm, E. & Jornayvaz, F. R. Fibroblast Growth Factor 15/19: From Basic Functions to Therapeutic Perspectives. *Endocr Rev* **39**, 960–989 (2018).

70. Han, S. & Chiang, J. Y. L. Mechanism of vitamin D receptor inhibition of cholesterol 7alpha-hydroxylase gene transcription in human hepatocytes. *Drug Metab Dispos* **37**, 469–478 (2009).

71. Jonker, J. W., Liddle, C. & Downes, M. FXR and PXR: Potential therapeutic targets in cholestasis. *J Steroid Biochem Mol Biol* **130**, 147 (2012).

72. Matijašić, M. *et al.* Gut Microbiota beyond Bacteria—Mycobiome, Virome, Archaeome, and Eukaryotic Parasites in IBD. *Int J Mol Sci* **21**, (2020).

73. Bourgin, M. *et al.* Bile Salt Hydrolases: At the Crossroads of Microbiota and Human Health. *Microorganisms* **9**, (2021).

74. Yang, M. *et al.* Bile Acid–Gut Microbiota Axis in Inflammatory Bowel Disease: From Bench to Bedside. *Nutrients 2021, Vol. 13, Page 3143* **13**, 3143 (2021).

75. Xie, J., Lee, K., Park, H., Jung, H. & Oh, J. M. Enhanced Emulsifying Ability of Deoxycholate through Dynamic Interaction with Layered Double Hydroxide. *Nanomaterials* **13**, 567 (2023).

76. Bera, T. & Fang, J. Optical detection of lithocholic acid with liquid crystal emulsions. *Langmuir* **29**, 387–392 (2013).

77. Collins, S. L., Stine, J. G., Bisanz, J. E., Okafor, C. D. & Patterson, A. D. Bile acids and the gut microbiota: metabolic interactions and impacts on disease. *Nature Reviews Microbiology 2022 21:4* **21**, 236–247 (2022).

78. Takeda, M. *et al.* Bile acid profiles in adult patients with biliary atresia who achieve native liver survival after portoenterostomy. *Scientific Reports 2024 14:1* **14**, 1–9 (2024).

79. Mousa, O. Y. *et al.* Bile Acid Profiles in Primary Sclerosing Cholangitis and their Ability to Predict Hepatic Decompensation. *Hepatology* **74**, 281 (2021).

80. Sarathy, J. *et al.* The Yin and Yang of bile acid action on tight junctions in a model colonic epithelium. *Physiol Rep* **5**, e13294 (2017).

81. Shulpekova, Y. *et al.* The Role of Bile Acids in the Human Body and in the Development of Diseases. *Molecules* **27**, (2022).

82. Lou, G. *et al.* GPBAR1/TGR5 mediates bile acid-induced cytokine expression in murine Kupffer cells. *PLoS One* **9**, (2014).

83. Le Bras, A. Humanized mouse models of drug metabolism. *Lab Animal 2024 53:4* **53**, 87–87 (2024).

84. Guo, G. L. & Chiang, J. Y. L. Is CYP2C70 the key to new mouse models to understand bile acids in humans? *J Lipid Res* **61**, 269 (2020).

85. Round, J. L. & Mazmanian, S. K. The gut microbiota shapes intestinal immune responses during health and disease. *Nature Reviews Immunology 2009 9:5* **9**, 313–323 (2009).

86. Zheng, D., Liwinski, T. & Elinav, E. Interaction between microbiota and immunity in health and disease. *Cell Research 2020 30:6* **30**, 492–506 (2020).

87. Allaire, J. M. *et al.* The Intestinal Epithelium: Central Coordinator of Mucosal Immunity. *Trends Immunol* **39**, 677–696 (2018).

88. Mowat, A. M. & Agace, W. W. Regional specialization within the intestinal immune system. *Nature Reviews Immunology 2014 14:10* **14**, 667–685 (2014).

89. Wu, R. Q., Zhang, D. F., Tu, E., Chen, Q. M. & Chen, W. The mucosal immune system in the oral cavity—an orchestra of T cell diversity. *International Journal of Oral Science 2014 6:3* **6**, 125–132 (2014).

90. Spence, J. R., Lauf, R. & Shroyer, N. F. Vertebrate intestinal endoderm development. *Dev Dyn* **240**, 501–520 (2011).

91. Santos, A. J. M., Lo, Y. H., Mah, A. T. & Kuo, C. J. The Intestinal Stem Cell Niche: Homeostasis and Adaptations. *Trends Cell Biol* **28**, 1062 (2018).

92. Sato, T. *et al.* Paneth cells constitute the niche for Lgr5 stem cells in intestinal crypts. *Nature* **469**, 415–418 (2011).

93. Cheroutre, H., Lambolez, F. & Mucida, D. The light and dark sides of intestinal intraepithelial lymphocytes. *Nature Reviews Immunology 2011 11:7* **11**, 445–456 (2011).

94. Denning, T. L., Wang, Y. C., Patel, S. R., Williams, I. R. & Pulendran, B. Lamina propria macrophages and dendritic cells differentially induce regulatory and interleukin 17–producing T cell responses. *Nature Immunology 2007 8:10* **8**, 1086–1094 (2007).

95. Macpherson, A. J. & Smith, K. Mesenteric lymph nodes at the center of immune anatomy. *J Exp Med* **203**, 497 (2006).

96. Jung, C., Hugot, J.-P. & Barreau, F. Peyer's Patches: The Immune Sensors of the Intestine. *Int J Inflam* **2010**, 1–12 (2010).

97. Mowat, A. M. & Agace, W. W. Regional specialization within the intestinal immune system. *Nature Reviews Immunology 2014 14:10* **14**, 667–685 (2014).

98. Neurath, M. F. Targeting immune cell circuits and trafficking in inflammatory bowel disease. *Nature Immunology 2019 20:8* **20**, 970–979 (2019).

99. De Mattos, B. R. R. *et al.* Inflammatory Bowel Disease: An Overview of Immune Mechanisms and Biological Treatments. *Mediators Inflamm* **2015**, (2015).

100. Peterson, L. W. & Artis, D. Intestinal epithelial cells: regulators of barrier function and immune homeostasis. *Nature Reviews Immunology 2014 14:3* **14**, 141–153 (2014).

101. Gustafsson, J. K. & Johansson, M. E. V. The role of goblet cells and mucus in intestinal homeostasis. *Nature Reviews Gastroenterology & Hepatology 2022 19:12* **19**, 785–803 (2022).

102. Song, C. *et al.* Intestinal mucus components and secretion mechanisms: what we do and do not know. *Experimental & Molecular Medicine 2023 55:4* **55**, 681–691 (2023).

103. Muniz, L. R., Knosp, C. & Yeretssian, G. Intestinal antimicrobial peptides during homeostasis, infection, and disease. *Front Immunol* **3**, 32484 (2012).

104. Mahapatro, M., Erkert, L. & Becker, C. Cytokine-Mediated Crosstalk between Immune Cells and Epithelial Cells in the Gut. *Cells* **10**, 1–24 (2021).

105. Song-Zhao, G. X. *et al.* Nlrp3 activation in the intestinal epithelium protects against a mucosal pathogen. *Mucosal Immunol* **7**, 763–774 (2014).

106. Price, A. E. *et al.* A map of Toll-like receptor expression in the intestinal epithelium reveals distinct spatial, cell type-specific, and temporal patterns. *Immunity* **49**, 560 (2018).

107. Mogensen, T. H. Pathogen Recognition and Inflammatory Signaling in Innate Immune Defenses. *Clin Microbiol Rev* **22**, 240 (2009).

108. Yang, D., Han, Z. & Oppenheim, J. J. Alarmins and immunity. *Immunol Rev* **280**, 41–56 (2017).

109. Fukata, M. & Arditi, M. The role of pattern recognition receptors in intestinal inflammation. *Mucosal Immunology 2013 6:3* **6**, 451–463 (2013).

110. Magarian Blander, J. & Blander, M. Phagocytosis and antigen presentation: a partnership initiated by Toll-like receptors. *Ann Rheum Dis* **67**, iii44–iii49 (2008).

111. Fore, F., Indriputri, C., Mamutse, J. & Nugraha, J. TLR10 and Its Unique Anti-Inflammatory Properties and Potential Use as a Target in Therapeutics. *Immune Netw* **20**, (2020).

112. McInturff, J. E., Modlin, R. L. & Kim, J. The Role of Toll-like Receptors in the Pathogenesis and Treatment of Dermatological Disease. *Journal of Investigative Dermatology* **125**, 1–8 (2005).

113. Janssens, S. & Beyaert, R. A universal role for MyD88 in TLR/IL-1R-mediated signaling. *Trends Biochem Sci* **27**, 474–482 (2002).

114. Annunziato, F., Romagnani, C. & Romagnani, S. The 3 major types of innate and adaptive cell-mediated effector immunity. *Journal of Allergy and Clinical Immunology* **135**, 626–635 (2015).

115. Kagnoff, M. F. The intestinal epithelium is an integral component of a communications network. *J Clin Invest* **124**, 2841–2843 (2014).

116. Das, S. T. *et al.* Monomeric and Dimeric CXCL8 Are Both Essential for In Vivo Neutrophil Recruitment. *PLoS One* **5**, e11754 (2010).

117. Hirota, K. *et al.* Preferential recruitment of CCR6-expressing Th17 cells to inflamed joints via CCL20 in rheumatoid arthritis and its animal model. *Journal of Experimental Medicine* **204**, 2803–2812 (2007).

118. Groom, J. R. & Luster, A. D. CXCR3 in T cell function. *Exp Cell Res* **317**, 620–631 (2011).

119. Sokol, C. L. & Luster, A. D. The Chemokine System in Innate Immunity. *Cold Spring Harb Perspect Biol* **7**, 1–20 (2015).

120. Hayashi, F. *et al.* The innate immune response to bacterial flagellin is mediated by Toll-like receptor 5. *Nature 2001 410:6832* **410**, 1099–1103 (2001).

121. Micheau, O. & Tschopp, J. Induction of TNF Receptor I-Mediated Apoptosis via Two Sequential Signaling Complexes. *Cell* **114**, 181–190 (2003).

122. Kolls, J. K., McCray, P. B. & Chan, Y. R. Cytokine-mediated regulation of antimicrobial proteins. *Nat Rev Immunol* **8**, 829 (2008).

123. Sharba, S. *et al.* Interleukin 4 induces rapid mucin transport, increases mucus thickness and quality and decreases colitis and Citrobacter rodentium in contact with epithelial cells. *Virulence* **10**, 97 (2019).

124. Mills, K. H. G. IL-17 and IL-17-producing cells in protection versus pathology. *Nature Reviews Immunology 2022 23:1* **23**, 38–54 (2022).

125. Liu, X. K., Lin, X. & Gaffen, S. L. Crucial Role for Nuclear Factor of Activated T Cells in T Cell Receptor-mediated Regulation of Human Interleukin-17. *Journal of Biological Chemistry* **279**, 52762–52771 (2004).

126. Xu, H. *et al.* IL-17-producing innate lymphoid cells are restricted to mucosal tissues and are depleted in SIV-infected macaques. *Mucosal Immunology 2012 5:6* **5**, 658–669 (2012).

127. Onishi, R. M. & Gaffen, S. L. Interleukin-17 and its target genes: mechanisms of interleukin-17 function in disease. *Immunology* **129**, 311 (2010).

128. Liew, F. Y., Girard, J. P. & Turnquist, H. R. Interleukin-33 in health and disease. *Nature Reviews Immunology 2016 16:11* **16**, 676–689 (2016).

129. Barbour, M. *et al.* IL-33 attenuates the development of experimental autoimmune uveitis. *Eur J Immunol* **44**, 3320–3329 (2014).

130. Ho, L. H. *et al.* IL-33 induces IL-13 production by mouse mast cells independently of IgE-FcepsilonRI signals. *J Leukoc Biol* **82**, 1481–1490 (2007).

131. Lindemans, C. A. *et al.* Interleukin-22 promotes intestinal-stem-cell-mediated epithelial regeneration. *Nature 2015 528:7583* **528**, 560–564 (2015).

132. Moore, K. W., De Waal Malefyt, R., Coffman, R. L. & O'Garra, A. Interleukin-10 and the interleukin-10 receptor. *Annu Rev Immunol* **19**, 683–765 (2001).

133. Okumura, R. & Takeda, K. Roles of intestinal epithelial cells in the maintenance of gut homeostasis. *Experimental & Molecular Medicine 2017 49:5* **49**, e338–e338 (2017).

134. Guan, Q. A Comprehensive Review and Update on the Pathogenesis of Inflammatory Bowel Disease. *J Immunol Res* **2019**, (2019).

135. Abraham, C. & Cho, J. H. Mechanisms of Disease Inflammatory Bowel Disease. *N Engl J Med* **361**, 2066–78 (2009).

136. Seyedian, S. S., Nokhostin, F. & Dargahi Malamir, M. A review of the diagnosis, prevention, and treatment methods of inflammatory bowel disease. *J Med Life* **12**, 113–122.

137. Mumolo, M. G. *et al.* From bench to bedside: Fecal calprotectin in inflammatory bowel diseases clinical setting. *World J Gastroenterol* **24**, 3681 (2018).

138. Stallmach, A. *et al.* Treatment Strategies in Inflammatory Bowel Diseases. *Dtsch Arztebl Int* **120**, 768–778 (2023).

139. Abraham, B. & Quigley, E. M. M. Antibiotics and probiotics in inflammatory bowel disease: when to use them? *Frontline Gastroenterol* **11**, 62–69 (2020).

140. McCormack, M. D., Wahedna, N. A., Aldulaimi, D. & Hawker, P. Emerging role of dual biologic therapy for the treatment of inflammatory bowel disease. *World J Clin Cases* **11**, 2621 (2023).

141. Cai, Z., Wang, S. & Li, J. Treatment of Inflammatory Bowel Disease: A Comprehensive Review. *Front Med (Lausanne)* **8**, (2021).

142. Torres, J. *et al.* Systematic Review of Effects of Withdrawal of Immunomodulators or Biologic Agents From Patients With Inflammatory Bowel Disease. *Gastroenterology* **149**, 1716–1730 (2015).

143. Alatab, S. *et al.* The global, regional, and national burden of inflammatory bowel disease in 195 countries and territories, 1990–2017: a systematic analysis for the Global Burden of Disease Study 2017. *Lancet Gastroenterol Hepatol* **5**, 17–30 (2020).

144. Caviglia, G. P. *et al.* Epidemiology of Inflammatory Bowel Diseases: A Population Study in a Healthcare District of North-West Italy. *J Clin Med* **12**, 641 (2023).

145. Schütz, L., Radke, M., Menzel, S. & Däbritz, J. Long-term implications of structured transition of adolescents with inflammatory bowel disease into adult health care: A retrospective study. *BMC Gastroenterol* **19**, 1–12 (2019).

146. Stallmach, A. *et al.* Treatment Strategies in Inflammatory Bowel Diseases. *Dtsch Arztebl Int* **120**, 768–778 (2023).

147. Christensen, C. *et al.* Diet, Food, and Nutritional Exposures and Inflammatory Bowel Disease or Progression of Disease: an Umbrella Review. *Adv Nutr* **15**, (2024).

148. Li, F., Liu, X., Wang, W. & Zhang, D. Consumption of vegetables and fruit and the risk of inflammatory bowel disease: A meta-analysis. *Eur J Gastroenterol Hepatol* **27**, 623–630 (2015).

149. Limketkai, B. N. *et al.* Dietary interventions for induction and maintenance of remission in inflammatory bowel disease. *Cochrane Database of Systematic Reviews* **2019**, (2019).

150. Li, T. *et al.* Systematic review and meta-analysis: Association of a pre-illness Western dietary pattern with the risk of developing inflammatory bowel disease. *J Dig Dis* **21**, 362–371 (2020).

151. Liu, J. Z. *et al.* Association analyses identify 38 susceptibility loci for inflammatory bowel disease and highlight shared genetic risk across populations. *Nature Genetics 2015 47:9* **47**, 979–986 (2015).

152. De Lange, K. M. *et al.* Genome-wide association study implicates immune activation of multiple integrin genes in inflammatory bowel disease. *Nature Genetics 2017 49:2* **49**, 256–261 (2017).

153. Ananthakrishnan, A. N. Environmental Risk Factors for Inflammatory Bowel Disease. *Gastroenterol Hepatol (N Y)* **9**, 367 (2013).

154. Kaser, A., Zeissig, S. & Blumberg, R. S. Genes and Environment: How Will Our Concepts on the Pathophysiology of IBD Develop in the Future? *Dig Dis* **28**, 395 (2010).

155. Linares, R., Francés, R., Gutiérrez, A. & Juanola, O. Bacterial Translocation as Inflammatory Driver in Crohn's Disease. *Front Cell Dev Biol* **9**, (2021).

156. Jaeger, N. *et al.* Single-cell analyses of Crohn's disease tissues reveal intestinal intraepithelial T cells heterogeneity and altered subset distributions. *Nature Communications 2021 12:1* **12**, 1–12 (2021).

157. Garrido-Trigo, A. *et al.* Macrophage and neutrophil heterogeneity at single-cell spatial resolution in human inflammatory bowel disease. *Nature Communications 2023 14:1* **14**, 1–18 (2023).

158. Neurath, M. F. Cytokines in inflammatory bowel disease. *Nature Reviews Immunology 2014 14:5* **14**, 329–342 (2014).

159. Laukoetter, M. G., Nava, P. & Nusrat, A. Role of the intestinal barrier in inflammatory bowel disease. *World Journal of Gastroenterology : WJG* **14**, 401 (2008).

160. Schmitz, H. *et al.* Altered tight junction structure contributes to the impaired epithelial barrier function in ulcerative colitis. *Gastroenterology* **116**, 301–309 (1999).

161. Meddings, J. B., Sutherland, L. R. & May, G. R. Intestinal permeability in patients with Crohn's disease. *Gut* **35**, 1675 (1994).

162. Wang, F. *et al.* Interferon-gamma and tumor necrosis factor-alpha synergize to induce intestinal epithelial barrier dysfunction by up-regulating myosin light chain kinase expression. *Am J Pathol* **166**, 409–419 (2005).

163. Meyer, F., Wendling, D., Demougeot, C., Prati, C. & Verhoeven, F. Cytokines and intestinal epithelial permeability: A systematic review. *Autoimmun Rev* **22**, (2023).

164. Asteria, C. R., Ficari, F., Bagnoli, S., Milla, M. & Tonelli, F. Treatment of perianal fistulas in Crohn's disease by local injection of antibody to TNF-α accounts for a favourable clinical response in selected cases: A pilot study. *Scand J Gastroenterol* **41**, 1064–1072 (2006).

165. Vancamelbeke, M. *et al.* Genetic and Transcriptomic Bases of Intestinal Epithelial Barrier Dysfunction in Inflammatory Bowel Disease. *Inflamm Bowel Dis* **23**, 1718–1729 (2017).

166. Khaloian, S. *et al.* Mitochondrial impairment drives intestinal stem cell transition into dysfunctional Paneth cells predicting Crohn's disease recurrence. *Gut* **69**, 1939–1951 (2020).

167. Baumdick, M. E. *et al.* HLA-DP on Epithelial Cells Enables Tissue Damage by NKp44+ Natural Killer Cells in Ulcerative Colitis. *Gastroenterology* **165**, 946-962.e13 (2023).

168. Bagur, R. & Hajnóczky, G. Intracellular Ca2+ sensing: role in calcium homeostasis and signaling. *Mol Cell* **66**, 780 (2017).

169. Görlach, A., Bertram, K., Hudecova, S. & Krizanova, O. Calcium and ROS: A mutual interplay. *Redox Biol* **6**, 260 (2015).

170. Gong, T., Yang, Y., Jin, T., Jiang, W. & Zhou, R. Orchestration of NLRP3 Inflammasome Activation by Ion Fluxes. *Trends Immunol* **39**, 393–406 (2018).

171. Csordás, G., Weaver, D. & Hajnóczky, G. Endoplasmic Reticulum–Mitochondrial Contactology: Structure and Signaling Functions. *Trends Cell Biol* **28**, 523–540 (2018).

172. Ribeiro, C. M. P. The role of intracellular calcium signals in inflammatory responses of polarised cystic fibrosis human airway epithelia. *Drugs R D* **7**, 17–31 (2006).

173. Liu, Q. *et al.* The Mechanosensitive Ion Channel PIEZO1 in Intestinal Epithelial Cells Mediates Inflammation through the NOD-Like Receptor 3 Pathway in Crohn's Disease. *Inflamm Bowel Dis* **29**, 103–115 (2023).

174. Murakami, T. *et al.* Critical role for calcium mobilization in activation of the NLRP3 inflammasome. *Proc Natl Acad Sci U S A* **109**, 11282–11287 (2012).

175. Feldmeyer, L. *et al.* Report The Inflammasome Mediates UVB-Induced Activation and Secretion of Interleukin-1b by Keratinocytes. *Current Biology* **17**, 1140–1145.

176. Lee, G. S. *et al.* The calcium-sensing receptor regulates the NLRP3 inflammasome through Ca2+ and cAMP. *Nature 2012 492:7427* **492**, 123–127 (2012).

177. Souza, C. O. *et al.* Extracellular ATP induces cell death in human intestinal epithelial cells. *Biochimica et Biophysica Acta (BBA) - General Subjects* **1820**, 1867–1878 (2012).

178. Prakriya, M. The molecular physiology of CRAC channels. *Immunol Rev* **231**, 88–98 (2009).

179. Letizia, M. *et al.* Store-operated calcium entry controls innate and adaptive immune cell function in inflammatory bowel disease. *EMBO Mol Med* **14**, e15687 (2022).

180. Berry, C. T., May, M. J. & Freedman, B. D. STIM- and Orai-mediated calcium entry controls NF-κB activity and function in lymphocytes. *Cell Calcium* **74**, 131–143 (2018).

181. Vaeth, M. *et al.* Store-Operated Ca2+ Entry Controls Clonal Expansion of T Cells through Metabolic Reprogramming. *Immunity* **47**, 664-679.e6 (2017).

182. McCarl, C. A. *et al.* ORAI1 deficiency and lack of store-operated Ca2+ entry cause immunodeficiency, myopathy, and ectodermal dysplasia. *Journal of Allergy and Clinical Immunology* **124**, 1311-1318.e7 (2009).

183. Di Sabatino, A. *et al.* Targeting Gut T Cell Ca2+ Release-Activated Ca2+ Channels Inhibits T Cell Cytokine Production and T-Box Transcription Factor T-Bet in Inflammatory Bowel Disease. *The Journal of Immunology* **183**, 3454–3462 (2009).

184. Kav, T. *et al.* P029 Azelnidipine, a novel calcium channel blocker, ameliorates severity of colitis in DSS induced colitis in mice possibly by modulating tissue levels of TNF-alpha and IL-6. *J Crohns Colitis* **11**, S93–S94 (2017).

185. Harris, G., KuoLee, R. & Chen, W. Role of Toll-like receptors in health and diseases of gastrointestinal tract. *World Journal of Gastroenterology : WJG* **12**, 2149 (2006).

186. Brown, M., Hughes, K. R., Moossavi, S., Robins, A. & Mahida, Y. R. Toll-like receptor expression in crypt epithelial cells, putative stem cells and intestinal myofibroblasts isolated from controls and patients with inflammatory bowel disease. *Clin Exp Immunol* **178**, 28–39 (2014).

187. Bank, S. *et al.* Polymorphisms in the Toll-Like Receptor and the IL-23/IL-17 Pathways Were Associated with Susceptibility to Inflammatory Bowel Disease in a Danish Cohort. *PLoS One* **10**, e0145302 (2015).

188. Sheridan, J. *et al.* A Non-Synonymous Coding Variant (L616F) in the TLR5 Gene Is Potentially Associated with Crohn's Disease and Influences Responses to Bacterial Flagellin. *PLoS One* **8**, (2013).

189. Gewirtz, A. T. *et al.* Dominant-negative TLR5 polymorphism reduces adaptive immune response to flagellin and negatively associates with Crohn's disease. *Am J Physiol Gastrointest Liver Physiol* **290**, 1157–1163 (2006).

190. Meena, N. K., Ahuja, V., Meena, K. & Paul, J. Association of TLR5 gene polymorphisms in ulcerative colitis patients of north India and their role in cytokine homeostasis. *PLoS One* **10**, (2015).

191. Sánchez-Muñoz, F. *et al.* Transcript levels of Toll-Like Receptors 5, 8 and 9 correlate with inflammatory activity in Ulcerative Colitis. *BMC Gastroenterol* **11**, (2011).

192. Lopetuso, L. R. *et al.* Epithelial-specific Toll-like Receptor (TLR)5 Activation Mediates Barrier Dysfunction in Experimental Ileitis. *Inflamm Bowel Dis* **23**, 392–403 (2017).

193. Massimino, L. *et al.* The Inflammatory Bowel Disease Transcriptome and Metatranscriptome Meta-Analysis (IBD TaMMA) framework. *Nature Computational Science 2021 1:8* **1**, 511–515 (2021).

194. De Souza, H. S. P. & Fiocchi, C. Immunopathogenesis of IBD: current state of the art. *Nature Reviews Gastroenterology & Hepatology 2015 13:1* **13**, 13–27 (2015).

195. Jaeger, N. *et al.* Single-cell analyses of Crohn's disease tissues reveal intestinal intraepithelial T cells heterogeneity and altered subset distributions. *Nature Communications 2021 12:1* **12**, 1–12 (2021).

196. Fujino, S. *et al.* Increased expression of interleukin 17 in inflammatory bowel disease. *Gut* **52**, 65 (2003).

197. Harbour, S. N., Maynard, C. L., Zindl, C. L., Schoeb, T. R. & Weaver, C. T. Th17 cells give rise to Th1 cells that are required for the pathogenesis of colitis. *Proc Natl Acad Sci U S A* **112**, 7061–7066 (2015).

198. Brand, S. *et al.* IL-22 is increased in active Crohn's disease and promotes proinflammatory gene expression and intestinal epithelial cell migration. *Am J Physiol Gastrointest Liver Physiol* **290**, 827–838 (2006).

199. Mahida, Y. R., Patel, S., Gionchetti, P., Vaux, D. & Jewell, D. P. Macrophage subpopulations in lamina propria of normal and inflamed colon and terminal ileum. *Gut* **30**, 826–834 (1989).

200. Aderem, A. & Underhill, D. M. Mechanisms of phagocytosis in macrophages. *Annu Rev Immunol* **17**, 593–623 (1999).

201. Denning, T. L., Wang, Y. C., Patel, S. R., Williams, I. R. & Pulendran, B. Lamina propria macrophages and dendritic cells differentially induce regulatory and interleukin 17–producing T cell responses. *Nature Immunology 2007 8:10* **8**, 1086–1094 (2007).

202. Dharmasiri, S. *et al.* Human Intestinal Macrophages Are Involved in the Pathology of Both Ulcerative Colitis and Crohn Disease. *Inflamm Bowel Dis* **27**, 1641–1652 (2021).

203. Martín-Orozco, N., Isibasi, A. & Ortiz-Navarrete, V. Macrophages present exogenous antigens by class I major histocompatibility complex molecules via a secretory pathway as a consequence of interferon-γ activation. *Immunology* **103**, 41 (2001).

204. Steinbach, E. C. & Plevy, S. E. The role of macrophages and dendritic cells in the initiation of inflammation in IBD. *Inflamm Bowel Dis* **20**, 166–175 (2014).

205. Baumgart, D. C. *et al.* Exaggerated inflammatory response of primary human myeloid dendritic cells to lipopolysaccharide in patients with inflammatory bowel disease. *Clin Exp Immunol* **157**, 423–436 (2009).

206. Liu, W., Wang, C., Tang, L. & Yang, H. Associations between Gene Polymorphisms in Pro-inflammatory Cytokines and the Risk of Inflammatory Bowel Disease: A Meta-analysis. *Immunol Invest* **50**, 869–883 (2021).

207. Mazzucchelli, L. *et al.* Expression of interleukin-8 gene in inflammatory bowel disease is related to the histological grade of active inflammation. *Am J Pathol* **144**, 997 (1994).

208. Kaser, A. *et al.* Increased expression of CCL20 in human inflammatory bowel disease. *J Clin Immunol* **24**, 74–85 (2004).

209. D'Haens, G. *et al.* Endoscopic and histological healing with infliximab anti-tumor necrosis factor antibodies in Crohn's disease: A European multicenter trial. *Gastroenterology* **116**, 1029–1034 (1999).

210. Franzosa, E. A. *et al.* Gut microbiome structure and metabolic activity in inflammatory bowel disease. *Nature Microbiology 2018 4:2* **4**, 293–305 (2018).

211. Lloyd-Price, J. *et al.* Multi-omics of the gut microbial ecosystem in inflammatory bowel diseases. *Nature 2019 569:7758* **569**, 655–662 (2019).

212. Jacobs, J. P. *et al.* A Disease-Associated Microbial and Metabolomics State in Relatives of Pediatric Inflammatory Bowel Disease Patients. *Cell Mol Gastroenterol Hepatol* **2**, 750–766 (2016).

213. Thomas, J. P., Modos, D., Rushbrook, S. M., Powell, N. & Korcsmaros, T. The Emerging Role of Bile Acids in the Pathogenesis of Inflammatory Bowel Disease. *Front Immunol* **13**, (2022).

214. Walters, J. R. F. *et al.* A new mechanism for bile acid diarrhea: defective feedback inhibition of bile acid biosynthesis. *Clin Gastroenterol Hepatol* **7**, 1189–1194 (2009).

215. Gadaleta, R. M. *et al.* Fibroblast Growth Factor 19 modulates intestinal microbiota and inflammation in presence of Farnesoid X Receptor. *EBioMedicine* **54**, (2020).

216. Lyutakov, I. *et al.* Serum Levels of Fibroblast Growth Factor 19 Correlate with the Severity of Diarrhea and Independently from Intestinal Inflammation in Patients with Inflammatory Bowel Disease or Microscopic Colitis. *Turkish Journal of Gastroenterology* **32**, 374–381 (2021).

217. Glassner, K. L., Abraham, B. P. & Quigley, E. M. M. The microbiome and inflammatory bowel disease. *Journal of Allergy and Clinical Immunology* **145**, 16–27 (2020).

218. Song, Z. *et al.* Taxonomic profiling and populational patterns of bacterial bile salt hydrolase (BSH) genes based on worldwide human gut microbiome. *Microbiome* **7**, 1–16 (2019).

219. Li, C., Peng, K., Xiao, S., Long, Y. & Yu, Q. The role of Lactobacillus in inflammatory bowel disease: from actualities to prospects. *Cell Death Discovery 2023 9:1* **9**, 1–12 (2023).

220. Wise, J. L. & Cummings, B. P. The 7-α-dehydroxylation pathway: An integral component of gut bacterial bile acid metabolism and potential therapeutic target. *Front Microbiol* **13**, 1093420 (2023).

221. Priya, S. *et al.* Identification of shared and disease-specific host gene–microbiome associations across human diseases using multi-omic integration. *Nature Microbiology 2022 7:6* **7**, 780–795 (2022).

222. Thomas, J. P., Modos, D., Rushbrook, S. M., Powell, N. & Korcsmaros, T. The Emerging Role of Bile Acids in the Pathogenesis of Inflammatory Bowel Disease. *Front Immunol* **13**, (2022).

223. Yoneno, K. *et al.* TGR5 signalling inhibits the production of pro-inflammatory cytokines by in vitro differentiated inflammatory and intestinal macrophages in Crohn's disease. *Immunology* **139**, 19–29 (2013).

224. Song, X. *et al.* Microbial bile acid metabolites modulate gut RORγ+ regulatory T cell homeostasis. *Nature 2019 577:7790* **577**, 410–415 (2019).

225. Broxmeyer, H. E., Cooper, S., Hangoc, G. & Chang, C. H. Class II transactivator-mediated regulation of major histocompatibility complex class II antigen expression is

important for hematopoietic progenitor cell suppression by chemokines and iron-binding proteins. *Exp Hematol* **34**, 1078–1084 (2006).

226. Hang, S. *et al.* Bile acid metabolites control TH17 and Treg cell differentiation. *Nature 2019 576:7785* **576**, 143–148 (2019).

227. Yui, S., Saeki, T., Kanamoto, R. & Iwami, K. Characteristics of Apoptosis in HCT116 Colon Cancer Cells Induced by Deoxycholic Acid. *The Journal of Biochemistry* **138**, 151–157 (2005).

228. Duboc, H. *et al.* Connecting dysbiosis, bile-acid dysmetabolism and gut inflammation in inflammatory bowel diseases. *Gut* **62**, 531–539 (2013).

229. Sorrentino, G. *et al.* Bile Acids Signal via TGR5 to Activate Intestinal Stem Cells and Epithelial Regeneration. *Gastroenterology* **159**, 956-968.e8 (2020).

230. Attinkara, R. *et al.* Association of genetic variation in the NR1H4 gene, encoding the nuclear bile acid receptor FXR, with inflammatory bowel disease. *BMC Res Notes* **5**, (2012).

231. Sasson, A. N. *et al.* The role of precision nutrition in the modulation of microbial composition and function in people with inflammatory bowel disease. *Lancet Gastroenterol Hepatol* **6**, 754–769 (2021).

232. Trefflich, I. *et al.* Associations between Dietary Patterns and Bile Acids—Results from a Cross-Sectional Study in Vegans and Omnivores. *Nutrients* **12**, (2020).

233. Chiba, M., Nakane, K. & Komatsu, M. Westernized Diet is the Most Ubiquitous Environmental Factor in Inflammatory Bowel Disease. *Perm J* **23**, 18–107 (2019).

234. Sato, T. *et al.* Single Lgr5 stem cells build crypt-villus structures in vitro without a mesenchymal niche. *Nature* **459**, 262–265 (2009).

235. Sato, T. *et al.* Long-term Expansion of Epithelial Organoids From Human Colon, Adenoma, Adenocarcinoma, and Barrett's Epithelium. *YGAST* **141**, 1762–1772 (2011).

236. Hu, H. *et al.* Long-Term Expansion of Functional Mouse and Human Hepatocytes as 3D Organoids. *Cell* **175**, 1591-1606.e19 (2018).

237. Leushacke, M. & Barker, N. Ex vivo culture of the intestinal epithelium: strategies and applications. *Gut* **63**, 1345–1354 (2014).

238. Lehmann, R. *et al.* Human organoids: a new dimension in cell biology. *Mol Biol Cell* **30**, 1129 (2019).

239. Zietek, T. *et al.* Organoids to Study Intestinal Nutrient Transport, Drug Uptake and Metabolism – Update to the Human Model and Expansion of Applications. *Front Bioeng Biotechnol* **8**, (2020).

240. Mithal, A. *et al.* Generation of mesenchyme free intestinal organoids from human induced pluripotent stem cells. *Nature Communications 2020 11:1* **11**, 1–15 (2020).

241. Qi, Z. *et al.* BMP restricts stemness of intestinal Lgr5+ stem cells by directly suppressing their signature genes. *Nature Communications 2017 8:1* **8**, 1–14 (2017).

242. Bar-Ephraim, Y. E., Kretzschmar, K. & Clevers, H. Organoids in immunological research. *Nature Reviews Immunology 2019 20:5* **20**, 279–293 (2019).

243. Schreurs, R. R. C. E., Baumdick, M. E., Drewniak, A. & Bunders, M. J. In vitro co-culture of human intestinal organoids and lamina propria-derived CD4+ T cells. *STAR Protoc* **2**, (2021).

244. Puschhof, J. *et al.* Intestinal organoid cocultures with microbes. *Nature Protocols 2021 16:10* **16**, 4633–4649 (2021).

245. Rubert, J. *et al.* Intestinal Organoids: A Tool for Modelling Diet–Microbiome–Host Interactions. *Trends in Endocrinology & Metabolism* **31**, 848–858 (2020).

246. Sato, T. *et al.* Single Lgr5 stem cells build crypt-villus structures in vitro without a mesenchymal niche. *Nature* **459**, 262–265 (2009).

247. Bremer, J. P. *et al.* GOAT: Deep learning-enhanced Generalized Organoid Annotation Tool. *bioRxiv* 2022.09.06.506648 (2022) doi:10.1101/2022.09.06.506648.

248. Sato, T. *et al.* Single Lgr5 stem cells build crypt-villus structures in vitro without a mesenchymal niche. *Nature* **459**, 262–265 (2009).

249. Pleguezuelos-Manzano, C. *et al.* Establishment and Culture of Human Intestinal Organoids Derived from Adult Stem Cells. *Curr Protoc Immunol* **130**, (2020).

250. Pleguezuelos-Manzano, C. *et al.* Establishment and Culture of Human Intestinal Organoids Derived from Adult Stem Cells. *Curr Protoc Immunol* **130**, (2020).

251. Hou, Q., Huang, J., Ayansola, H., Masatoshi, H. & Zhang, B. Intestinal Stem Cells and Immune Cell Relationships: Potential Therapeutic Targets for Inflammatory Bowel Diseases. *Front Immunol* **11**, 623691 (2021).

252. Dekkers, J. F. *et al.* High-resolution 3D imaging of fixed and cleared organoids. *Nat Protoc* **14**, 1756–1771 (2019).

253. Barker, N. Adult intestinal stem cells: critical drivers of epithelial homeostasis and regeneration. *Nature Reviews Molecular Cell Biology 2013 15:1* **15**, 19–33 (2013).

254. Bremer, J. P. *et al.* GOAT: Deep learning-enhanced Generalized Organoid Annotation Tool. *bioRxiv* 2022.09.06.506648 (2022) doi:10.1101/2022.09.06.506648.

255. Clapham, D. E. Calcium Signaling. *Cell* **131**, 1047–1058 (2007).

256. Sui, J. *et al.* Dual role of Ca2+-activated Cl− channel transmembrane member 16A in lipopolysaccharide-induced intestinal epithelial barrier dysfunction in vitro. *Cell Death & Disease 2020 11:5* **11**, 1–12 (2020).

257. Jiang, L. H., Mousawi, F., Yang, X. & Roger, S. ATP-induced Ca2+-signalling mechanisms in the regulation of mesenchymal stem cell migration. *Cell Mol Life Sci* **74**, 3697–3710 (2017).

258. Corre, B. *et al.* Integration of intermittent calcium signals in T cells revealed by temporally patterned optogenetics. *iScience* **26**, (2023).

259. Feng, S. *et al.* TLR5 Signaling in the Regulation of Intestinal Mucosal Immunity. *J Inflamm Res* **16**, 2491 (2023).

260. Casper, J. M. *et al.* The c-myc DNA-unwinding element-binding protein modulates the assembly of DNA replication complexes in vitro. *J Biol Chem* **280**, 13071–13083 (2005).

261. Chen, W. *et al.* MUC1: Structure, Function, and Clinic Application in Epithelial Cancers. *Int J Mol Sci* **22**, (2021).

262. Sheng, Y. H. *et al.* MUC1 and MUC13 differentially regulate epithelial inflammation in response to inflammatory and infectious stimuli. *Mucosal Immunology 2013 6:3* **6**, 557–568 (2012).

263. Xu, S. *et al.* Oxidative stress gene expression, DNA methylation, and gut microbiota interaction trigger Crohn's disease: a multi-omics Mendelian randomization study. *BMC Med* **21**, 1–16 (2023).

264. van Haaften, W. T. *et al.* Intestinal stenosis in Crohn's disease shows a generalized upregulation of genes involved in collagen metabolism and recognition that could serve as novel anti-fibrotic drug targets. *Therap Adv Gastroenterol* **13**, (2020).

265. Mussunoor, S. & Murray, G. I. The role of annexins in tumour development and progression. *Journal of Pathology* **216**, 131–140 (2008).

266. Zhang, C. *et al.* ANXA10 is a prognostic biomarker and suppressor of hepatocellular carcinoma: a bioinformatics analysis and experimental validation. *Sci Rep* **13**, (2023).

267. Lloyd-Price, J. *et al.* Multi-omics of the gut microbial ecosystem in inflammatory bowel diseases. *Nature 2019 569:7758* **569**, 655–662 (2019).

268. Ning, L. *et al.* Microbiome and metabolome features in inflammatory bowel disease via multi-omics integration analyses across cohorts. *Nature Communications 2023 14:1* **14**, 1–17 (2023).

269. Northfield, T. C. & McColl, I. Postprandial concentrations of free and conjugated bile acids down the length of the normal human small intestine. *Gut* **14**, 513–518 (1973).

270. Hamilton, J. P. *et al.* Human cecal bile acids: Concentration and spectrum. *Am J Physiol Gastrointest Liver Physiol* **293**, 256–263 (2007).

271. Barrasa, J. I. *et al.* Deoxycholic and chenodeoxycholic bile acids induce apoptosis via oxidative stress in human colon adenocarcinoma cells. *Apoptosis* **16**, 1054–1067 (2011).

272. Pérez-Ramos, P. *et al.* Effect of Bile Acids on Butyrate-Sensitive and -Resistant Human Colon Adenocarcinoma Cells. *Nutr Cancer* **53**, 208–219 (2005).

273. Barrasa, J. I., Santiago-Gómez, A., Olmo, N., Lizarbe, M. A. & Turnay, J. Resistance to butyrate impairs bile acid-induced apoptosis in human colon adenocarcinoma cells via up-regulation of Bcl-2 and inactivation of Bax. *Biochimica et Biophysica Acta (BBA) - Molecular Cell Research* **1823**, 2201–2209 (2012).

274. Villalpando-Rodriguez, G. E. & Gibson, S. B. Reactive Oxygen Species (ROS) Regulates Different Types of Cell Death by Acting as a Rheostat. *Oxid Med Cell Longev* **2021**, (2021).

275. Lih-Brody, L. *et al.* Increased oxidative stress and decreased antioxidant defenses in mucosa of inflammatory bowel disease. *Dig Dis Sci* **41**, 2078–2086 (1996).

276. Shahinfar, H. *et al.* Administration of dietary antioxidants for patients with inflammatory bowel disease: A systematic review and meta-analysis of randomized controlled clinical trials. *Complement Ther Med* **63**, 102787 (2021).

277. Bommelaer, G. *et al.* Oral Curcumin No More Effective Than Placebo in Preventing Recurrence of Crohn's Disease After Surgery in a Randomized Controlled Trial. *Clinical Gastroenterology and Hepatology* **18**, 1553-1560.e1 (2020).

278. Reis, J. *et al.* Targeting ROS production through inhibition of NADPH oxidases. *Nature Chemical Biology 2023 19:12* **19**, 1540–1550 (2023).

279. Zhang, C. *et al.* ANXA10 is a prognostic biomarker and suppressor of hepatocellular carcinoma: a bioinformatics analysis and experimental validation. *Scientific Reports 2023 13:1* **13**, 1–23 (2023).

280. Dotti, I. *et al.* Alterations in the epithelial stem cell compartment could contribute to permanent changes in the mucosa of patients with ulcerative colitis. *Gut* **66**, 2069–2079 (2017).

281. Chowdhury, A. *et al.* The DNA unwinding element binding protein DUE-B interacts with Cdc45 in preinitiation complex formation. *Mol Cell Biol* **30**, 1495–1507 (2010).

282. Laukoetter, M. G., Nava, P. & Nusrat, A. Role of the intestinal barrier in inflammatory bowel disease. *World Journal of Gastroenterology : WJG* **14**, 401 (2008).

283. Thornberry, N. A. *et al.* A novel heterodimeric cysteine protease is required for interleukin-1 beta processing in monocytes. *Nature* **356**, 768–774 (1992).

284. Gong, Z. *et al.* Chenodeoxycholic acid activates NLRP3 inflammasome and contributes to cholestatic liver fibrosis. *Oncotarget* **7**, 83951 (2016).

285. Mazzucchelli, L. *et al.* Expression of interleukin-8 gene in inflammatory bowel disease is related to the histological grade of active inflammation. *Am J Pathol* **144**, 997 (1994).

286. Olsen, T. *et al.* Tissue levels of tumor necrosis factor-alpha correlates with grade of inflammation in untreated ulcerative colitis. *Scand J Gastroenterol* **42**, 1312–1320 (2007).

287. Cambier, S., Gouwy, M. & Proost, P. The chemokines CXCL8 and CXCL12: molecular and functional properties, role in disease and efforts towards pharmacological intervention. *Cellular & Molecular Immunology 2023 20:3* **20**, 217–251 (2023).

288. van Unen, V. *et al.* Identification of a Disease-Associated Network of Intestinal Immune Cells in Treatment-Naive Inflammatory Bowel Disease. *Article* **13**, 1 (2022).

289. Russo, R. C., Garcia, C. C., Teixeira, M. M. & Amaral, F. A. The CXCL8/IL-8 chemokine family and its receptors in inflammatory diseases. *Expert Rev Clin Immunol* **10**, 593–619 (2014).

290. Williams, I. R. CCR6 and CCL20: partners in intestinal immunity and lymphorganogenesis. *Ann N Y Acad Sci* **1072**, 52–61 (2006).

291. Jaeger, N. *et al.* Single-cell analyses of Crohn's disease tissues reveal intestinal intraepithelial T cells heterogeneity and altered subset distributions. *Nature Communications 2021 12:1* **12**, 1–12 (2021).

292. Lee, H. J. *et al.* Iron chelator induces MIP-alpha/CCL20 in human intestinal epithelial cells: implication for triggering mucosal adaptive immunity. *Exp Mol Med* **37**, 297–310 (2005).

293. Kalliolias, G. D. & Ivashkiv, L. B. TNF biology, pathogenic mechanisms and emerging therapeutic strategies. *Nat Rev Rheumatol* **12**, 49 (2016).

294. Chen, S. *et al.* Macrophages in immunoregulation and therapeutics. *Signal Transduction and Targeted Therapy 2023 8:1* **8**, 1–35 (2023).

295. Zhu, W. *et al.* Disequilibrium of M1 and M2 macrophages correlates with the development of experimental inflammatory bowel diseases. *Immunol Invest* **43**, 638–652 (2014).

296. Lissner, D. *et al.* Monocyte and M1 Macrophage-induced Barrier Defect Contributes to Chronic Intestinal Inflammation in IBD. *Inflamm Bowel Dis* **21**, 1297–1305 (2015).

297. Thakur, B. K., Dasgupta, N., Ta, A. & Das, S. Physiological TLR5 expression in the intestine is regulated by differential DNA binding of Sp1/Sp3 through simultaneous Sp1 dephosphorylation and Sp3 phosphorylation by two different PKC isoforms. *Nucleic Acids Res* **44**, 5658–5672 (2016).

298. Liao, C. *et al.* Inflammatory-Dependent Bidirectional Effect of Bile Acids on NLRP3 Inflammasome and Its Role in Ameliorating CPT-11-Induced Colitis. *Front Pharmacol* **13**, (2022).

299. Calkhoven, C. F. & Ab, G. Multiple steps in the regulation of transcription-factor level and activity. *Biochemical Journal* **317**, 329 (1996).

300. Benasciutti, E. *et al.* MAPK and JNK transduction pathways can phosphorylate Sp1 to activate the uPA minimal promoter element and endogenous gene transcription. *Blood* **104**, 256–262 (2004).

301. Trisciuoglio, D. *et al.* bcl-2 induction of urokinase plasminogen activator receptor expression in human cancer cells through Sp1 activation: involvement of ERK1/ERK2 activity. *J Biol Chem* **279**, 6737–6745 (2004).

302. Dent, P. *et al.* Conjugated bile acids promote ERK1/2 and AKT activation via a pertussis toxin–sensitive mechanism in murine and human hepatocytes. *Hepatology* **42**, 1291–1299 (2005).

303. Liu, D. *et al.* Activation of extracellular-signal regulated kinase (ERK1/2) by fluid shear is Ca2+- and ATP-dependent in MC3T3-E1 osteoblasts. *Bone* **42**, 644–652 (2008).

304. Guo, Y.-J. *et al.* ERK/MAPK signalling pathway and tumorigenesis. *Exp Ther Med* **19**, 1997 (2020).

305. Price, A. E. *et al.* A map of Toll-like receptor expression in the intestinal epithelium reveals distinct spatial, cell type-specific, and temporal patterns. *Immunity* **49**, 560 (2018).

306. Liu, H. *et al.* TLR5 mediates CD172α(+) intestinal lamina propria dendritic cell induction of Th17 cells. *Sci Rep* **6**, (2016).

307. Rhee, S. H. *et al.* Pathophysiological role of Toll-like receptor 5 engagement by bacterial flagenllin in colonic inflammation. *Proc Natl Acad Sci U S A* **102**, 13610–13615 (2005).

308. Brestoff, J. R. & Artis, D. Commensal bacteria at the interface of host metabolism and the immune system. *Nature Immunology 2013 14:7* **14**, 676–684 (2013).

309. Möller, K. J. *et al.* Expanded ILC2s in human infant intestines promote tissue growth. *Mucosal Immunol* **16**, 408–421 (2023).

310. Venegas, D. P. *et al.* Short chain fatty acids (SCFAs)mediated gut epithelial and immune regulation and its relevance for inflammatory bowel diseases. *Front Immunol* **10**, 424615 (2019).

311. Gulhane, M. *et al.* High Fat Diets Induce Colonic Epithelial Cell Stress and Inflammation that is Reversed by IL-22. *Scientific Reports 2016 6:1* **6**, 1–17 (2016).

312. Straniero, S. *et al.* Of mice and men: murine bile acids explain species differences in the regulation of bile acid and cholesterol metabolism contains a supplement. *J Lipid Res* **61**, (2020).

313. Takahashi, S. *et al.* Cyp2c70 is responsible for the species difference in bile acid metabolism between mice and humans. *J Lipid Res* **57**, 2130–2137 (2016).

314. Ding, S. *et al.* High-fat diet: bacteria interactions promote intestinal inflammation which precedes and correlates with obesity and insulin resistance in mouse. *PLoS One* **5**, (2010).

315. Stentz, F. B. & Kitabchi, A. E. Palmitic acid-induced activation of human T-lymphocytes and aortic endothelial cells with production of insulin receptors, reactive oxygen species, cytokines, and lipid peroxidation. *Biochem Biophys Res Commun* **346**, 721–726 (2006).

316. Henkel, J. *et al.* Enhanced palmitate-induced interleukin-8 formation in human macrophages by insulin or prostaglandin E2. *Biomedicines* **9**, (2021).

317. Lancaster, G. I. *et al.* Evidence that TLR4 Is Not a Receptor for Saturated Fatty Acids but Mediates Lipid-Induced Inflammation by Reprogramming Macrophage Metabolism. *Cell Metab* **27**, 1096-1110.e5 (2018).

318. Nicholas, D. A. *et al.* Palmitic acid is a toll-like receptor 4 ligand that induces human dendritic cell secretion of IL-1β. *PLoS One* **12**, (2017).

319. Ghezzal, S. *et al.* Palmitic acid damages gut epithelium integrity and initiates inflammatory cytokine production. *Biochimica et Biophysica Acta (BBA) - Molecular and Cell Biology of Lipids* **1865**, 158530 (2020).

320. Geurts, M. H. & Clevers, H. CRISPR engineering in organoids for gene repair and disease modelling. *Nature Reviews Bioengineering 2023 1:1* **1**, 32–45 (2023).

321. Leung, C. M. *et al.* A guide to the organ-on-a-chip. *Nature Reviews Methods Primers 2022 2:1* **2**, 1–29 (2022).

Acknowledgments

First, I would like to thank Madeleine for the supervision during this project and the scientific input. Special thanks also to Julia as the first reviewer of the thesis. Also, special thanks to Björn, Jörg and Mira for the great collaboration.

Furthermore, I would like to thank several members of the Virus Immunology and the Immune Ontogeny and Viral Infections research groups. Thank you to Heike, Christin, Martin, Malte, Sebastian, Ana, Mareike, Timo, Jenny, Bene, Deborah, and Johann for all kinds of support during the last years. It was a pleasure working with you.

Special thanks to Lotte and Nils for always being supportive in every sense.

Lastly, I would like to express my immense thanks to my family for supporting me during my academic career and my whole life.

Eidesstattliche Versicherung

Hiermit versichere ich an Eides statt, die vorliegende Dissertationsschrift selbst verfasst und keine anderen als die angegebenen Hilfsmittel und Quellen benutzt zu haben.

Sofern im Zuge der Erstellung der vorliegenden Dissertationsschrift generative KünstlicheIntelligenz (gKI) basierte elektronische Hilfsmittel verwendet wurden, versichere ich, dass meine eigene Leistung im Vordergrund stand und dass eine vollständige Dokumentation aller verwendeten Hilfsmittel gemäß der Guten wissenschaftlichen Praxis vorliegt. Ich trage die Verantwortung für eventuell durch die gKI generierte fehlerhafte oder verzerrte Inhalte, fehlerhafte Referenzen, Verstöße gegen das Datenschutz- und Urheberrecht oder Plagiate.

Affidavit:

I hereby declare and affirm that this doctoral dissertation is my own work and that I have not used any aids and sources other than those indicated.

If electronic resources based on generative artificial intelligence (gAI) were used in the course of writing this dissertation, I confirm that my own work was the main and value-adding contribution and that complete documentation of all resources used is available in accordance with good scientific practice. I am responsible for any erroneous or distorted content, incorrect references, violations of data protection and copyright law or plagiarism that may have been generated by the gAI.

Hamburg, den 17.10.2024 Unterschrift